LINKING X-BAND RADAR BACKSCATTERING AND OPTICAL REFLECTANCE WITH CROP GROWTH MODELS

Promotor: dr. ir. R.A. Feddes,
hoogleraar in de Bodemnatuurkunde en Agrohydrologie

Co-promotor: dr. ir. J. Goudriaan,
universitair hoofddocent, vakgroep Theoretische Produktie-ecologie

BAS A.M. BOUMAN

LINKING X-BAND RADAR BACKSCATTERING AND OPTICAL REFLECTANCE WITH CROP GROWTH MODELS

Proefschrift

ter verkrijging van de graad van
doctor in de landbouw- en milieuwetenschappen,
op gezag van de rector magnificus,
dr. H.C. van der Plas,
in het openbaar te verdedigen
op dinsdag 17 september 1991
des namiddags te vier uur in de aula
van de Landbouwuniversiteit te Wageningen

This thesis contains results of a research project carried out at the Centre for Agrobiological Research (CABO-DLO) at Wageningen, from 1987 to 1991. The project was funded by The Netherlands Remote Sensing Board (BCRS) and the Ministry of Education and Science.

NNO 701, 1436

STELLINGEN

1. Modellen zijn vereenvoudigde percepties van de werkelijkheid. Doordat onze perceptie van werkelijke systemen gedicteerd wordt door de metingen die we daaraan kunnen verrichten, is het in principe juister om modellen aan te passen aan nieuwe waarnemingstechnieken, zoals remote sensing, dan vice versa.

2. X-band radarreflectie van landbouwgewassen wordt met name bepaald door de structuur van het gewas. De interpretatie van radarbeelden voor het monitoren van groei en ontwikkeling van landbouwgewassen moet dan ook vooral gericht zijn op de detectie van veranderingen in de structuur en de morfologie.
(Dit proefschrift, Hoofdstuk 3)

3. Radar remote sensing, en radar polarimetrie in het bijzonder, is zeer geschikt voor herkenning en areaalbepaling van landbouwgewassen ten behoeve van oogstverwachting op regionale schaal.

4. X-band radarreflectie data zijn over het algemeen ongeschikt voor het voldoende nauwkeurig schatten van gewasgroei-parameters als de hoeveelheden droge stof en water in het vegetatiedek, en de bedekking van de bodem door het gewas.
(Dit proefschrift, Hoofdstuk 4)

5. X-band radarreflectie data zijn slechts bruikbaar voor de initialisatie en het bijsturen van gewasgroeisimulatiemodellen in het begin van het groeiseizoen voor een beperkt aantal gewassen. Optische reflectie data daarentegen, zijn hiervoor geschikt gedurende het gehele groeiseizoen en voor een groot aantal gewassen.
(Dit proefschrift, Hoofdstuk 7)

6. De bodembedekkingsgraad van landbouwgewassen kan met voldoende nauwkeurigheid uit optische reflectie data worden geschat om als input in gewasgroeimodellen te kunnen dienen.
(Dit proefschrift, Hoofdstuk 8)

7. De onderkenning van de *mondiale* problematiek van veranderingen in het klimaat en ons leefmilieu is mede een gevolg van de opkomst van remote sensing technieken die de observatie van onze aarde op mondiale schaal mogelijk maken.

8. De kracht van aardobservatie vanuit satellieten is het verschaffen van overzichten in ruimte en tijd, en niet de nauwkeurige bepaling van bio/geo-fysische parameters op een vierkante meter aardoppervlak.

9. De praktische toepasbaarheid van gewasgroei-simulatiemodellen voor voorspellingsdoeleinden is omgekeerd evenredig met de complexiteit van die modellen.

10. Bij de presentatie van berekeningen met simulatiemodellen voor gewasgroei en uit 'Multiple Goal Programming' studies krijgt een discussie over gevoeligheden van uitkomsten voor onnauwkeurigheden in inputwaardes zelden de nodige aandacht.

11. Om de milieu-vervuiling door autoverkeer tegen te gaan zijn maatregelen gericht op het verminderen van het gebruik van de auto niet meer dan hoogstnoodzakelijke lapmiddelen. Een uiteindelijke oplossing kan alleen liggen in het gebruik van energiebronnen zonder vervuilende afvalprodukten, of in het gecontroleerd opslaan van de afvalprodukten.

12. Het zou de kwaliteit van de samenleving ten goede komen als een deel van de taken van het leger omgebogen zou worden van de bewaking van de landsgrenzen naar de bewaking van het milieu.

13. Het autobezit en rijgedrag van de mannelijke *Homo sapiens* vertoont vaak treffende gelijkenis met het balts- en pochgedrag van de mannelijke *Philomachus pugnax* (Kemphaan).

14. Vanwege het niet-determinstische karakter van de natuur bestaat de kans dat U deze stelling niet op deze plaats zult aantreffen.

15. Een toetje is pas lekker als het veel is.
(Rijnsteeg 8-15A, 1986-1989)

Stellingen behorende bij het Proefschrift van B.A.M. Bouman: Linking X-band radar backscattering and optical reflectance with crop growth models. Wageningen, 17 september 1991.

ABSTRACT

Bouman, B.A.M., 1991. Linking X-band radar backscattering and optical reflectance with crop growth models. Ph.D. Thesis, Wageningen Agricultural University, The Netherlands. 169 pages, 21 Tables, 44 Figures.

This thesis describes an investigation into the possibilities of linking X-band radar backscattering and optical remote sensing data with crop growth models for the monitoring of crop growth. The emphasis is on the usability of X-band radar data, with a detailed analysis of the main backscattering influencing factors of agricultural crops in The Netherlands.

Six-years of ground-based X-band radar observations (VV and HH polarized, 10° to 80° incidence angle) were used to study the temporal radar backscattering of sugar beet, potato, wheat, barley and oats. The geometry of the crop canopy was found to be a major backscattering influencing factor, especially for the cereals. The possibilities of crop growth parameter (soil cover, biomass, height) estimation from the radar data were investigated using empirical and simple physical relationships. Except for sugar beet in the early growing season, the accuracies of parameter estimation were generally too low to be used in crop growth models.

In the optical region, the accuracy of estimating the leaf area index (*LAI*) from vegetation indices was studied. In a case study for sugar beet, the *LAI* was fairly accurately estimated from the so-called Weighted Difference Vegetation Index (*WDVI*).

Two methodologies were developed to link X-band radar and optical remote sensing data with crop growth models. In the first method, remote sensing data were used to estimate the fraction soil cover of a crop as input for a simple light-interception growth model. This method was especially suitable for the use of optical remote sensing data. The use of X-band radar data was only feasible for sugar beet.

In the second method, X-band radar and optical remote sensing data were used to initialize and re-parameterize the crop growth simulation model SUCROS (Simple and Universal Crop Growth Simulator). In six years of sugar beet observations, this method improved the simulation of canopy biomass over the use of SUCROS only. The radar and optical reflectance data were very effective in the initialization of SUCROS, and in adjusting the model during early, exponential crop growth. Optical data also adjusted SUCROS in the middle of the growing season.

Key words: remote sensing, radar, crops, growth model.

ACKNOWLEDGEMENTS

During the investigation and the writing of this thesis, I had the help of a number of people that I wish to thank here.

First of all, I want to thank H.W.J. van Kasteren. Together with the members of the team 'Radar Observation on Vegetation' (ROVE) in 1976-1981, he designed and carried out the field experiments with the ground-based radar that were used in this study. He pre-processed and stored the data in an organized data-base on the computer, which enabled me to start immediately with data analysis. I remember with pleasure our many fruitful, and sometimes fierce discussions on the interpretation of the data and on strategies for possible use in growth monitoring. His ideas have been a great inspiration for this work.

I express my gratitude to prof. R.A. Feddes and J. Goudriaan for their assistance to this work as promotor and co-promotor respectively. Their inspiration for this work, and later their valuable comments on this manuscript are greatly appreciated.

At the Centre for Agrobiological Research (CABO), D. Uenk collected most of the reflectance and ground-truth data used in this study. Moreover, he has been a very pleasant room-mate. B.E. Pengel and M.A.M. Vissers taught me the efficient use of a personal computer (PC), and kept my PC updated with the newest versions of software. Without their work, I would still have been writing this thesis, and the many figures in it, with pencil and graph-paper. W. Stol showed me how to debug and 'forcheck' FORTRAN simulation models on the computer mainframe.

H. Breman is thanked for his critical reviewing of most of the papers presented in this thesis. His critical viewpoint with regard to the use of remote sensing in agriculture stimulated careful consideration and formulation of results and conclusions.

Members of the ROVE team in 1987-1991 have helped me to understand the complexity of the physics and technology behind radar remote sensing. Especially the many conversations with D. Hoekman and G.P de Loor on this subject, and their enthusiasm for radar remote sensing have been very stimulating. As participant in ROVE, and in the Agriscatt and Maestro campaigns, I had interesting exchange of ideas with many other radar remote sensing colleagues, especially E. Attema, J. Groot, P. Hoogeboom, L. Krul and P. Snoeij.

I had fruitful discussions on strategies for integrating remote sensing data with crop growth models with J.G.P.W. Clevers, J. Goudriaan, A. Haverkort, H. van Keulen, H. van Leeuwen and C.J.T. Spitters († 1990).

Finally, I want to express my gratitude to The Netherlands Remote Sensing Board (BCRS) and the Ministery of Education and Science whose financial support made this study possible.

J. Engelsman has prepared the manually drawn figures in this thesis. The lay-out has been kindly supplied by 'captain' N. van Duivenbooden.

CONTENTS

ACCOUNT

The chapters in this thesis have been published or are in press by the following journals:

2. Bouman, B.A.M. and H.W.J. van Kasteren, 1990, Ground-based X-band (3-cm wave) radar backscattering of agricultural crops. I sugar beet and potato; backscattering and crop growth, Remote Sensing of Environment, 34: 93-105.

3. Bouman, B.A.M. and H.W.J. van Kasteren, 1990, Ground-based X-band (3-cm wave) radar backscattering of agricultural crops. II Wheat, barley and oats, the impact of canopy structure, Remote Sensing of Environment, 34: 107-118.

4. Bouman, B.A.M., Crop parameter estimation from ground-based X-band (3-cm wave) radar data, Remote Sensing of Environment (*in press*).

5. Bouman, B.A.M. and J. Goudriaan, 1989, Estimation of crop growth from optical and microwave soil cover, International Journal of Remote Sensing, 10(12): 1843-1855.

6. Bouman, B.A.M., Accuracy of estimating the leaf area index from vegetation indices derived from crop reflectance characteristics, a simulation study, International Journal of Remote Sensing (*in press*).

7. Bouman, B.A.M., Linking physical remote sensing models with crop growth simulation models, applied for sugar beet, International Journal of Remote Sensing (*in press*).

LIST OF USED SYMBOLS

Symbol	Interpretation	Units	Dimensions
$C(\theta)$	Backscattering coefficient of an optically thick crop canopy	dB	-
D	Coefficient of attenuation	$m^2.kg^{-1}$	$L^2.M^{-1}$
f	Fraction green soil cover	-	-
f'	Microwave soil cover	-	-
$G(\theta)$	Backscattering coefficient of dry soil	dB	-
h	Canopy height	m	L
k	Light extinction coefficient	-	-
K	Moisture coefficient of soil	-	-
m	Volumetric soil moisture content	-	-
R	Canopy growth rate	$kg.m^{-2}.d^{-1}$	$M.L^{-2}.t^{-1}$
S	Incoming global radiation	$J.m^{-2}.d^{-1}$	$M.t^{-3}$
W	Amount of water in canopy	$kg.m^{-2}$	$M.L^{-2}$
W_d	Dry canopy biomass	$kg.m^{-2}$	$M.L^{-2}$
α	Conversion efficiency of solar radiation to dry weight	$kg.J^{-1}$	$T2.L^{-2}$
γ	Normalised radar cross section per unit projected area of the radar beam	dB	-
σ'	Normalised radar cross section per unit illuminated surface	dB	-
θ	Incidence angle (grazing angle in H5)	(°)	-

LIST OF USED ABBREVIATIONS

Abbreviation	Description
LAI	Leaf Area Index (ratio of total leaf area in a crop canopy to area ground surface underneath the crop)
GR	Green reflectance of crop
GR_s	Green reflectance of soil
IR	Infra-red reflectance of crop
IR_s	Infra-red reflectance of soil
R	Red reflectance of crop
R_s	Red reflectance of soil
VI	Vegetation Index:
NDVI	Normalized Difference Vegetation Index $= (IR-GR)/(IR+GR)$
PVI	Perpendicular Vegetation Index: $= \sqrt{[(IR-IR_s)^2+(GR-GR_s)^2]}$
WDVI	Weighted Difference Vegetation Index $= IR - (IR_s/GR_s)*GR$
HH	Horizontal co-polarization (horizontal transmit, horizontal receive)
VV	Vertical co-polarization (vertical transmit, vertical receive)

FREQUENTLY USED ACRONYMS AND MODEL NAMES

Name	Description
Cloud	Model for radar backscattering of vegetation
EXTRAD	EXTinction of RADiation (model for crop canopies)
SUCROS	Simple and Universal CROp growth Simulator

1 INTRODUCTION

1.1 Yield prediction and crop growth models

In agriculture, monitoring of crop growth and development, and early estimates of final yield are of general interest. At a local level, individual farmers want to know how their crops perform for optimum crop management. At a regional and national level, local governments need data on type, location and acreage of crops for land use planning and management. Early yield forecasts may be helpful for market orientation. For some crops that are not marketed by wholesalers, but, like maize in The Netherlands, are more or less privately marketed, insight into annual production and distribution figures is still scarce. Timely yield forecasting is also crucial for some agricultural industries. Sugar beet factories must have an idea about expected dates of delivery and yields of sugar beets in order to plan their processing capacity.

At an international level, like the European Community (EC), yield estimates are an indispensable tool for pricing policies and the setting of import/export quotas. For Third World countries, early yield forecasting to mitigate possible food-shortage is of utmost importance.

Traditionally, yield forecasts are made on the basis of samples taken from individual farms, e.g. field visits or written enquiries. Problems encountered concern subjectivity in responses, respondent differences and non-response (Heath, 1990). At regional and (inter-) national level, the processing of these sample data is an expensive and time consuming procedure. Moreover, in the EC for example, there is a need for greater objectivity and inter-country comparability in the agricultural statistics delivered by the member states (Heath, 1990). In general, a more objective, standardized and possibly cheaper and faster methodology for collecting yield estimations is needed.

Over the last few years, attention has been given to the possibility of using remote sensing techniques and crop growth models as new tools for crop growth monitoring and yield prediction. The Council of the EC began, for example, in September 1988 a pilot project on the application of remote sensing for the improvement of agricultural statistics (Toselli and Meyer-Roux, 1990). Beside remote sensing, crop growth models were recognized as a promising tool for regional yield prediction.

Most deterministic crop growth models try to explain the growth and development of crops from an understanding of the physiological and physical processes involved (King, 1988). The complexity of these models ranges from very simple, consisting of only one equation (Monteith, 1981), to very complex, like the ones developed and described by van Keulen and Wolf (1986), Jones and

Kiniry (1986), van Keulen and Seligman (1987), and Spitters et al. (1989) for example. This last category of growth models generally computes the daily growth and development rate of the crop from meteorological parameters like solar radiation, maximum and minimum temperature, precipitation, relative humidity and wind speed.

Most deterministic growth models were developed as research tools to synthesize available knowledge on crop growth and development. Not so surprisingly, these crop growth models often appear to fail when applied to practical field conditions for the purpose of yield estimations (Kanemasu et al, 1984). Detailed field data necessary as input for the model, such as sowing date, empirical and physiological crop parameters and physical soil properties, are often lacking, and the effects of the possible occurrence of stress factors on yield formation are insufficiently known. Therefore, simulated crop growth in any regional environment will nearly always deviate from the crop growth that actually occurs.

For practical application of growth models, there is a need to update the model in the course of the growing season with information on the actual status of the crops. Such information can be obtained, in a non-destructive way, using remote sensing techniques.

1.2 Remote sensing

Remote sensing is basically the measurement of electromagnetic radiation that is reflected or emitted from the surface of the earth. Reflected electromagnetic waves may have been emitted by the sun (optical remote sensing) or by artificial sources (e.g. radar). An illustration of the electromagnetic spectrum and the regions used for remote sensing is given in Figure 1.1. An introduction to the fundamental physical aspects of electromagnetic radiation and its use for remote sensing is given by Schanda (1986).

Through repeated remote sensing observations of agricultural crops during the growing season, a so-called temporal signature of the crops is obtained. The problem is to translate this temporal signature of remote sensing signals, like reflected solar radiation or radar backscattering, into crop biomass and final yield. Direct relationships between remote sensing signals and yields of crops are generally too inaccurate to be used successfully in yield prediction systems. Relationships between remote sensing signals and 'secondary' crop variables like fraction soil cover or leaf area index (*LAI*) appear more reliable. Crop growth models are then needed to proceed from these variables to crop biomass and final yield figures.

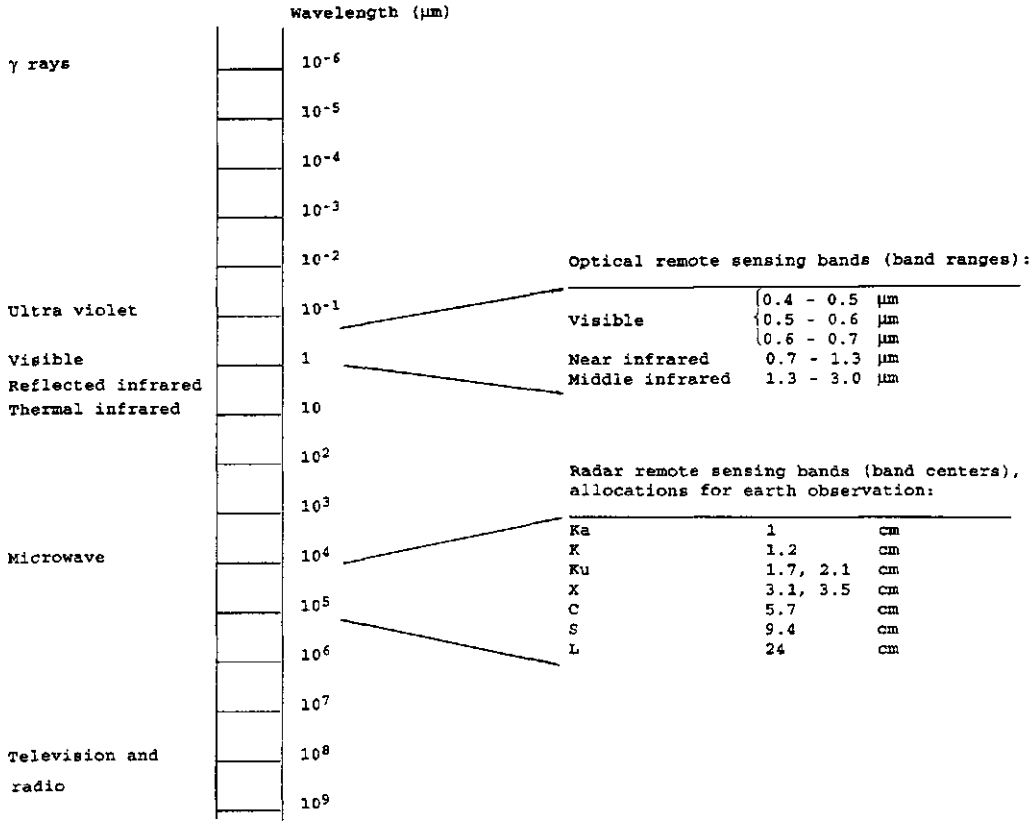

Figure 1.1. The electromagnetic spectrum (partly from Lillesand and Kiefer, 1974), with the regions used for optical and radar remote sensing. The radar band nomenclature and the wavelength assignment for remote sensing agree with the 1975 International Telecommunication Union assignment for frequency ranges (partly from Hoekman, 1990).

1.2.1 Optical remote sensing

The most widely used remote sensing technique so far is optical remote sensing: the measurement of the amount of reflected solar radiation from the earth's surface. Reflectance values are calculated by dividing the reflected amount of radiation by the incident radiation, or by the reflected amount of radiation from an ideal reflector (Suits, 1975). Reflectances are mainly measured in different optical spectrum wavelength bands, for instance in the blue (0.4-0.5 μm), green (0.5-0.6 μm) or red (0.6-0.7 μm) part of the visible region, or in parts of the near infrared (0.7-1.3 μm) and the middle-infrared (1.3-2.5/3.0 μm) spectrum. Because of the differences in the interaction of electromagnetic radiation of different wavelengths with vegetation, the various wavelength bands have different information contents (Bunnik, 1978). For in-depth studies of the physics of optical remote sensing, see Wendlandt and Hecht (1966), Lavin (1971) and Schanda (1986).

A number of operational satellite systems provide regular images of the earth in different wavelength bands in the optical region, e.g. METEOSAT, NIMBUS, NOAA, Landsat and SPOT (Buiten and Clevers, 1990). The availability of these data has stimulated scientists to study the reflectance properties of crops, and to use these data for crop growth monitoring (Wiegand et al., 1979; Tucker et al., 1979, 1980). However, a main drawback of optical systems in tropical and temperate climates is cloud occurrence. Since a frequency of observations is necessary for monitoring purposes, optical space-borne systems are less suitable in these regions. At a sub-regional level, air-borne systems may be used, and at farm and field level, portable reflectance meters.

The optical reflectance of crops is determined by the interaction of solar radiation with the crop canopy. From the late sixties, this interaction process has been extensively studied and modelled (Allen and Richardson, 1968; Allen at al., 1969; Suits 1972a; de Wit, 1965; Goudriaan 1977; Bunnik 1978; Verhoef, 1984; Den Dulk, 1989; Kuusk and Nilson, 1989). From these studies and numerous field observations (Suits, 1972b; Bunnik, 1978; Clevers, 1986; Nilson, 1988; Schellberg, 1990), the interaction of optical radiation with vegetation canopies is relatively well understood.

The spectral (i.e. as function of wavelength) optical reflectance of crops is a function of canopy factors, viewing and illumination conditions, and of the properties of the underlying soil. Canopy factors are the optical properties of elements like stems and leaves, and the amount and spatial distribution of these elements (canopy structure). Viewing conditions are the azimuth and incidence angle of the view direction of the sensor. Illumination conditions are the azimuth and incidence angle of the sun, and the fraction between diffuse and direct solar radiance. The reflectance properties of soil are mainly a function of mineralogical and organic composition, water content and the surface roughness.

When monitoring crop growth and development by means of optical remote sensing, a number of the above mentioned factors remain stable or can be standardized. For consecutive measurements, the sensor can be placed in a standard position with respect to the crop, and measurements can be performed at comparable solar elevation angles. Furthermore, some changes in factors during the growing season, that disturb relationships between reflectance and significant crop parameters (e.g. *LAI*), may be corrected through the calculation of so-called Vegetation Indices (*VI*'s). An example is the much-used Normalized Difference Vegetation Index *NDVI* (first described as *VI* by Rouse, 1973):

$$NDVI = (IR-R)/(IR+R)$$

where IR = infrared reflectance of crop, and R = red reflectance of crop.

A number of authors have successfully correlated spectral reflectances and *VI*'s to crop parameters like *LAI*, fraction soil cover, light interception or the chlorophyll content of different types of crops (Kumar and Monteith, 1981; Steven at al., 1983; Asrar et al., 1984; Wiegand at al., 1986; Birnie et al., 1987; Huete, 1988; Clevers, 1986, 1989; Schellberg, 1990). These crop parameters play an important role in crop growth and can be used in crop growth simulation models. However, there is no agreement yet on the most suitable *VI* for the estimation of specific crop parameters from optical remote sensing measurements.

1.2.2 Radar remote sensing

A radar system generally consists of a transmitter in which microwaves of the desired wavelength (usually between 1 and 30 cm) are generated, and an antenna for spatial distribution of the generated radiation. After reflection in a backward direction by an object on the earth's surface, the microwaves are received by the antenna and detected on the radar receiver (radar backscattering). The radar backscattering of an object is expressed by its radar cross-section, which may be defined as its microwave reflective power in the direction of the source.

Microwaves that are used in radar remote sensing are relatively unhindered by atmospheric conditions. Wavelengths longer than 3 cm are hardly affected by clouds or fog and wavelengths longer than 10 cm are very little attenuated by rain (Goodman, 1980). The used radar wavelengths for remote sensing and their nomenclature are given in Figure 1.1. Basic principles of radar and radar remote sensing are given by Ulaby, Moore and Fung (1981, 1982 and 1986).

Compared to optical systems, the use of radar in remote sensing is relatively new. Up to 1991 there had been one satellite mission, the Seasat in 1978: a mission which only lasted for about three months. Other space observations were

performed during the SIR-A and -B Space Shuttle missions in 1981 and 1984 respectively. Most radar images have been collected using air-borne systems. Compared to optical remote sensing, very little use has been made of ground-based systems.

In land applications, radar data have mostly been studied for the mapping and inventorization of impenetrable marshes and tropical forests with near-permanent cloud cover (Hoekman, 1990). Research into agricultural applications has focussed mainly on crop type classification (Batliva and Ulaby, 1975; van Kasteren, 1981; Hoogeboom, 1983; Wooding, 1988; Wegmüller, 1990), whereas the monitoring of crop growth has, so far, received little attention. Overviews of the achievements of radar remote sensing in agriculture are given by Cihlar (1984), Krul (1984) and Ulaby et al. (1986).

The radar backscattering from a crop depends on the properties of the incident microwaves, and on those of the canopy and the underlying soil. Properties of microwaves are wavelength, state of polarization and angle of incidence. In microwave scattering models, a crop canopy can be considered as a dielectric mixture of discrete inclusions (e.g. leaves and stems) distributed in a host material of air (Ulaby and Jedlicka, 1984). Fundamental models generally describe the scattering strength and the microwave attenuation through crop canopies from the dielectric constant, the volume fraction and the geometry of the various types of inclusions (Ulaby et al., 1982, 1986; Allen and Ulaby, 1984; Eom and Fung, 1984; Ulaby and Wilson, 1985; Lang et al, 1986; Karam and Fung, 1988). These models have not yet been validated for different crops and growing conditions. Moreover, some of the input parameters could not be successfully related to measurable physical properties of the crop.

Another class of (simple) physical models has been developed that treat the canopy as a collection of water droplets (Attema and Ulaby, 1978; Ulaby et al. 1982, 1984; Hoekman et al., 1982). The possibilities of crop parameter estimation with this type of models has to some extent been investigated (Ulaby et al., 1984; Prévot et al., 1988; de Loor, 1985, 1987), but a large-scale effort by the research community has been hindered by the lack of sufficient temporal radar data with supporting ground-truth.

Overall, information about the radar backscattering of crops is less wide-spread than that on the optical reflectance of crops. Attempts to use radar backscattering data for monitoring of crop growth have, so far, been very few.

1.3 Objective and scope of thesis

The research presented in this thesis focuses on two objectives. Firstly, the application possibilities of X-band radar backscattering in crop growth monitoring are studied. The second objective is the development of methodologies which link remote sensing data in general to crop growth models for monitoring crop biomass development. For this, optical remote sensing data are used in addition to radar data.

Radar remote sensing is applied because of its unique all-weather capability. A number of earth observation satellites that are scheduled in the coming decade will carry radar sensors (e.g. ERS-1, JERS-1, Radarsat, EOS). Optical remote sensing is used because of the proven relationships with canopy parameters, and because of the many optical remote sensing satellites that are operational.

The scale of research is the 'field' level. Ground-based radar and optical remote sensing data collected from the agricultural fields of experimental stations and private farmers are used. The field level has the advantage that, on agricultural stations, growth and management conditions can be manipulated to study the effects on remote sensing signals. Also, on field level, detailed ground-truth can be collected on the near-exact location of the remote sensing measurement. Finally, the field level agrees with the scale on which most crop growth models have been developed.

Organisation of thesis

Chapter 2 introduces the experiments on the X-band radar backscattering of crops. The radar backscattering of sugar beet and potato is described in relation to crop growth and development. The backscattering is studied in vertical and horizontal like-polarization, VV and HH respectively, and at incidence angles from 10°-80°.

In Chapter 3, the backscattering of wheat, barley and oats is investigated. Special emphasis is placed on the influence of canopy structure on the backscattering. From the analyses in both Chapters 2 and 3, conclusions are drawn with regard to the application possibilities of X-band radar remote sensing in agriculture.

In Chapter 4, the possibilities of estimating crop parameters from X-band radar backscattering data are investigated using empirical and simple physical relationships. The crops investigated are sugar beet, potato, wheat and barley. The investigated crop parameters are dry canopy biomass, fraction soil cover, crop height and canopy plant water. The empirical and physical relationships use multi-temporal and muti-angle backscattering data in both VV and HH polarization.

In Chapter 5, X-band radar backscattering data are applied in a simple growth model for sugar beet. Using the 'Cloud' equations (Attema and Ulaby, 1978), a so-called 'microwave soil cover' is estimated from the radar backscattering at a high and a low angle of incidence. This microwave soil cover is related to the optical soil cover and used in a light-interception growth model. This model calculates the rate of growth from the product of the amount of intercepted solar radiation and a light use efficiency factor. The intercepted solar radiation is computed from daily measured values of total incoming solar radiation and the estimated soil cover of the crop.

Chapter 6 introduces optical remote sensing with an analysis of the estimation accuracy of *LAI* from different spectral Vegetation Indices. A physical interaction model (EXTRAD; Goudriaan, 1977) is used to simulate the effects of so-called 'disturbing factors', such as canopy structure, illumination condition and soil moisture, on the *VI-LAI* relationships. The effects of the disturbing factors on the accuracy of *LAI* estimation are quantified along the *LAI* trajectory. From this quantification, the most suitable *VI* for the estimation of *LAI* is derived. The simulation experiment is supported by field measurements of sugar beet crops.

In Chapter 7, a methodology for linking physical remote sensing models with physiological crop growth models is presented that allows for the use of multi-sensor information. A crop growth model (SUCROS; Spitters et al., 1989) is extended with the 'Cloud' equations and the EXTRAD model to calculate the X-band radar backscattering and the optical reflectance of the simulated crop. The simulated time series of remote sensing signals is compared to a measured time series of remote sensing signals. From this comparison, the combined SUCROS-Cloud-EXTRAD model is re-initialized and re-parameterized to fit the simulated remote sensing signals to the measured remote sensing signals. The methodology is applied on 11 fields of sugar beet, using both radar and optical remote sensing data. The simulated canopy biomass is compared with values measured in the field, before and after the re-initialization and re-parameterization of SUCROS.

Chapter 8 presents the main conclusions and discussions on the usability of X-band radar for crop growth monitoring, and on the methodologies developed for linking remote sensing data with crop growth models.

2 GROUND-BASED X-BAND (3-CM WAVES) RADAR BACKSCATTERING OF AGRICULTURAL CROPS. I: SUGAR BEET AND POTATO; BACKSCATTERING AND CROP GROWTH

Abstract Six years of ground-based radar observations were used to study backscattering influencing factors of agricultural crops. The X-band, 3 cm wavelength, radar backscattering of sugar beet and potato was studied at vertical and horizontal like-polarization and at several angles of incidence. For both crops the backscattering increased with crop growth until a saturation level was reached at about 80% soil cover. The average radar backscattering of a closed sugar beet canopy varied between -2 and 0 dB at all angles of incidence. The average backscattering of potato ranged from -2 to 0 dB at 20° incidence angle, to -7 to -5 dB at 70° incidence angle.

The geometry of the crop-soil system was an important backscattering influencing factor. In potato, the orientation of the ridges with respect to the incident radar beam dominated the backscattering in the early growing season. The architecture of individual beet plants, and their distribution in space affected the radar backscatter of sugar beet. For both beet and potato, changes in the canopy architecture due to strong winds affected the radar backscattering by 1-2 dB.

2.1 Introduction

In recent years the usefulness of remote sensing in agriculture is increasingly recognized. Applications vary from large scale crop inventory and disease detection to the monitoring of growth and development. The availability of satellite data from the Landsat, NOAA and SPOT satellites has stimulated research and applications in the optical region. For arid and semi-arid areas, these satellites deliver useful data on a regular basis. In many regions with a tropical or temperate climate, however, cloud cover frequently hampers remote sensing of the land surface. In The Netherlands the average number of cloud free imagery of a sector of 40x50 km, using the Landsat satellite is only four to six times a year (van der Laan, 1989). Therefore the attention of researchers is shifting to a remote sensing technique which is relatively unhindered by atmospheric conditions. Microwaves have the capability of penetrating clouds and fog and are therefore in principle suitable for remote sensing. Knowledge of the behaviour of microwave backscattering of agricultural crops is, however, still scarce while the lack of a remote sensing satellite with radar has hindered general investigations. This has prompted scientists in Europe to participate in communal airborne radar campaigns

such as Agrisar 1986 (Fiumara, 1988) and Agriscatt 1987-1988 (Attema, 1988). Such campaigns deliver a wealth of data under actual field conditions. However, because airborne campaigns are quite expensive, the number of observations is often limited to no more than four to seven in a growing season. This may be a handicap when the object of study is the monitoring of crop growth. Another drawback is that ground conditions can not be manipulated to investigate the effects of specific surface parameters. Therefore, airborne observations - giving area coverage at specific moments in time - have to be supported by ground-based measurements - which give continuity in time - in well conditioned environments like agricultural test farms.

In this series of two papers, the relationship between ground-based, X-band (3 cm-waves) radar backscattering of agricultural crops and agronomic (e.g. crop type, crop growth, management practices) and environmental factors (e.g. weather influences) is investigated. The objective is to assess main backscattering influencing factors of crops. Where possible, the effects of these factors on the radar backscattering are quantified. At the end, the potential role of X-band radar in agricultural application is discussed.

The present paper, part I of the series, presents an overview of the measurement methodology and deals with the relatively broad-leaved crops sugar beet and potato. The relationship between the radar backscattering and crop growth is investigated. With two special experiments, the importance of the geometry of the crop-soil system will be demonstrated. The consecutive paper, part II, discusses the backscattering of wheat, barley and oats with special emphasis on the influence of canopy structure. The canopies of these small-grain cereals consist of long, narrow leaves and stalks. The differences in general canopy architecture of sugar beet and potato on the one hand, and wheat, barley and oats on the other, caused specific differences in backscattering from these two crop groups.

2.2 Measurement methodology

The data used for this study were collected by the Dutch team ROVE (Radar Observation on Vegetation) during 1975-1981. The team consisted of:

- The Centre for Agrobiological Research (CABO), Wageningen
- The Microwave Department of the Delft University of Technology
- The Physics and Electronics Laboratory TNO, The Hague
- The National Aerospace Laboratory (NLR), Amsterdam
- The Department of Soils and Fertilizers of the Agricultural University, Wageningen

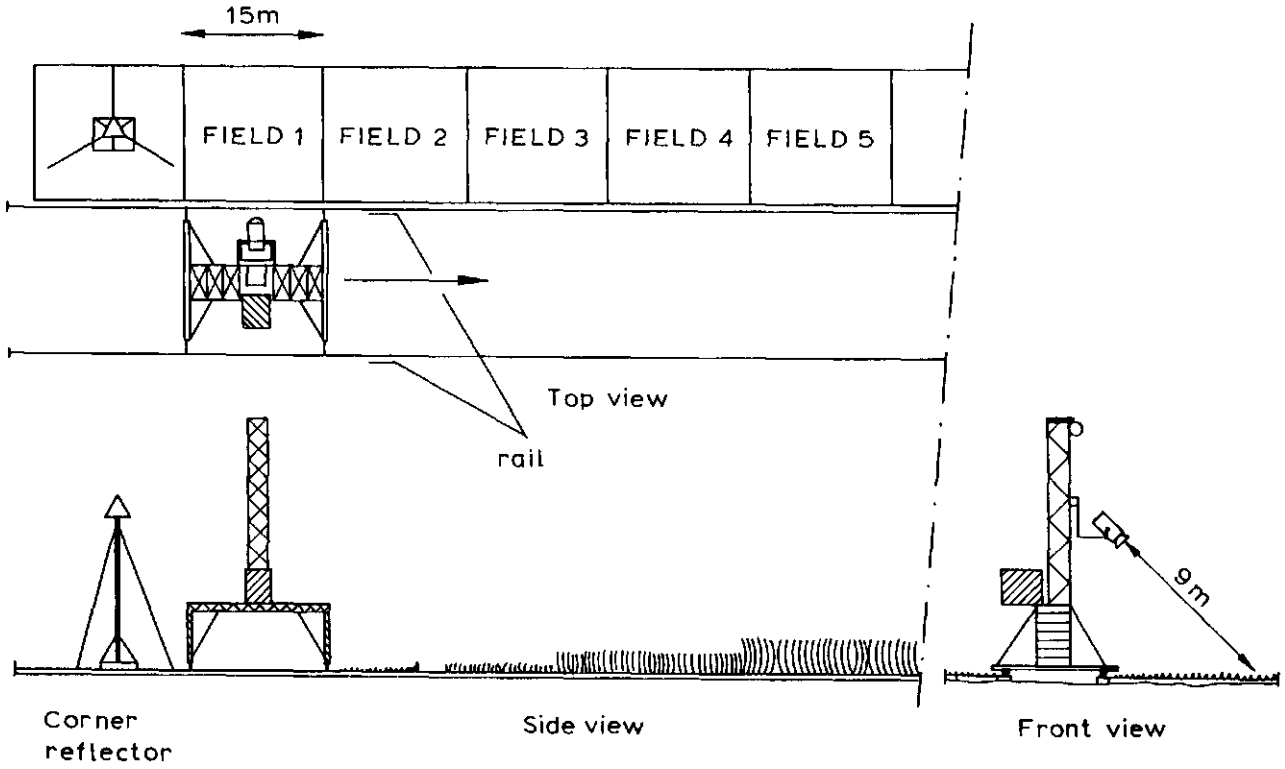

Figure 2.1. Illustration of the ground-based X-band radar system as deployed at test farm Droevendaal in Wageningen. Source: de Loor et al., 1982.

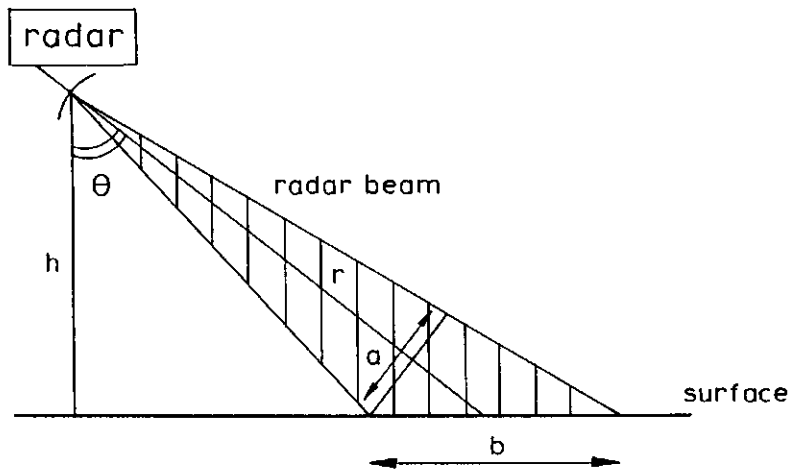

Figure 2.2. Schematic representation of the illumination geometry of the radar beam. The symbols in the figure have the following meaning: θ = angle of incidence; h = height of the radar; r = axis of the radar beam; a = projected area of the cross-section of the radar beam; b = area illuminated by the radar beam.

The X-band radar backscattering was measured with a FM-CW scatterometer mounted on a trailer. This trailer could be moved along the test field to measure the different plots at angles of incidence from 10° to 80° (Fig. 2.1). The distance of the scatterometer to the target could remain 10 m along the axis of the beam, at all angles of incidence. The antenna beam width was 4° (at the half power or 3 dB points), so the cross section of the antenna beam at the place of the target was 0.6 m^2. The central frequency of the scatterometer was 9.5 GHz (corresponding to a wavelength of about 3 cm) with a frequency sweep of about 0.4 GHz. Measurements could be made at different combinations of polarization VV, HH, HV and VH. In these abbreviations, the first letter stands for the polarization of transmitting, the second for the polarization of reception of the microwaves. 'V' denotes the vertical state and 'H' denotes the horizontal state.

The radar was calibrated by directing the radar beam to a corner reflector of known radar cross-section. This calibration was done for each state of polarization at the beginning and end of each measurement day. More information on the

calibration procedure is given by van Kasteren and Smit (1977) and by de Loor et al. (1982).

The radar backscattering was expressed as γ: the radar cross-section of the target per unit projected area of the cross-section of the radar beam (m^2/m^2). The relationship between γ and σ° (the Normalised Radar Cross Section NRCS, which is the radar cross-section per unit area illuminated by the antenna) is:

$$\gamma = \sigma^\circ/\cos\theta \qquad (1)$$

where θ is the angle of incidence, defined as the angle between the incident radar beam and the vertical (Fig. 2.2). In the text, a low angle of incidence refers to angles of 10°-30°, a medium angle to 40°-60° and a high angle to 60°-80°. Furthermore, as a standard, γ is expressed in dB:

$$\gamma\,(dB) = 10*\log10(\gamma\,(m^2/m^2)) \qquad (2)$$

The total measurement accuracy (as determined by the inaccuracies in the scatterometer, in the calibration procedure, in the data processing, and due to averaging over independent samples in a plot) was about 0.5 dB. The radar measurements were repeated during the growing season with intervals of about two to five days. This resulted in the following number of observations (per incidence angle and per state of polarization) per year: 27 in 1975, 24 in 1976, 32 in 1977, 36 in 1979, 39 in 1980 and 19 in 1981.

The experiments were done at three different test farms in The Netherlands: "Droevendaal" at Wageningen (1975-1977), "De Bouwing" at Randwijk (1978-1979) and "De Schreef" near Dronten (1980-1981). These farms are located in different environments on sandy soil, alluvial clay and marine clay respectively. All crops were given the best treatment for a healthy growth and development (with regard to fertilizer, weed control, pesticides, etc.). However, since no irrigation was possible, a natural water shortage caused in a limited number of occasions an under-developed or failing crop.

Together with the radar measurements, visual observations were made of the soil surface and of the crop morphology, phenological stage, and any anomalies like weeds or diseases. Quantitative measurements were made of the volumetric soil moisture content of five cm top soil, fresh and dry weight of the above ground biomass, crop height, soil cover, row spacing, number of stems/m^2 and for some crops the dimensions and number of leaves per plant. The measurements on biomass were done only a few times in the growing season. A fitted growth function was used to interpolate between the measurements to all dates of radar observations. Overviews of the experiments are given by van Kasteren (1981), de Loor (1982, 1985), Bouman (1987) and Bouman and van Kasteren (1989).

2.3 Crop description

The description of the crops applies to those in the ROVE data set and concerns the variety Monohil for sugar beet and Bintje for potato. Although in general it will apply to crops grown under various growing conditions, deviations may occur in, for instance the size of the canopy elements or the yield.

The canopy of *Sugar beet* is characterized by a relatively uniform architecture during its growth cycle. The leaves are placed in rosettes on the root and have approximately a plagiophile or uniform angle distribution during the whole growing period (de Wit, 1965). Depending on variety and growth conditions, the dimensions of the leaves varied from some 5 x 10 cm in the first month after emergence to some 25 x 35 cm in the late growing season. Thus, the leaves were relatively large in comparison with the 3-cm wavelength of X-band microwaves.

After about two months of growth, a healthy crop covered the soil completely and nearly no bare soil was visible. Under average, non-stressed growing conditions the above ground biomass attained seven to eight ton of dry matter/ha. The average plant water content was 93% throughout the growing season.

Potato was cultivated on ridges of some 25 cm height and 50-75 cm apart. Potato leaves were made up by small leaflets with an average size of about 4 x 8 cm for fully grown plants. This size was of the same order as the wavelength of X-band microwaves. Potato leaflets have a planophile angle distribution (de Wit, 1965), which means that horizontal leaves are most frequent.

A healthy potato crop covered the soil surface almost completely after six weeks from emergence. In the midst of the growing season a period of flowering occurred. The flowers were small (about 2 cm in diameter) and stood in the top of the canopy. At the end of the growing season, sometimes individual plants would lodge and spots of bare soil appeared in the canopy. Leaves clustered together on the ground and the stems became visible.

The above ground biomass attained some three ton of dry matter/ha, which is considerably less than that of sugar beet. The average plant water content was 90-95% throughout the growing season.

Examples of the growth of the above ground canopy of sugar beet and potato in 1975, 1979 and 1980 are given in Figure 2.3. The potato of 1975 is not included because this crop had a ridge direction perpendicular to the incident radar beam, where the other crops had a ridge direction parallel to the beam (see § 2.5). For sugar beet, the growth in 1979 and 1980 was comparable with a somewhat earlier start in 1980. The crop in 1975 had a much faster start but the maximum biomass was already reached at two months after emergence.

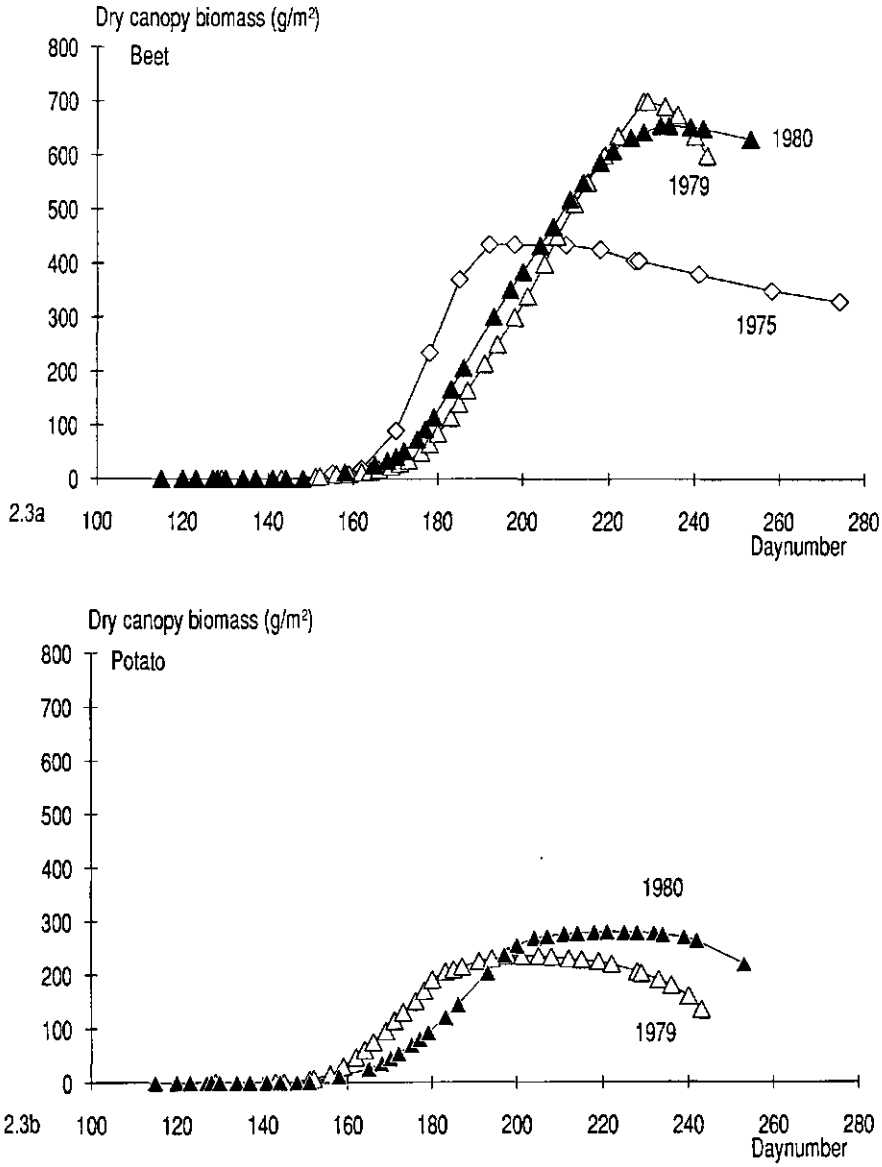

Figure 2.3. Examples of the development of the above ground canopy biomass in the course of the growing season for sugar beet (2.3a) in 1975 (◊), 1979 (Δ) and 1980 (◆), and for potato (2.3b) in 1979 and 1980.

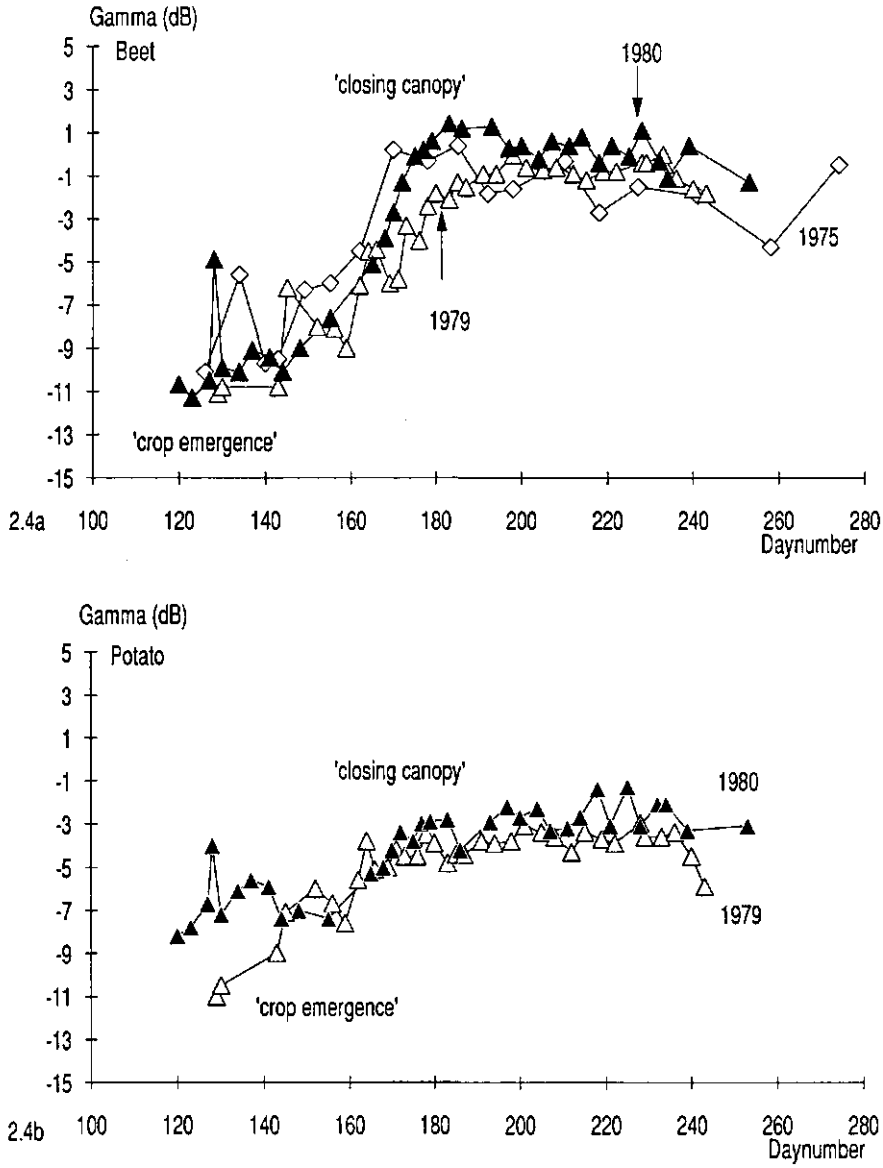

Figure 2.4. Vertical (VV) polarized X-band radar backscattering at 40° incidence angle in the course of the growing season for the same crops as in Figure 2.3.

Because of drought, the final weight of the above ground biomass was about twice as low as in the other two years. Contrary to sugar beet, potato in 1979 had a much faster start than in 1980. After about two months from emergence, no more growth in canopy biomass took place. All newly assimilated matter was transported to the tubers. At the end of the growing season, canopy biomass declined due to dying and loss of leaves.

2.4 Detailed radar backscattering in time

2.4.1 Backscattering and crop growth

The VV radar backscattering at a medium angle of incidence is plotted against time in Figure 2.4 for the same crops as in Figure 2.3.

For *sugar beet*, a 'radar-growth' curve is recognized in the temporal radar backscattering. Until day 150, no vegetation was present and the peaks in the backscattering curve coincided with peaks in the moisture content of the top soil. After day 150, the beets started to grow (Fig. 2.3) and the radar backscattering increased. The relative early growth of the crop in 1975, and the relative late growth of the crop in 1980 corresponded with a similar pattern in the backscattering curves until day 180-190. Around day 180-190, the radar backscattering saturated for all three crops relatively early in the growing season with biomass values of only two to three ton/ha. Because of this early saturation of the backscattering, the spectacular difference in biomass between 1975, and 1979 and 1980 (Fig. 2.3) was unnoticed. The radar backscattering remained on a more or less stable level for the rest of the growing season until harvest. The differences in the level of saturation, some 3 dB between the crops of 1975 and 1979, could not be explained by ground-truth observations.

The temporal curves of the radar backscattering of *potato* were less pronounced. Before emergence, day 140, there was a difference of about 4 dB between the bare soil (relatively smooth and weed-free) of 1979 and of 1980. With the growth of the crops after day 150, the backscattering increased until day 180-190. The earlier growth of the crop between day 160 and day 190 in 1979 is not recognized in the backscattering curves. From day 180, the backscattering appeared saturated for both crops after biomass values of one to two tons/ha. The flowering in the midst of the growing season and the lodging at the end, are not recognized as distinct features in the backscattering curves.

2.4.2 Fluctuations in the backscattering curves

Both the backscattering curves of sugar beet and potato had a large number of small fluctuations (peaks and dips) in the order of 1 to 2 dB (Fig. 2.4). These fluctuations were no measurement errors or inaccuracies. Firstly, a peak or dip in the curve of a specific crop on a certain day was repeated in several measurement series on that day. Secondly, most peaks and dips were not the same for different crop types, but were clearly related to specific crops. Therefore, the causes for these fluctuations must be looked for in the crops themselves.

Before emergence and in the early stages of growth, peaks and dips were explained by similar features in the moisture content of the top soil. The relationship between the radar backscattering and the moisture content of a soil surface is generally recognized (Attema and Ulaby, 1978; Waite, et al., 1984). With the saturation of the backscattering, the influence of the soil background was reduced. The fluctuations were then caused by other factors, namely the changes in the geometry of the canopy induced by the weather. Strong winds can enforce preference in orientation of the canopy elements. Little variation in wind in 1979 was generally reflected in relatively small fluctuations in the temporal curves. Large variations in wind speed and direction in 1980 produced relatively more and larger fluctuations. For potato, wind directed towards the radar often coincided with a relatively high backscattering value. Wind directed away from the radar often coincided with a relatively low backscattering value. The opposite effect was observed for sugar beet: high backscattering values often coincided with wind directed away from the radar and low backscattering values often coincided with wind directed towards the radar. This effect of wind direction occurred only when the wind speed exceeded 5 m/s, and it was stronger for sugar beet than for potato.

The canopy structure is not only affected by wind but also by other environmental conditions. Rain may cause drooping of leaves while prolonged drought may cause wilting in sugar beet. Moreover, the condition of the crop itself plays an important role in determining resistance to changes in the canopy's geometry. Because of these complex relationships between canopy structure on the one hand and crop condition and weather on the other, the relation between weather and radar backscattering could not be further elaborated.

2.4.3 Polarization and incidence angle

For both sugar beet and potato, the backscattering was nearly identical at VV and at HH polarization. The general shape of the temporal curves, the absolute level and the many small fluctuations at the different angles of incidence were faithfully reproduced at both states of polarization (Bouman, 1987). The coefficient of correlation (between VV and HH) was 0.98 for sugar beet and 0.94-0.97 for potato at the different angles of incidence. The data for the correlation calculations

were taken for the crops in Figure 2.4 from sowing to harvest and numbered 66 for beet and 57 for potato, at each angle of incidence.

The coefficients of correlation between the VV radar backscattering at different angles of incidence are given in Table 2.1. The radar backscattering of sugar beet was highly correlated between the different angles of incidence. The correlations were only slightly lower between the backscattering at 20° and at 50° to 70°.

Table 2.1. Correlation matrix for the VV radar backscattering at different angles of incidence for sugar beet and potato, using data from sowing to harvest.

SUGAR BEET (number of data = 6 x 75)						
20°	1.00					
30°	0.97	1.00				
40°	0.95	0.99	1.00			
50°	0.94	0.98	0.99	1.00		
60°	0.93	0.97	0.99	0.99	1.00	
70°	0.90	0.96	0.98	0.98	0.99	1.00
	20°	30°	40°	50°	60°	70°
POTATO (number of data = 6 x 64)						
20°	1.00					
30°	0.97	1.00				
40°	0.94	0.98	1.00			
50°	0.89	0.95	0.98	1.00		
60°	0.83	0.90	0.94	0.98	1.00	
70°	0.77	0.85	0.89	0.95	0.98	1.00
	20°	30°	40°	50°	60°	70°

The radar backscattering of potato was correlated between most angles of incidence. However, the coefficients of correlation decreased faster with increasing difference between the angles of incidence than for beet. The coefficient of correlation between 20° and 70° had dropped to 0.77 where it still was 0.90 for sugar beet. These lower correlations were caused by the fluctuations in the temporal curves of the radar backscattering. For sugar beet, most peaks and dips

coincided at all angles of incidence. For potato, peaks at low angles of incidence sometimes coincided with dips at high angles, and vice versa. This resulted in lower correlations between these incidence angles.

The shape of the temporal backscattering curves of sugar beet and potato at different angles of incidence is discussed in the next paragraph.

2.5 Average temporal trends

The many small fluctuations in the temporal backscattering curves hinder the derivation of general trends. Moreover, the time scale of the temporal curves should be normalized to compare the different years on a similar basis. Normalizing is generally done by plotting the data on a development scale. The steps in a development scale are related to characteristic morphological and physiological phenomena that occur during the development of the crop. For instance the four-grammes sugar weight of the root is a characteristic point of sugar beet. However, radar data of sugar beet and potato plotted on these conventional scales were not consistent. The radar backscattering of crops reacted on the above-ground crop canopy and did not respond to phenomena that occurred in roots and tubers below-ground. Also some above-ground phenomena like flowering in potato were not noticed by the radar. Therefore a special 'radar-growth' scale was constructed to accommodate characteristics of the crop that put the radar data on a consistent basis (Table 2.2).

Table 2.2. Proposed 'radar-growth' scale to put the temporal X-band radar backscattering data of sugar beet and potato in various years on a consistent basis.

Stage	Crop	Description
R0	beet, potato	seed-bed
R1	beet, potato	soil cover 0-10 %
R2	beet, potato	soil cover 11-20 %
R3	beet, potato	soil cover 21-50 %
R4	beet, potato	soil cover 51-80 %; biomass < 200 g/m^2
R5	beet, potato	soil cover > 80 %; biomass 200-500 g/m^2
R6	beet	biomass > 500 g/m^2
R7	potato	yellowing in bottom of canopy
R8	potato	yellowing in top of canopy
R9	potato	leaf-deformation, patches of lodged crop

The first four stages of the radar-growth scale were related to soil cover. After 80% cover, a further differentiation was based on biomass. For potato, the stages were further extended to include loss of leaves and the lodging at the end of the growing season. The steps in the scale were necessarily large to smooth the fluctuations in the temporal backscattering curves and to get reliable average values per stage.

The radar measurements on a crop falling within a growth stage were averaged for 20°, 40° and 70° incidence angle and plotted on the radar-growth scale (Fig. 2.5). The standard deviation was about 0.8 dB for most averages. For stage R0 and R1 of potato, the standard deviation was about 1.5 dB. The averages for sugar beet were derived from five plots with non-stressed growth and development and those for potato from three. All plots had a row or ridge direction parallel to that of the incident radar beam. For beet, a total number of about 104 data was used per incidence angle, and for potato some 95.

The backscattering of *beet* increased after emergence until it saturated at about 80% soil cover in stage R5. At all angles of incidence, the temporal curves converged to a common level of saturation. This common level may be explained by the uniform leaf angle distribution of the crop: the canopy reflects the microwaves in backward direction equally well at all incidence angles. After stage R5, the backscattering remained at the same level at all angles of incidence until harvest. The average range in radar backscattering from crop emergence to full crop cover was about 3 dB at 20°, 7 dB at 40° and 10 dB at 70° incidence angle.

The backscattering of *potato* increased after crop emergence until 80% soil cover in stage R5. During these stages, the backscattering curves ran completely parallel at all angles of incidence. This reflects the planophile leaf angle distribution of the crop: the microwaves are more reflected in backward direction at a low angle of incidence than at a high angle of incidence. After stage R5, the backscattering at 70° incidence angle further increased some 1.5 dB until the end of the growing season. The backscattering at 40° incidence angle remained the same, where that at 20° decreased 2 dB with the yellowing and lodging of the crop. In a low incidence angle, patches of bare soil were 'visible' which might be the cause of this small decrease in the radar backscattering.

The average range in radar backscattering from crop emergence to full crop cover was about 4.5 dB at all angles of incidence.

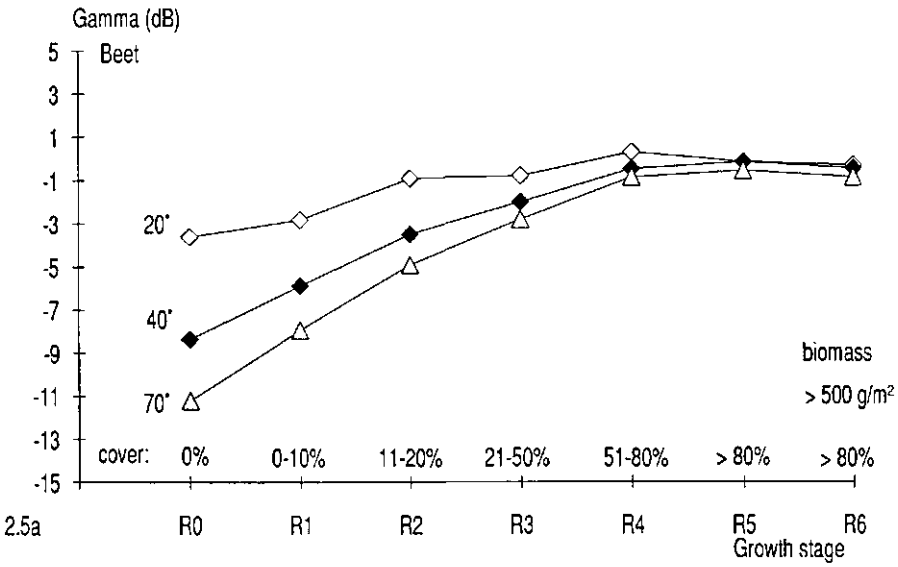

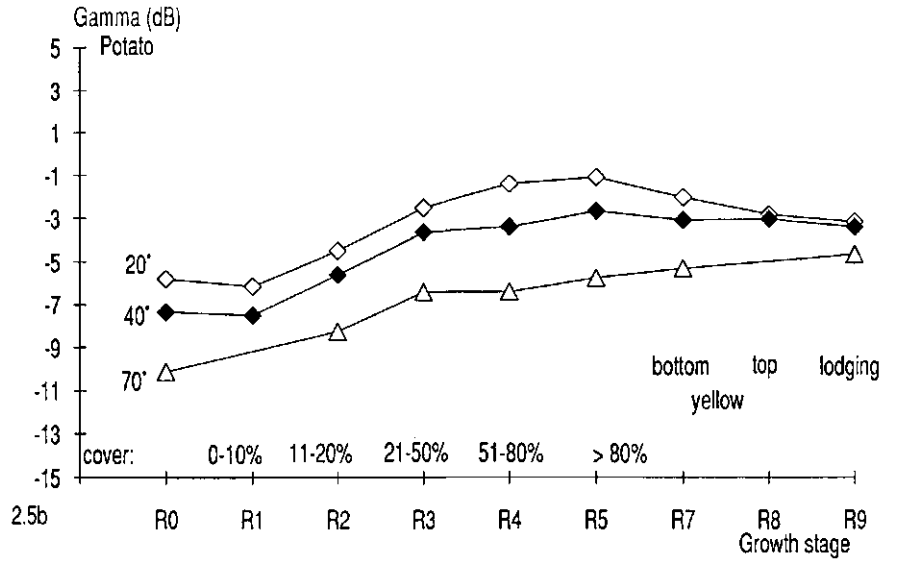

Figure 2.5. Average VV radar backscattering of five sugar beet crops (2.5a) and three potato crops (2.5b) at 20° (◊), 40° (◆) and 70° (Δ) degrees incidence angle versus introduced 'radar-growth' stage.

2.6 Special experiments

In 1981 two experiments were held to investigate the relationships between the architecture of the crop-soil system and the radar backscattering. The first concerned the effect of ridge direction in potato, and the second the effect of plant thinning in sugar beet.

2.6.1 Ridge orientation in potato

In 1981 the effect of the orientation of ridges on the radar backscattering of potato was investigated using two plots with different ridge orientations. The plot with the ridges parallel to the incident radar beam was labelled 'parallel plot', and the plot with the ridges perpendicular to the beam 'across plot'. On the parallel plot, the ridges had an East-West direction, and on the across plot a North-South direction. The effect of ridge orientation depended on the angle of incidence and on the stage of development of the crop (Fig. 2.6).

At 10° incidence angle, the radar backscattering of the parallel plot increased with the growth of the crop until some 80% crop cover on day 160 (Fig. 2.6a). For the across plot this familiar 'radar-growth' curve was absent. When the soil was still bare, the microwaves were especially scattered in backward direction from the sides of the ridges. This resulted in a relatively high radar backscattering. The difference in backscattering between the two bare plots averaged some 6 dB. After day 170, the crop covered the soil for 90% and formed a homogeneous layer over the ridges. The microwaves did not penetrate the canopy and there was no influence of the soil background. The level of radar backscattering of the two plots was now the same.

With *increasing incidence angle* the radar beam became more perpendicular to the slope angle of the ridges on the across plot. The backscattering from the 'across' ridges increased and the difference between the plots became larger. When the radar beam was most perpendicular to the slope angle of the ridges, at 30°, the backscattering from the bare soil of the across plot was highest (Fig. 2.6b). The difference in backscattering between the two plots amounted to 13 dB. The familiar 'radar-growth' curve of the across plot was now reversed: after a small initial increase, the backscattering decreased with the growth of the crop until 95% soil cover on day 180. Again, with full cover, the differences between the two plots vanished.

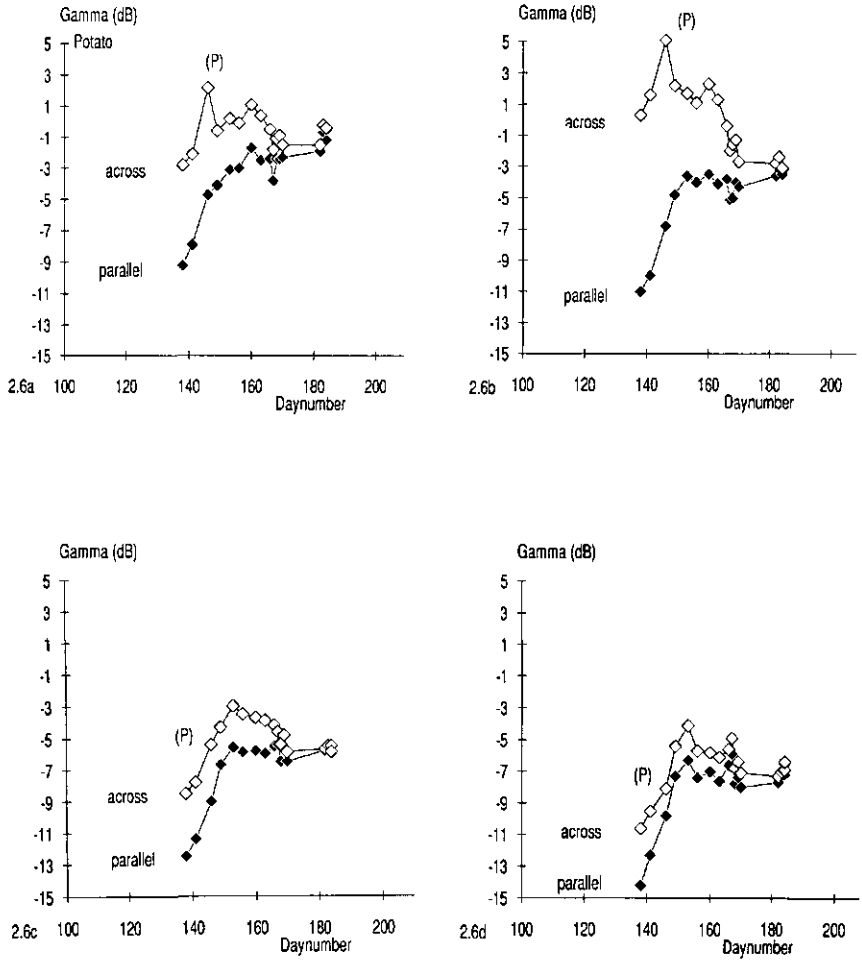

Figure 2.6. VV radar backscattering at 10° (2.6a), 30° (2.6b), 50° (2.6c) and 70° (2.6d) incidence angle versus time; potato 1981 with a row direction parallel to that of the incident radar beam (◆), and with a row direction across (◊). The (P) indicates a peak in the radar backscattering caused by a high moisture content of the top soil between the ridges of the across plot.

With *still further increasing incidence angle*, the backscattering from the ridges on the across plot decreased again, and the difference between the two plots became smaller (some 4 dB at 50°). At 50° incidence, the backscattering of the across plot first increased with the growth of the crop, and then decreased again from 60% to 90% soil cover (Fig. 2.6c). This pattern, which was also to some extent present at the other angles of incidence, illustrates the complex relationship between the radar backscattering and the changing architecture of the crop-soil system. At 70° incidence, the field of view of the radar beam was dominated by the flat top of the ridges for both plots. The effect of ridge orientation was minimized and the difference in backscattering was reduced to some 2-3 dB (Fig. 2.6d).

The effect of ridge orientation was also notable in the peak in the radar backscattering curves of the across row plot on day 146. This peak is marked with (P) in Figure 2.6. That day, the bottom between the ridges on the across plot was still wet from previous rain. The North-South direction of the ridges had prevented the rising sun in the East to dry the soil between the ridges. The high soil moisture content caused a peak in the temporal backscattering curve. This peak only appeared at low incidence angles that permitted the wet soil between the dry ridges to be 'seen' by the radar. On the parallel plot, the sun had dried the soil between the ridges and there was no peak in the temporal backscattering curves.

2.6.2 Plant thinning in sugar beet

In the midst of the growing season of 1981, beets were thinned from 100% soil cover to 50%, 25%, 12.5% and 6% cover in an attempt to quantify the effect of plant reduction (Fig. 2.7). In this figure, the backscattering of a neighbouring smooth, weed-free bare soil is also plotted as a reference field with 0% cover. Between each thinning, the soil was raked to get a smooth surface. The canopy biomass before thinning was about 4.5 ton/ha.

At all angles of incidence, the reduction in plant number was only notable after thinning to less than 25%. The decrease in radar backscattering from 100% to 25% beet cover was only about 0.5 dB at low angles of incidence to 1 dB at medium and high angles. Thus only a quarter of the surface covered with fully grown sugar beet (above ground) still dominated the radar backscattering of the whole plot!

With a further reduction in plant number to 12.5% and 6% soil cover the shape of the angular curve changed from horizontal to concave. Between low and medium angles of incidence, the curve resembled more and more that of the neighbouring bare soil: the backscattering decreased with increasing incidence angle. The largest decrease in backscattering with thinning was at the medium angles of incidence, respectively about 3 dB and 5 dB from 25% to 12.5% and 6% cover.

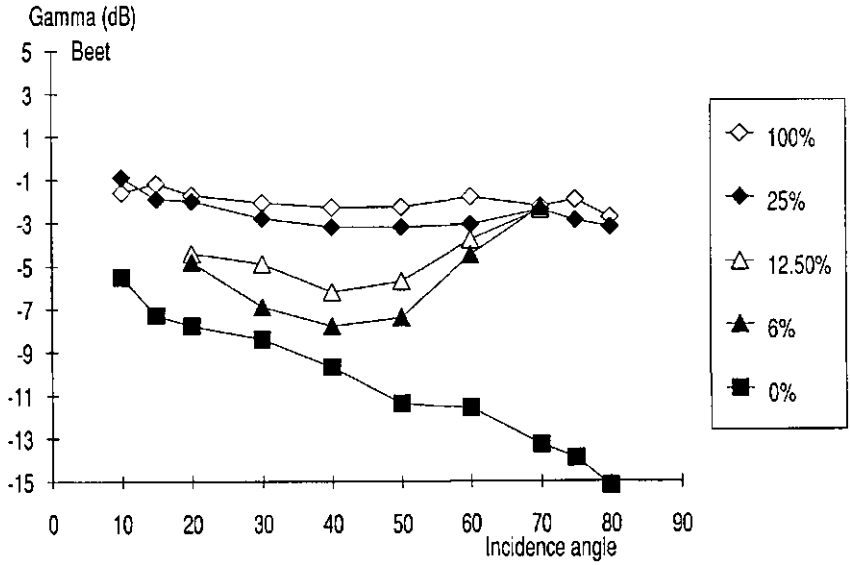

Figure 2.7. VV radar backscattering of sugar beet in the midst of the growing season of 1981 versus angle of incidence. Beet plants were thinned from 100% (◊) to 25% (◆), 12.5% (Δ) and 6% (▲) soil cover. The backscattering of a neighbouring bare soil is plotted for comparison [0% soil cover (■), weed-free, smooth surface).

At high angles of incidence the field of view of the radar beam was still dominated by the 6% sugar beet plants and the backscattering hardly decreased. Also, a corner effect between the soil surface and the sides of the plants may have added to the high backscattering. At 70°, there was no decrease in backscattering at all from 100% to 6% soil cover!

The observed reaction of the radar backscattering on the thinning of plants does not agree with the relations found between backscattering and soil cover in the early growing season. Generally, the radar backscattering increased with soil cover until it saturated at a cover of about 80% at high incidence angles and of 70%-80% at medium to low incidence angles. In terms of biomass the 'saturation values' were about two and three ton/ha respectively. However, when the sugar beet field was thinned in the midst of the growing season, the backscattering only started to decrease after less than 25% crop cover and about one ton/ha canopy biomass. This suggests that the architecture of the canopy and of the individual plants largely affects the radar backscattering. A same cover or amount of canopy

biomass made up by small, developing plants, or by large, fully grown plants has a different level of (X-band) radar backscattering.

2.7 Discussion

An important (X-band) backscattering influencing factor of sugar beet and potato was the geometry of the crop-soil system. The thinning experiment in beet suggested that the architecture of individual beet plants, and their distribution in space dominated the radar backscattering of the crop. The increase in radar backscattering with crop growth of beet may then be associated with architectural changes in the plants from small saplings to fully grown plants with large and broad leaves. In potato, the direction of the ridges with respect to the incident microwaves dominated the radar backscattering from bare soil to an 80% crop cover. For both beet and potato, changes in the canopy architecture due to strong winds affected the radar backscattering by 1-2 dB.

The importance of the geometry of the crop-soil system affects the potential applications of X-band radar in agriculture. The different backscattering levels at medium to high angles of incidence of sugar beet and potato will result in a high probability of discrimination between these two crop types. The differences in angular behaviour of the crops can be exploited by using more than one incidence angle. The best single angle of observation for discrimination appears to be a high one. At 70° incidence angle, possible disturbing effects on the radar backscattering like ridge orientation in potato and canopy architecture of sugar beet are minimal.

The possibilities of X-band radar for the monitoring of crop growth are different for sugar beet and for potato. For sugar beet, the possibilities seem good for monitoring early growth until a soil cover of about 80% and biomass values of two to three ton/ha. At full crop cover the radar backscattering no longer reacted on any further increase in biomass (Figs. 3a and 4a). Also, the thinning experiment showed that any decrease in biomass and/or soil cover in the midst of the growing season (such as may be caused by pests or diseases) will most likely not be detected.

The monitoring of the growth of potato will be more troublesome than that of sugar beet because of the large effect of ridge orientation in the early growing season. Thus, it is necessary that this direction be either known from other sources of information, or be derived from the measurements themselves.

3 GROUND-BASED X-BAND (3-CM WAVES) RADAR BACKSCATTERING OF AGRICULTURAL CROPS. II: WHEAT, BARLEY AND OATS; THE IMPACT OF CANOPY STRUCTURE

Abstract The ground-based, X-band radar backscattering of wheat, barley and oats was investigated through the growing season at VV and HH polarization, and at incidence angles from 10°-80°. The VV and HH backscattering of wheat and barley decreased at all incidence angles with crop growth until it fluctuated around a stable level from grain filling to dying of the canopy. The VV backscattering of oats at low to medium angles of incidence decreased during vegetative growth and sharply increased to a steady level with the appearance of the panicles.

The geometrical architecture of the crop canopy was a major factor that influenced the X-band radar backscattering of wheat, barley and oats. Row spacing, crop variety, lodging and ear orientation of barley had a large effect on the radar backscattering. The architecture of the canopy also influenced the impact of the soil background on the radar backscattering of the whole crop. Stubble and straw largely determined the radar backscattering of harvested fields. Because of the many complex factors that influence the canopy structure, the radar backscattering was highly variable through the years.

3.1 Introduction

This paper is the second in a series of two on the ground-based X-band (3-cm waves) radar backscattering of agricultural crops. The objective is to investigate main backscattering influencing properties of agricultural crops. The first paper presented the experiments and measurement methodology of the ground based ROVE (Radar Observation on VEgetation) programme. It also described the radar backscattering of the relatively broad-leaved crops sugar beet and potato. The geometry of the crop-soil system was identified as an important backscattering influencing factor.

In this second paper, the X-band radar backscattering of wheat, barley and oats will be described and the influence of the geometry of the crop-soil system will be further analysed. First, average trends in the temporal backscattering curves of six years of observation will be presented on a specially constructed 'radar-growth' scale. The influence of the canopy structure as a main backscattering influencing factor will then be elaborated and where possible quantified. The effect of harvesting and post-harvest management activities on the radar backscattering will

be investigated. After this analysis the implications for potential agricultural application of X-band radar remote sensing will be discussed.

3.2 Crop development

Table 3.1. Proposed radar-growth scale to put the temporal X-band radar backscattering of wheat, barley and oats in various years on a consistent basis. The Zadoks code is given for comparison as a morpho-physiological growth scale commonly used in agriculture.

Stage	Description	Zadoks code
R0	seed-bed	00
R1	soil cover 0-20%	10-25
R2	soil cover 20-50%	25-30
R3	soil cover >50%; beginning stem extension	30-37
R4	shooting 1st and 2nd leaf; booting	37-47
R5	ear formation from the opening of the flag leaf sheath	47-60
R6	ear stem formation	60-70
R7	grain filling; yellowing at the bottom	70-75
R8	grain filling; yellowing 2nd leaf	75-80
R9	ripening; yellowing 1st leaf; dry weight% ear> 40%	80-93
R10	dying; brown leaves; dry weight% ear> 50%	80-93
R11	thresh ready; ears bent; dry weight% ear> 80%	93-99
R21	lodged in grain filling stage (7,8)	70-90
R22	lodged in ripening stage (9,10,11)	99-99
R30	harvest	-
R31	stubble field	
R32	ploughed field	
R33	harrowed field	

To consider average trends in the temporal radar backscattering curves of wheat, barley and oats, the time scale had to be normalized to crop growth and development. For cereals, normalization is usually done by plotting data on the

Zadoks scale of development (Zadoks et al., 1974). However, radar data of different years of observation plotted on this scale were not consistent. The radar backscattering did not react on many of the morpho-phenological events that form the basis of the Zadoks scale, e.g. seedling emergence, booting or flowering. On the other hand, the radar backscattering reacted on specific changes in the canopy architecture that make no part of the Zadoks scale, e.g. ear-stem formation and lodging. Therefore, like for sugar beet and potato, a 'radar-growth' scale was constructed that put the temporal radar data of different years of observation on a consistent base (Table 3.1). The 'radar-growth' scale for cereals is based on morphological characteristics of the crop during its development cycle that had some effect on the X-band radar backscattering.

The stages R1-R11 describe the development of the crop from seed-bed to harvest. The stages R21 and R22 designate lodging in respectively the period of grain filling and the period of ripening. Stage R30 indicates the harvested crop with optionally the stages R31-R33 to designate respectively a stubble field, ploughed soil or harrowed soil.

3.2.1 Wheat

In Figure 3.1 the average VV radar backscattering per growth stage of wheat is plotted on the 'radar-growth' scale for three angles of incidence. The standard deviation of the averages was about 1.5-2.0 dB. The average values were calculated from some 325 data per incidence angle, from 10 plots between 1975 and 1979. All data that fell within the same growth stage were averaged. The crops had a row direction parallel to the incident radar beam, and a non-stressed growth and development.

During *vegetative* growth, the radar backscattering at 50° and 70° incidence angle initially increased a little during stages R1-R3. Seedling growth and tillering took place and the height of the crop remained relatively low. At these angles of incidence, the minor increase in backscattering was probably the result of directed scattering in backward direction from the canopy. At the end of stage R3 stem extension began and the backscattering at 50° and 70° started to decrease. At 20° incidence angle the backscattering decreased already from the first stage of development. The decrease in radar backscattering, as opposite to the increase observed for sugar beet and potato, was caused by the relatively open structure of the canopy and the small dimensions of its elements. Microwaves penetrated relatively deeply in the canopy where they were eventually extinct through absorption by the canopy elements (stems, leaves). While the crop increased in height through the stages of shooting, booting and ear formation the radar backscattering kept decreasing. During these stages two things were remarkable. First, from the stage of shooting the radar backscattering decreased more at medium angles of incidence than at low and high angles of incidence. The angular

dependency-curve (i.e. the radar backscattering versus incidence angle) is said to become hollow and remained so until the cultivation of the soil after harvest. The second remarkable feature was the lack of a pronounced response of the radar backscattering to the emergence of the ears in stage R5. The radar backscattering just kept decreasing at all angles of incidence and the shape of the angular dependency-curve remained unchanged.

During stage R6 the ear-stems were formed and anthesis took place. The backscattering decreased further until no more growth in height took place at the beginning of stage R7.

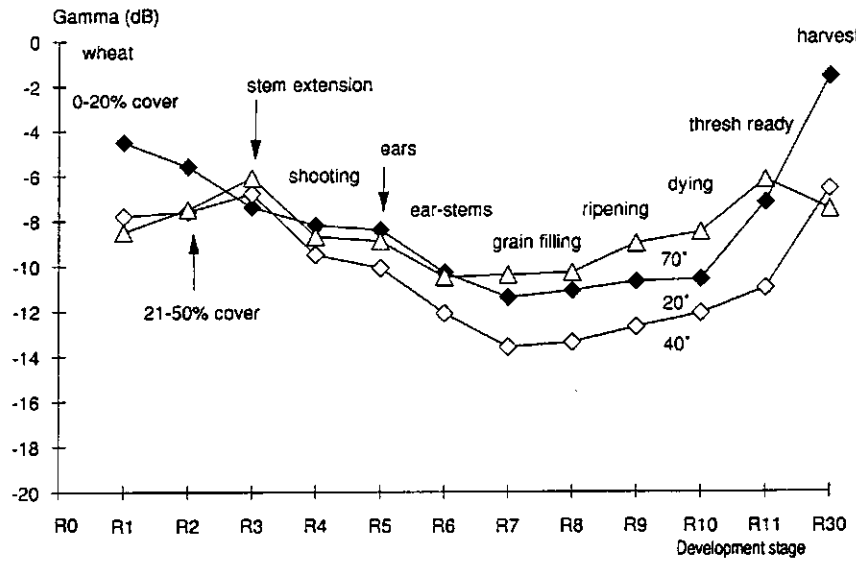

Figure 3.1. Average VV polarized radar backscattering of 10 wheat crops at 20° (◆), 40° (◊) and 70° (Δ) incidence angle versus introduced radar-growth stage.

In the *generative* stage after flowering, the crop started to yellow and wither from the bottom of the canopy upwards and it lost crop water. Since this loss may affect the radar backscattering (Attema and Ulaby, 1978; Ulaby et al., 1982), the further division in development stages was based on this yellowing and dying of the canopy. The backscattering of wheat was stable at all angles of incidence through both stages of grain filling and yellowing R7 and R8. Only during the stages R9 and R10 did the backscattering increase some 2 dB at medium and high

angles of incidence where it was still hardly affected at low angles of incidence. From this, it is concluded that the increase in backscattering at medium and high angles of incidence did not result from an increased contribution of the underlying soil background (increasing transparency of the crop), but from changes in the backscattering from the canopy itself. An increase in soil background would have been especially notable at the lowest angle of incidence. At stage R11 the crop was completely ripe and the radar backscattering increased at all angles of incidence.

3.2.2 Barley

The average VV radar backscattering of barley is given in Figure 3.2. The standard deviation of the averages varied per incidence angle. At 20° incidence angle the standard deviation was some 3 dB, at 50° incidence angle it was 2 dB in stages R0-R6 and 3-4 dB in stages R7-R30, and at 70° incidence angle it was 2 dB. The average values were calculated from 225 data per incidence angle, from seven plots between 1975-1980.

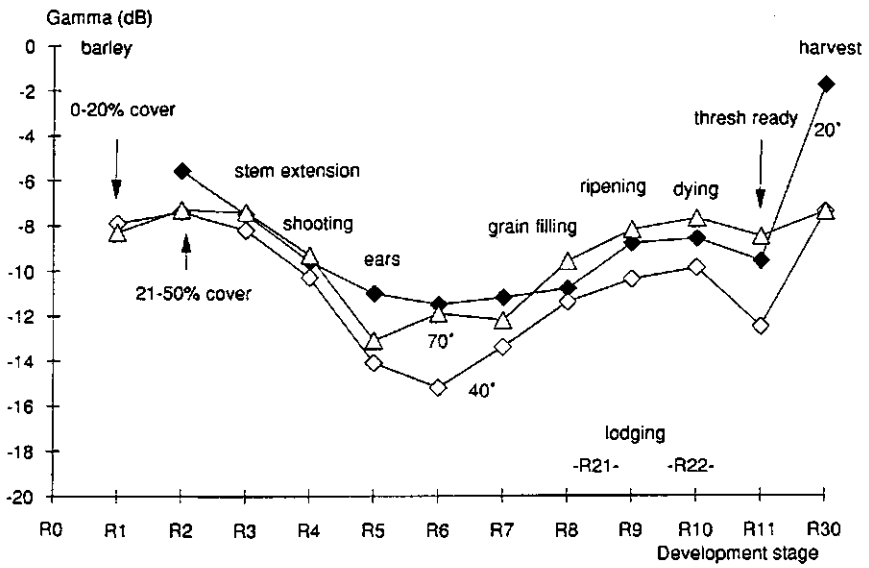

Figure 3.2. Average VV polarized radar backscattering of seven barley crops at 20° (◆), 40° (◊) and 70° (Δ) incidence angle versus introduced radar-growth stage.

In general, the trends were the same as for wheat with two main exceptions. First, barley did hardly form ear-stems and the radar backscattering reached a minimum level already in stage R6. This minimum level was some 2 dB lower than that of wheat, indicating that barley was a stronger absorbent of microwaves than wheat. Secondly, the backscattering of barley was less stable during the phases of grain filling than that of wheat. Already at stage R7 the backscattering increased at medium and high angles of incidence with some 2 dB. This was not caused by yellowing but by the lodging of the crops (see § 3.3.2). The backscattering then increased further through the stages R8-R10 by the combined effects of ripening, dying and lodging. At low angles of incidence the backscattering only rose during stage R9 when the crop ripened to the phase of dying.

3.2.3 Oats

For oats the VV radar backscattering was only averaged per growth stage for the crop in 1979 (Fig. 3.3). The standard deviation of the averages was about 1 dB. The number of data was 36 per incidence angle.

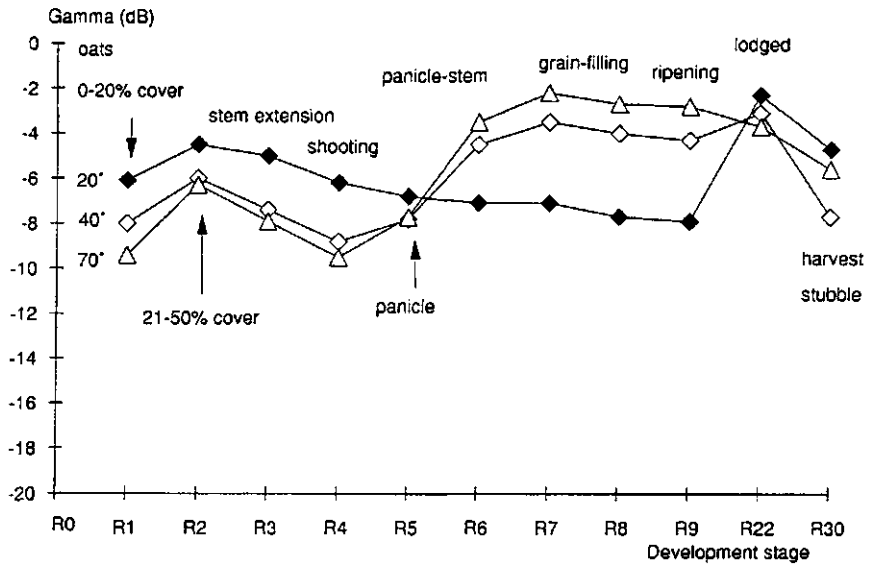

Figure 3.3. Average VV radar backscattering of one oats crop at 20° (◆), 40° (◊) and 70° (Δ) incidence angle versus introduced radar-growth stage.

After an initial increase from stage R1 to stage R2, the backscattering decreased at the beginning of stem extension in stage R3. At medium and high angles of incidence the backscattering further decreased until the beginning of panicle formation. With the emergence of the panicles, the backscattering sharply increased during the stages R5-R7. The panicles with their cloud of small, elongated grains were highly reflective for the VV polarized microwaves. During grain filling and early ripening the backscattering remained at a stable level. Contrary to the backscattering at medium and high angles of incidence, that at low angles did not react on the appearance of the panicles. From the stage of stem extension onwards, the backscattering steadily decreased without any marked features until the end of the ripening phase.

In stage R22 the crop lodged and was manually beaten down to some 30 cm height. The result was a dramatic increase in the backscattering at low angles of incidence and a comparatively small increase at medium angles. At high angles of incidence the backscattering decreased about 1 dB but this may also have been caused by the ripening and dying of the crop. At harvest the backscattering had returned to the level of that of the bare soil.

3.2.4 State of polarization.

The previous section only described the radar backscattering at VV polarization. The differences between the VV and HH backscattering were generally small, in the order of 0-3 dB. They were related to the development of the crop and to the angle of incidence.

For *wheat*, the average VV backscattering at low angles of incidence was similar to that at HH before ear formation, and a bit lower (1-2 dB) somewhere from ear formation to harvest. At medium angles it was somewhat higher (0-1 dB) than at HH before, and lower (1-2 dB) after ear formation. At high angles of incidence the average VV backscattering was somewhat higher (0-1 dB) before ear formation and significantly higher (0-3 dB) from grain filling to harvest. It should be noted that these differences applied to average values (from some 325 data per incidence angle and per state of polarization). For single crops, and especially for individual measurements, the differences were sometimes higher (Fig. 3.4).

For *barley*, the comparison between the backscattering at VV and at HH gave about the same results as for wheat. The difference was that the cross-over point between VV and HH was more at the stage of shooting than at that of ear formation.

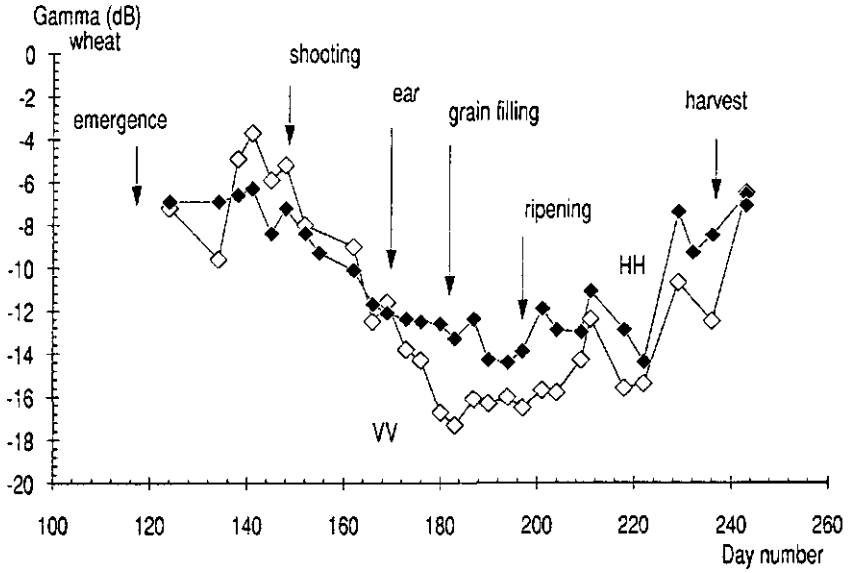

Figure 3.4. VV (◊) and HH (◆) radar backscattering of spring wheat with 12.5 cm row spacing, in the course of the growing season of 1977, at 50° incidence angle.

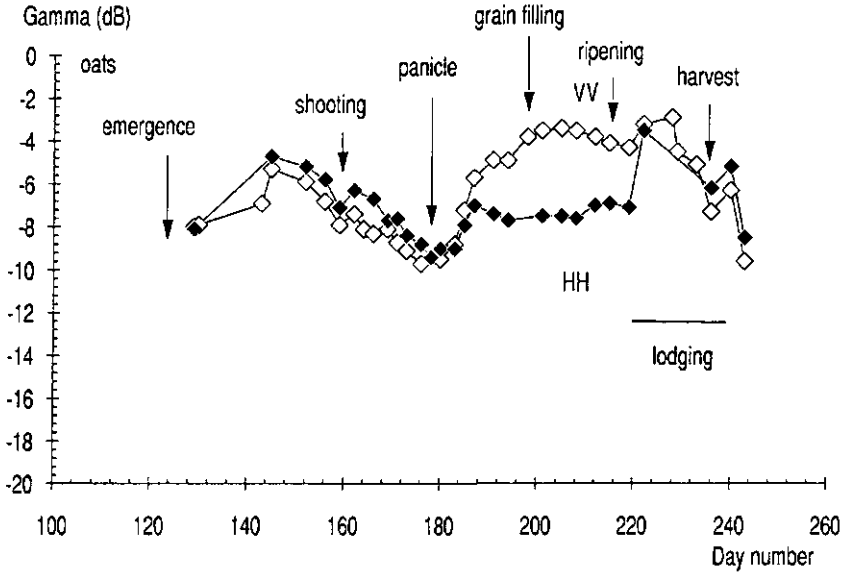

Figure 3.5. VV (◊) and HH (◆) radar backscattering of oats in the course of the growing season of 1979, at 50° incidence angle.

For *oats*, the situation differed again from that of wheat and barley (Fig. 3.5). At low angles of incidence there was practically no difference between the backscattering at VV and at HH during the whole growing season. At medium angles the backscattering was generally somewhat lower at VV than at HH (0-1 dB) during tillering and shooting. With the emergence of the panicles the backscattering at VV rose sharply while that at HH only initially rose until the formation of the ear-stems. From the formation of ear-stems to harvest the backscattering was then considerably higher (1-4 dB) at VV polarization. The panicles with the vertical needles were more reflective for microwaves in VV polarization than in HH polarization. At high angles of incidence the situation was comparable to that at medium angles, except that the backscattering was similar between VV and HH during tillering and shooting.

These observations were derived from about 102 measurements at each angle of incidence and state of polarization.

3.3 The influence of canopy structure

Although an average shape was given for the radar backscattering curves of each crop, large variations occurred between the curves from individual plots, and between single measurements. This variation was only to a limited extent related to parameters which are of direct agronomic interest like biomass, soil cover or crop water (Bouman and van Kasteren, 1989). Most variation was caused by differences in the geometry of the canopy. This geometry was affected by management practices (e.g. row direction, row spacing, crop variety), and environmental factors (e.g. wind and soil background). Table 3.2 lists the average variation and its causes for wheat, barley and oats between 1975 and 1981.

3.3.1 Management practice

Row spacing was varied in an experiment with wheat and barley in 1977. The crops were sown parallel to the direction of the radar beam with 12.5, 25.0 and 37.5 cm row spacing. The total number of measurements was 288 per incidence angle and state of polarization. All plots of the same crop type showed comparable development in height, biomass and crop water. Only the soil cover of the crops differed, with the 12.5 cm crops having the highest cover and the 37.5 cm crop the lowest.

Table 3.2. Average variation and its causes in X-band radar backscattering (dB) at VV polarization during the period of grain filling and ripening for cereals in 1975-1981.

Effect	Crop	Incidence angle 20°	50°	70°
Row spacing 12.5-37.5 cm	wheat 1977	3	1.5	2.2
	barley 1977	6.5	2.5	0.5
Row direction parallel-perpendicular	barley 1976	2.5	0.5	0
	wheat 1981	2.5	0.5	0.5
Crop variety	wheat 1979	1.5	1	0.5
	wheat 1981	3.0	3.0	2.0
Lodging	barley 1980	4.5	11	11.5
	wheat 1979	5.0	1.5	4.0
	oats	5.5	2	0.5
Ear orientation	barley 1977	6.5	7.5	7.5
	wheat 1977	0	0	3
Annual variation	wheat 1975-1979	5	5	4
	barley 1975-1980	6	6	3
	oats 1975-1980	3	1.5	1.5

A close row spacing resulted in an enhancement of the typical features in the temporal curves of the radar backscattering at low and medium angles of incidence. This is illustrated for barley in Figure 3.6. The typical features were the relatively high radar backscattering during early vegetative growth at medium angles of incidence, and the low backscattering during grain filling and ripening at low and medium angles of incidence. At high angles of incidence no significant effect of row spacing was notable. Since there were no differences between the growth and development of the crops, the differences in backscattering must be attributed to the spatial distribution of the canopy elements. This distribution was relatively homogeneous with a close row spacing, and 'clustered' in rows with a large row spacing.

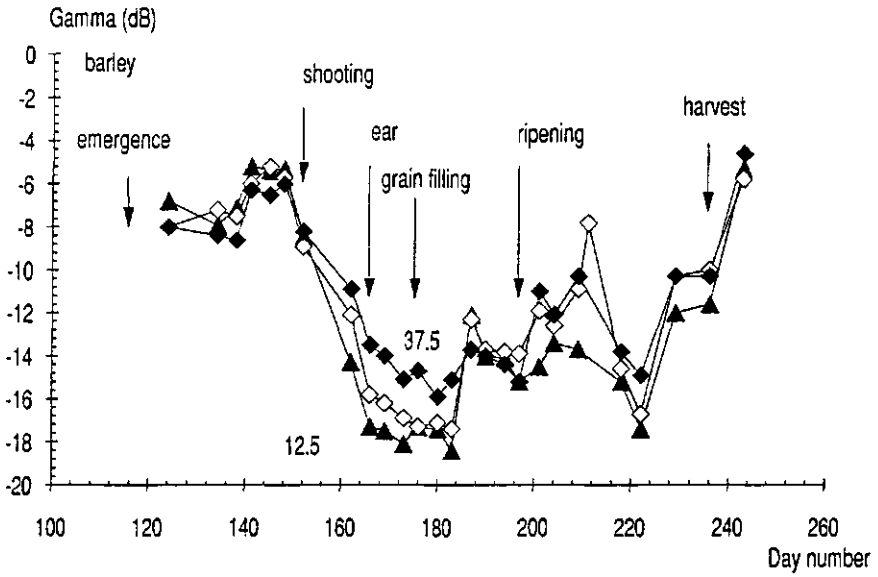

Figure 3.6. VV radar backscattering of barley with 12.5 (▲) , 25.0 (◊) and 37.5 (◆) cm row spacing, in the course of the growing season of 1977, at 50° incidence angle.

The row spacing of the crop also affected the radar backscattering through the influence of the underlying soil surface. In Figure 3.6, the increase in backscattering between days 200 and 220 was caused by an increase in the moisture content of the top soil. The crop with 12.5 cm row spacing was completely closed between the rows and the effect of the soil moisture was relatively small. The open rows of the crops with 25 and 37.5 cm row spacing permitted a considerable fraction of bare soil to be 'seen' (lower soil cover) and the effect of the soil background was larger.

The effect of *row direction* of wheat and barley was much smaller than that of row spacing. At medium and high angles of incidence there was practically no (consistent) difference between the backscattering with a radar beam direction parallel or perpendicular to the row direction. A marked difference was only present at low angles of incidence: the backscattering was some 2.5 dB lower with a perpendicular beam direction than with a parallel beam direction.

The number of observations was 86 per incidence angle and state of polarization, throughout the growing season.

Different *crop varieties* influenced the radar backscattering according to the geometry of the canopy. In 1981 four wheat varieties were sown with a considerable difference in canopy structure, resulting in some differences in the

radar backscattering. The number of data was 76 per incidence angle and state of polarization, from sowing to the beginning of grain filling.

A variety with a short and dense canopy, and with broad top leaves with a large horizontal component, Durin, had a relatively high level of radar backscattering at medium and low angles of incidence. The 3-cm microwaves did not enter the canopy very deeply but were reflected from the broad leaves in the top of the canopy. A tall and thin variety with narrow top leaves with a small horizontal component, Okapi, had a relatively low level of radar backscattering. The microwaves could penetrate deeper in the canopy and were absorbed. The average difference in radar backscattering between the 'dense' crop Durin and the 'open' crop Okapi in 1981 was about 2-3 dB.

3.3.2 External conditions

The effect of *lodging* on the radar backscattering is illustrated for barley in 1980 (Fig. 3.7). Already on day 187 the first observations were made of patches of lodged crop which caused an irregular appearance of the canopy. These patches increased in size and degree of lodging with initially no reaction on the radar backscattering until it suddenly increased on day 197. The changes in the canopy structure before this day were apparently not significant enough to affect the radar backscattering. On day 197, however, lodging became complete. This resulted in a large increase in radar backscattering at medium and high angles of incidence. The effect was somewhat larger at VV than at HH polarization. Other examples of lodging indicated a high variability of the effect of lodging on the radar backscattering. Beside the common feature of an increase in the backscattering, the effects were different in magnitude at different angles of incidence and at the different states of polarization. In general, however, the increases were largest at high angles of incidence.

Strong wind can influence the radar backscattering of crops through its effect on the orientation of the canopy elements (van Kasteren, 1981). A specific example of the effect of *ear orientation* is given in Figure 3.8 for barley in 1977. During the period of grain filling the stems of the ears were bent and the ears lied almost horizontally in the top of the canopy. On day 182 the ears were directed towards the radar, while on day 186 winds had reversed their orientation and they pointed away from the radar. The result of this change on the backscattering depended on the state of polarization, and in this specific example also on the spacing between the rows. For the 12.5 cm row crop the backscattering increased about 7 dB at nearly all angles of incidence at VV polarization, and about 2.5 dB at HH polarization. The effect of ear orientation became small when the angle of incidence became very low, at about 10° incidence.

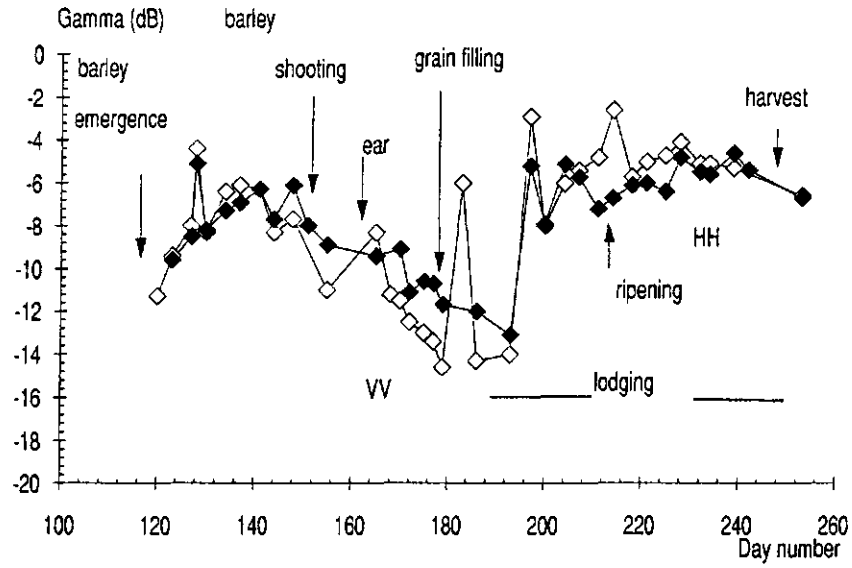

Figure 3.7. VV (◊) and HH (◆) radar backscattering of barley in lodged and non-lodged situation in the course of the growing season of 1980, at 50 ° incidence angle.

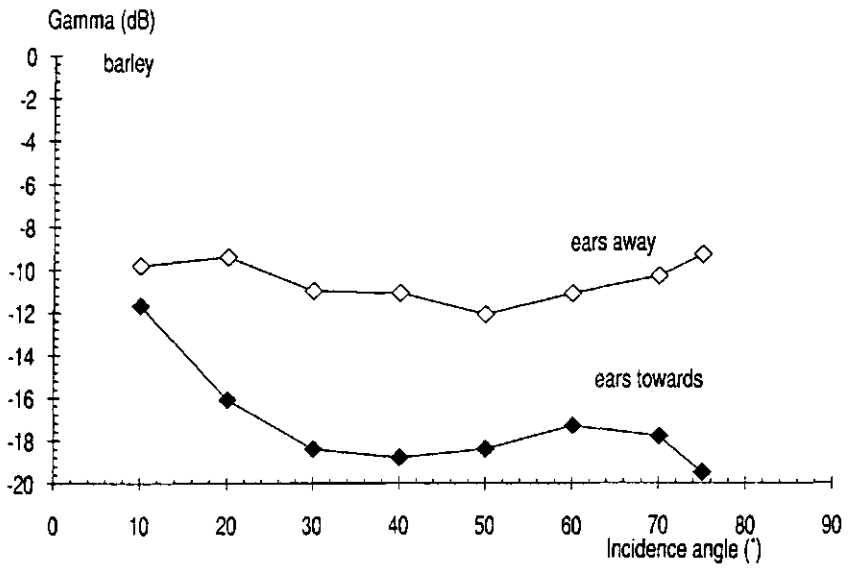

Figure 3.8. VV radar backscattering of barley in the stage of ear filling in 1980 versus angle of incidence. The ears were directed towards (◆) and away (◊) from the radar.

For the 37.5 cm row crop there was practically no effect at all angles of incidence. This is explained by the "ear-less" space between the rows of the crop which attenuated the effect of the ears in the rows.

The above examples illustrate the complex relationships between X-band radar backscattering and crop type, crop conditions, management practices and external factors. The combination of these effects resulted in large fluctuations in the backscattering curves and in a large annual variation in the level of the backscattering (Fig. 3.9).

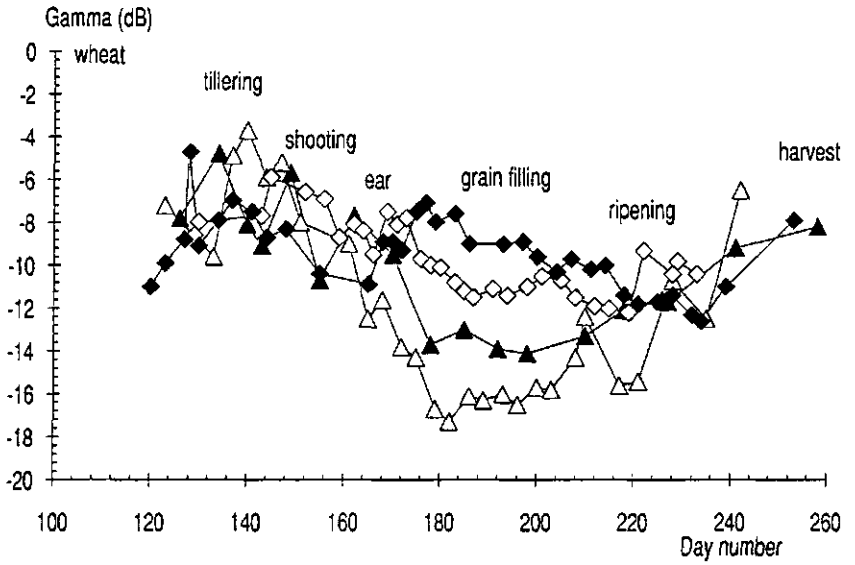

Figure 3.9. VV radar backscattering in the course of the growing season of wheat in 1975 (▲), 1977 (Δ), 1979 (◊) and 1980 (◆), at 50° incidence angle.

Especially remarkably in this Figure is the backscattering curve of wheat in 1980. That year, the familiar shape of a wheat curve was completely absent at all angles of incidence. Instead, the general pattern and most of the fluctuations largely resembled the backscattering curves of two neighbouring bare soil plots (one plot ploughed and rough, the other harrowed and smooth; both plots weed-free). The explanation is that soil cover, height and biomass of the crop were extremely low during the growing season. The crop was therefore relatively transparent for microwaves which resulted in a dominant contribution from the underlying soil

surface. Since the weather was very rainy, the moisture content of the top soil was high. As a result the radar backscattering of the soil surface and that of the whole crop was also high.

3.4 Harvest

A special point of interest was the radar backscattering at the end of the growing season and the effect of harvesting and post-harvest practices. At the end of the growing season, canopies of cereals are ripened and dried to some 25-30% moisture content. Where the amount of crop water in a green canopy may attain values of 3 Kg/m^2, values decreased to some 0.25-0.5 Kg/m^2 just before harvest. Because of these low amounts of crop water one would expect the soil background to play a major role on the radar backscattering (Ulaby et al., 1982). However, the data showed that the influence of the soil background depended much on the architecture of the ripened crop canopy. For thin crops with an open row structure, temporal fluctuations in the moisture content of the top soil clearly showed up in the backscattering curves of the crop. Crops with a dense canopy could mask the influence of the soil background completely until they were harvested.

After harvest fields were left as stubble-field with or without straw, or they were ploughed and/or harrowed immediately. There was no consistent change in the radar backscattering of a ripe crop to that of a harvested field. The changes in backscattering were generally small (0-3 dB) and depended on the state of the crop before, and on the management practices after harvest. For stubble-fields with the straw removed from the field, the temporal backscattering resembled that of neighbouring bare soil plots (both rough and smooth, weed-free) at all angles of incidence. The fluctuations in the temporal backscattering curves were caused by corresponding fluctuations in the soil moisture content. The levels of the curves however differed because of differences in surface roughness and the presence of the stubbles. When straw was left on the field between the stubbles, it appeared to mask the influence of the soil background at medium and high angles of incidence. Only at low angles of incidence did fluctuations in the temporal backscattering curves always correspond with similar fluctuations in the soil moisture content.

An interesting feature of stubble was its angular dependency-curve (Fig. 3.10). The shape of this curve was hollow and resembled more that of ripened wheat and barley than that of bare soils (rough or smooth). The level of the stubble-curve was either higher, lower, or similar to that of the ripened crop. The differences between the backscattering at VV and HH polarization also resembled those of a ripe crop. At high angles of incidence the backscattering was mostly larger at VV than at HH, while at medium and low angles of incidence it was mostly smaller.

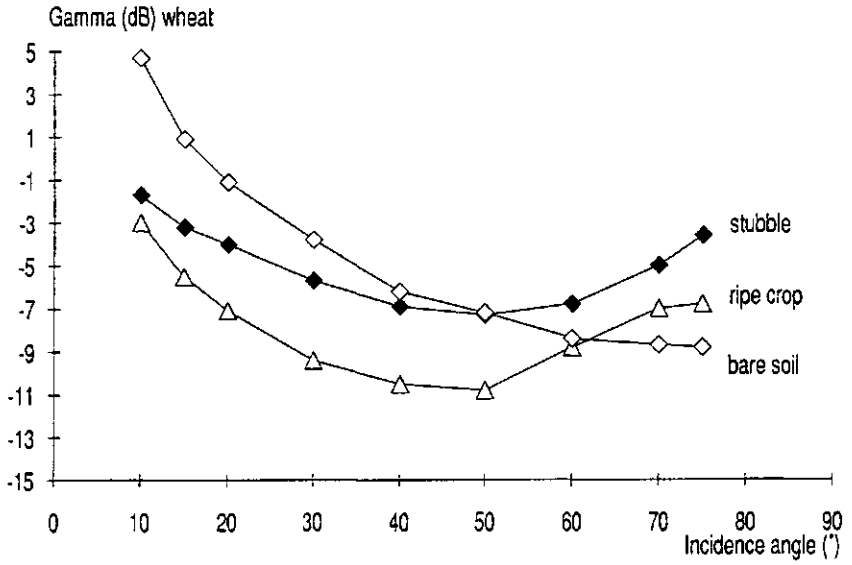

Figure 3.10. VV radar backscattering of ripened crop (Δ) and stubble (◆) of wheat in 1979 versus angle of incidence. The backscattering of a neighbouring bare soil (ploughed, rough surface; weed-free) (◊) is also given. The volumetric soil moisture content in all three cases was 18%. The amount of water in the ripened crop canopy was 0.75 Kg/m^2, that in the stubbles was about 0.04 Kg/m^2. The tiller density of crop and stubbles was 445/m^2. The crop was 90 cm high, the stubbles were 15 cm high.

The large effect of stubbles and straw on the X-band radar backscattering was surprising because of the very low amount of water it contained (measured values of stubble water varied between 0.02 and 0.05 Kg/m^2). The geometry of the material (vertical structures) apparently had a determining influence. A large effect of stubbles on the radar backscattering of harvested cereals was also reported by Bouman and Uenk (1987) for C-band radar imagery. They found that the azimuthal direction of stubbles towards and away from the radar resulted in dark respectively light colours on VV polarized images.

3.5 Discussion

The X-band (3-cm waves) radar backscattering of wheat, barley and oats was much determined by the general architecture of the canopy. Canopy architecture is the result of a complex of interacting factors: crop development stage, crop variety, row spacing and weather influences. Other factors that were not investigated in this paper will probably have to be added to this list, e.g. general crop condition (for

instance nitrogen status in relation to resistance to lodging), pest, disease and weed infection, sowing practice (broad-cast or in rows), tiller density. The architecture of the canopy also influenced the impact of the soil background on the radar backscattering of the whole crop. Stubble and straw, that are theoretically relatively transparent to microwaves, even largely determined the radar backscattering of harvested fields.

Because of the large effect of canopy structure, the radar backscattering of cereals was highly variable in time, both on daily and on yearly scales. For wheat and barley, the variation in radar backscattering in the stages of grain filling and ripening between the years 1975-1981 was about 5-6 dB at low and medium incidence angles. This variability nearly equalled the total 'radar-growth' range from sowing to closed crop canopy in a single (average) year. The interpretation of X-band radar data, acquired with remote sensing, should therefore be done with great care and preferably be based on a large number of measurements.

In agricultural application, the use of X-band radar remote sensing seems to offer good perspectives for crop classification. The large differences between the radar backscattering of cereals and that of beet and potato (first article of this series) will result in a high probability of discrimination between these crop types. Hoogeboom (1985) and Binnenkade and Uenk (1987) reported good classification results in the HH polarized X-band using the Dutch absolute and digital SLAR (Side Looking Airborne Radar). The differences between the backscattering properties of wheat and barley are relatively small and differentiation between these crops may be troublesome. On the other hand, the typical backscattering properties of oats will result in a high probability of identification.

Detailed temporal signatures of wheat, barley and oats can be used to discriminate between generalized crop development phases, e.g. emergence-tillering, stem extension-heading, grain filling-ripening. Crop emergence was not very prominent in temporal radar backscattering curves. It was mostly masked by peaks and dips caused by changes in soil moisture content. Also, the harvesting of cereals was often unnoticed because of the similarity in backscattering characteristics of ripened crop and stubble. Moreover, management practices such as the leaving-behind or the removal of the straw, or the ploughing and harrowing of the stubble affected the radar backscattering of harvested fields.

Finally, it is stressed that these conclusions are derived from a specific data set of ground-based, X-band scatterometer measurements in VV and HH polarization.

Acknowledgements.

The authors are indebted to the ROVE team of 1975-1981 for the collection of the extensive data set used for this study. The critical comments of H. Breman, R. Feddes, J. Goudriaan and G.P. de Loor on this paper were much appreciated.

This study was sponsored by the Netherlands Remote Sensing Board (BCRS).

4 CROP PARAMETER ESTIMATION FROM GROUND-BASED X-BAND (3-CM WAVE) RADAR BACKSCATTERING DATA

Abstract The possibilities of crop parameter estimation from X-band radar backscattering measurements were investigated using empirical and simple physical relationships. The study used ground-based, multitemporal, multi-angle and co-polarized radar data. The investigated crops were beet, potato, wheat and barley. The investigated crop parameters were dry canopy biomass, amount of crop water, soil cover and crop height. The implications of the results and recommendations for further research were discussed.

Empirical relations and the 'Cloud' equations were inapt for accurate estimations of crop parameters from X-band radar data at one state of co-polarization and one angle of incidence. The use of both vertical and horizontal co-polarized radar data did not improve the estimation accuracy. The use of both a medium and a high angle of incidence improved the estimation accuracy of the amount of crop water in the early growing season of (only) beet. The use of more angles of incidence did not further improve the estimation accuracy.

The low estimation accuracies were attributed to speficic features of the X-band (early saturation, low soil-crop contrast), and to the simplicity of the mono/bi-variate inversion schemes used.

4.1 Introduction

The general use of remote sensing in land observation is the characterization of surface conditions. In agriculture this means often the estimation of crop parameters that can be used for e.g. crop type identification or growth monitoring. In the radar domain of remote sensing, crop type identification has relatively often been studied (Batliva and Ulaby, 1975; van Kasteren, 1981; Hoogeboom, 1983; Wooding, 1988, Wegmüller, 1990), but the estimation of crop parameters has been less addressed (Ulaby et al., 1984; Prévot et al., 1988). However, because of the all-weather capability of radar, the estimation and monitoring of crop parameters from radar data deserves ample attention.

Crop parameters may be estimated from radar backscattering measurements through empirical regressions, or through the inversion of simple physical models. The use of more fundamental physical models (e.g. Eom and Fung, 1984; Karam and Fung, 1988) appears, up to now, not yet feasible because: 1) the models have not yet been calibrated for different crops and growing conditions, 2) some of the input parameters can not successfully be related to measurable physical properties

of the crop, and 3) the inversion of such models will be a complicated and cumbersome task. Therefore, the use of more fundamental models was not pursued here (see § 4.5.2).

In this study, the possibilities of crop parameter estimation from radar data were investigated using empirical and simple physical relationships. The radar data concern ground-based, multitemporal X-band radar measurements in vertical and horizontal co-polarization at different angles of incidence.

The investigated crops were beet, potato, wheat and barley. Beet and potato represent a class of relatively broad-leaved crops (compared to the wavelength of X-band microwaves) and wheat and barley represent a class of relatively narrow-leaved crops. The relative dimensions of the leaves cause a specific behaviour of the X-band radar backscattering. In our data set, the backscattering of beet and potato increases with crop growth between 0 and ≈0.8 fraction soil cover. The backscattering of wheat and barley increases a little with very early crop growth, and then decreases between stem extension and grain filling (Bouman and van Kasteren, 1990a, 1990b), (Fig. 4.1). The decreasing temporal backscattering of wheat is confirmed by ground-based measurements by Wegmüller (1990), and partly by measurements by Ulaby (Ulaby et al., 1984; de Loor, 1984). In Ulaby's measurements (1984), the radar backscattering increases between emergence and booting, and only then decreases to the end of anthesis. The increasing radar backscattering of beet and potato is confirmed by Wegmüller (1990), and Bouman et al. (1991).

The selected crop parameters for estimation from the radar data were above-ground, dry canopy biomass, fraction soil cover, crop height and the amount of above-ground crop water. Dry canopy biomass and soil cover have direct agricultural relevance. Crop height plays an important role in modelling energy fluxes at the earth's surface boundary layer, and the amount of crop water was selected because of its importance in modelling radar backscattering (Ulaby et al., 1982).

4.2 Materials

The data for this study were collected by the Dutch ROVE team (Radar Observation on Vegetation; de Loor, 1982), between 1975 and 1981 on agricultural test farms in The Netherlands. The test farms were Droevendaal (1975-1977) on sandy soil at Wageningen, De Bouwing (1978-1979) on alluvial clay at Randwijk, and De Schreef (1980-1981) on marine clay near Dronten.

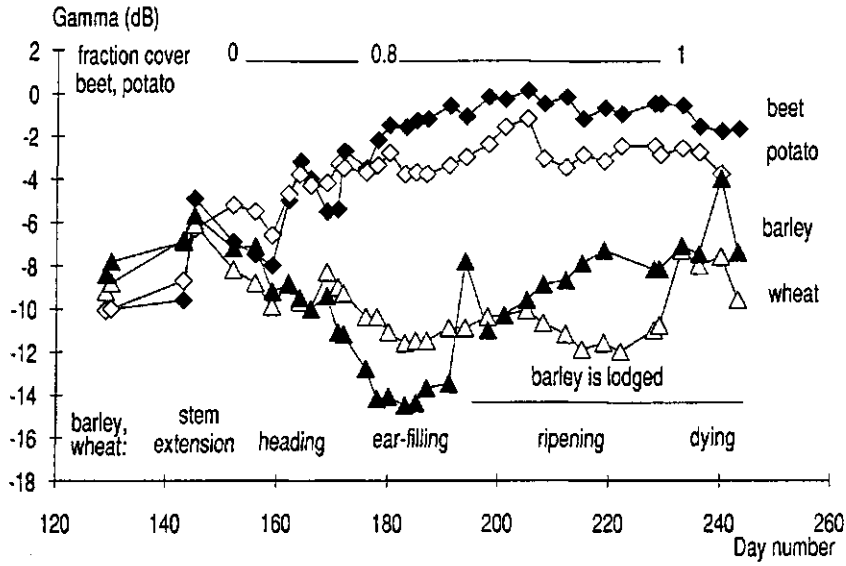

Figure 4.1. Temporal, X-band radar backscattering of beet (◆), potato (◊), wheat (Δ) and barley (▲) at test farm De Bouwing in 1979. The incidence angle was 40° and the state of polarization was VV: vertical transmitting and vertical receiving. Note the increase in backscattering of barley caused by lodging of the canopy.

An X-band FM-CW radar was mounted on a trailer and could be moved to measure the radar backscattering of plots with different crops. The radar backscattering was measured at angles of incidence between 10° and 80°, and at vertical co- (VV), horizontal co- (HH), and cross-polarization (VH, HV). However, the received power of the cross polarized signal was not sufficient to give reliable measurements, and the cross polarized data were discarded for this analysis. The radar system was externally calibrated at the end and beginning of each measurement day to ensure compatibility of the data during the growing season, and over the years. Details on the radar system, the calibration procedure and data handling are given by Attema (1974), van Kasteren and Smit (1977), Smit (1978), and de Loor et al. (1982).

The radar backscattering was expressed in γ: the radar cross-section of the target per unit projected area of the radar beam. From comparison with repetitive measurements (and from the calibration procedure), the overall accuracy of a field-average value of γ was supposed to be ≈ 0.5 dB.

On each day of radar observation, the height of the crops was measured, and the fraction soil cover was visually estimated. The standard error of estimate of

crop height generally ranged between 1 cm at the beginning of the growing season to 5 cm in the midst of the growing season. The visual estimations of soil cover were supported by grid measurements on photographs of the crops. The average (absolute) accuracy of the estimated fraction soil cover was ≈ 0.05. Dry canopy biomass and the amount of crop water were measured at a number of times in the growing season: 1975, 1979 and 1980: 8-10 times; 1976 and 1977: at all radar observation days; 1981: 3 times in early growing season. These measurements were smoothed by growth functions and missing values for days of radar observation were interpolated. No accuracies were attributed to these smoothed values, but they were consistent in time and with measured crop height and cover.

For this study, five plots of sugar beet were available (one in 1975, 1979 and 1980 each, two in 1981), three of potato (one in 1979, 1980 and 1981 each), 15 of wheat (one in 1975 and 1976 each, six in 1977, three in 1979, four in 1981), and seven of barley (one in 1975, 1976, 1979 and 1980 each, three in 1977). All crops had a good, non-stressed growth and development. The soil background was always harrowed at the beginning of the growing season by seed-bed preparations. On potato fields, ridges were created of some 20 cm height and 75 cm apart. The row directions of the crops were all parallel to the incident radar beam. Between some experiments, differences existed in row spacing, variety, plant density, soil background and meteorological conditions. Bouman and van Kasteren (1990a, 1990b) presented descriptions of the experiments, and of the radar backscattering of the crops.

4.3 Empirical relations

4.3.1 Linear regression

For all crop types, the radar measurements and ground-truth from sowing to harvest, of all years, were lumped. As a first insight in the relationships between radar backscattering and the crop parameters, linear coefficients of correlation r were calculated (Table 4.1).

The coefficients of correlation were higher for *beet and potato* than for wheat and barley, with all crop parameters and at all angles of incidence. The radar backscattering had the highest correlation at a medium angle of incidence with crop height and soil cover (Fig. 4.2). For beet, the coefficients of correlation were about 0.15-0.20 lower with canopy biomass and crop water. These differences in correlation with crop height and soil cover on the one hand, and canopy biomass and crop water on the other, were explained by the seasonal trends of these parameters. Crop height and soil cover increased after crop emergence to reach a stable level in the midst of the growing season. This trend was matched by that in the radar backscattering at most angles of incidence, leading to relatively high coefficients of correlation.

Table 4.1. Correlation matrix between canopy biomass, crop water, soil cover and height, and the VV radar backscattering at different angles of incidence, using data from sowing to harvest. Except for the values marked with (*), all coefficients are statistically significant with 99% confidence.

Angle	Can. biomass (kg/m^2)	Crop Water (kg/m^2)	Cover (fraction)	Height (m)
BEET (N = 75 per incidence angle)				
20°	0.54	0.56	0.71	0.71
30°	0.61	0.64	0.79	0.79
40°	0.66	0.69	0.84	0.84
50°	0.68	0.70	0.85	0.85
60°	0.68	0.70	0.86	0.85
70°	0.67	0.69	0.86	0.85
POTATO (N = 64 per incidence angle)				
20°	0.76	0.78	0.82	0.86
30°	0.77	0.79	0.82	0.87
40°	0.79	0.80	0.82	0.86
50°	0.77	0.77	0.77	0.83
60°	0.78	0.76	0.75	0.79
70°	0.77	0.75	0.73	0.77
WHEAT (N = 230 per incidence angle)				
20°	-0.39	-0.36	-0.47	-0.66
30°	-0.53	-0.29	-0.22	-0.76
40°	-0.63	-0.29	-0.16	-0.81
50°	-0.61	-0.32	-0.16	-0.80
60°	-0.51	-0.41	-0.19	-0.72
70°	-0.24	-0.39	-0.17	-0.50
BARLEY (N = 145 per incidence angle)				
20°	-0.21	-0.44	-0.57	-0.73
30°	-0.23	-0.32	-0.45	-0.76
40°	-0.20	-0.26	-0.37	-0.76
50°	-0.17	-0.25	-0.32	-0.75
60°	-0.09*	-0.32	-0.32	-0.77
70°	-0.02*	-0.42	-0.31	-0.62

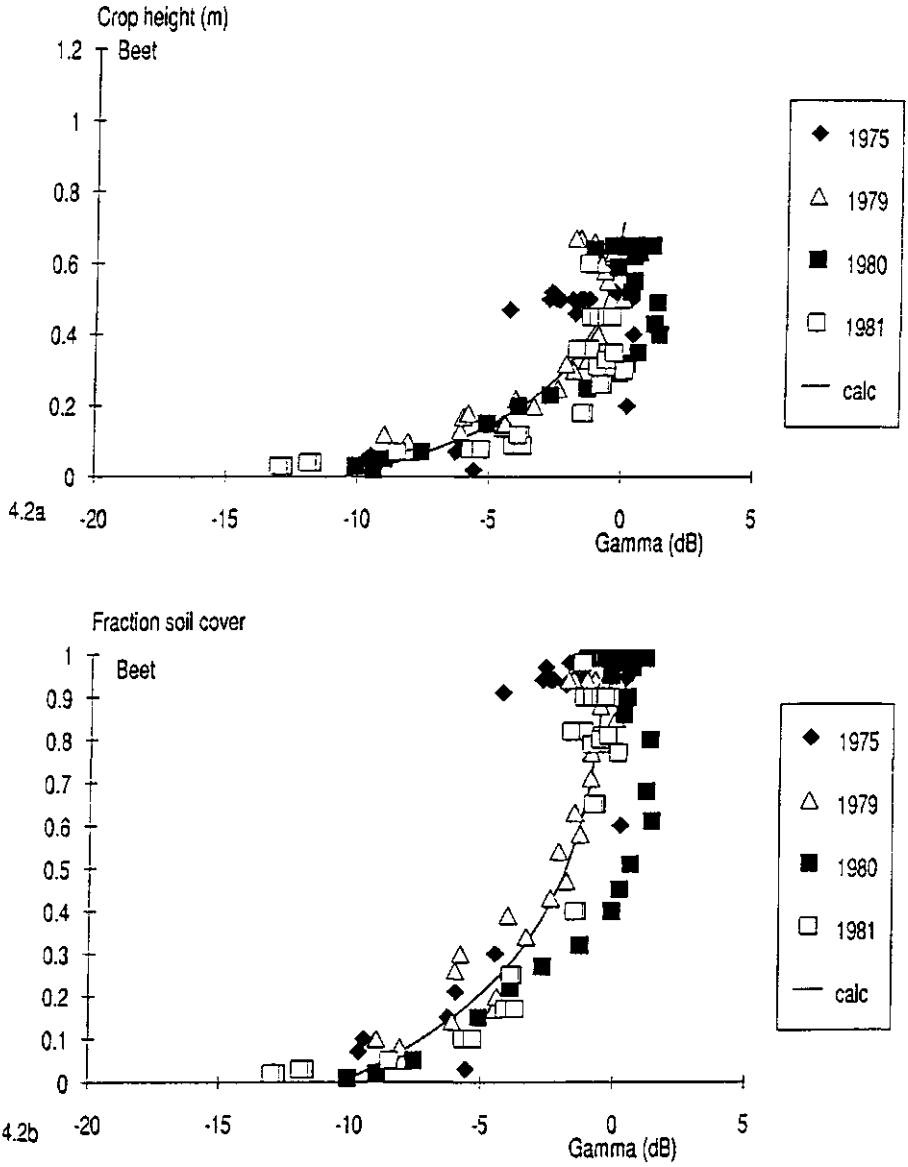

Figure 4.2. VV radar backscattering at 50° incidence angle of beet versus crop height (4.2a) and soil cover (4.2b). The data were taken from sowing to harvest, from five different plots in four different years (N = 75). The drawn lines indicate the fitted logarithmic expressions.

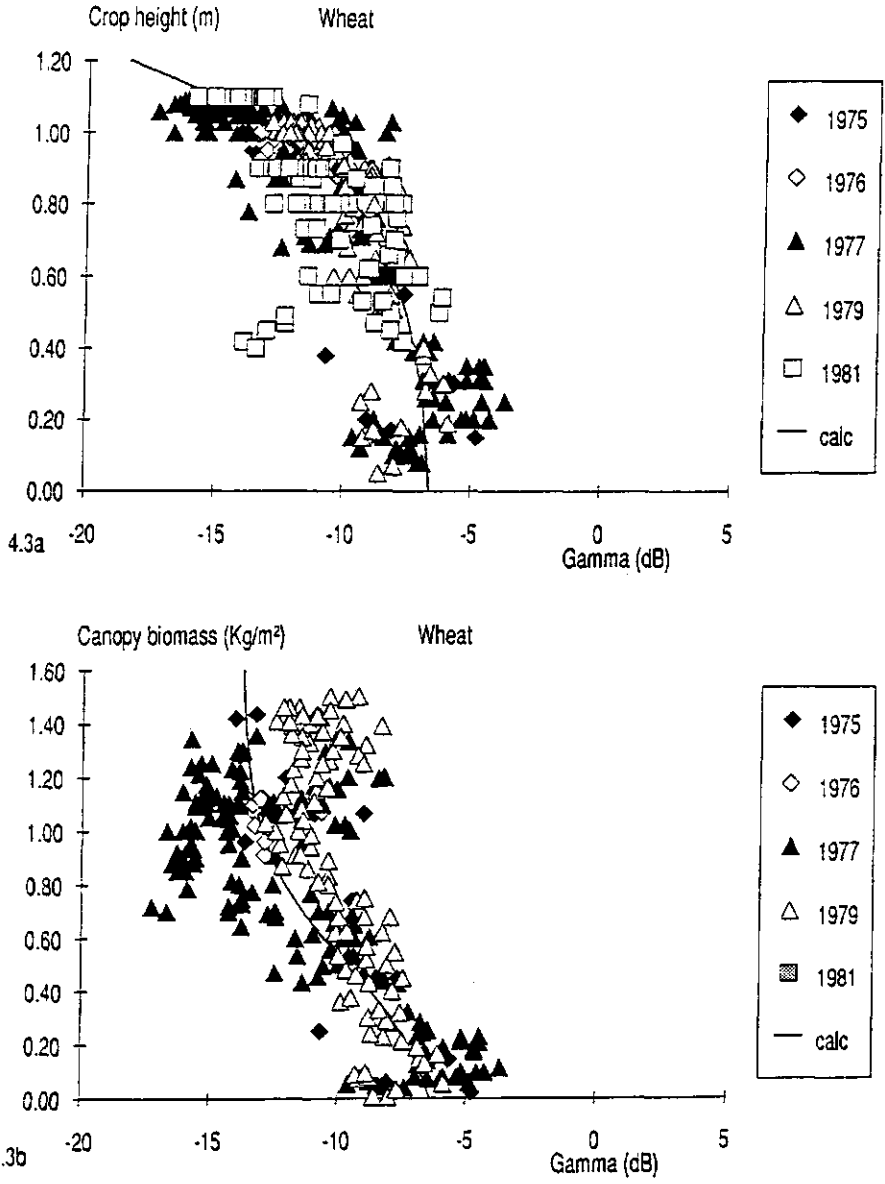

Figure 4.3. VV radar backscattering at 50° incidence angle of wheat versus crop height (4.3a) and dry canopy biomass (4.3b). The data were taken from sowing to harvest, from 15 different plots in five different years (N = 230). The drawn lines indicate the fitted logarithmic expressions.

Canopy biomass and crop water, on the other hand, kept increasing from crop emergence until the end of the growing season. For potato, canopy biomass and crop water also reached a stable level in the midst of the growing season and the coefficients of correlation were higher than for beet.

The coefficients of correlation for *wheat and barley* were negative because of the decreasing radar backscattering from stem extension to ripening. The radar backscattering only correlated with crop height, with the highest coefficients of correlation for wheat at medium angles of incidence (Fig. 4.3a). For wheat the radar backscattering at medium angles of incidence also correlated somewhat with canopy biomass (Fig. 4.3b).

The scatter in the data points of Figure 4.3 is quite large. This was partly caused by radar observations on lodged and dying crops at the end of the growing season. The changes in canopy structure through lodging and dying greatly affected the radar backscattering (Bouman and van Kasteren, 1990b), see also Figure 4.1.

For further analysis, data on lodged or on ripened wheat and barley, i.e. after stage 8 of the Zadoks growth scale (Zadoks et al., 1974), were excluded from the data set. This exclusion led to increased coefficients of correlation, especially at medium angles of incidence (Table 4.2).

Table 4.2. Average coefficients of correlation r between canopy biomass, crop water, soil cover and crop height, and the VV radar backscattering at 40°-60° incidence angle, using data on non-lodged crops from sowing to growth stage 8 on the Zadoks growth scale, i.e. ≈ ripening. The number of data for wheat was 184 per incidence angle, and for barley 116 per incidence angle. All coefficients are statistically significant with 99.5% confidence.

Crop	Biomass (kg/m^2)	Crop water (kg/m^2)	Cover (-)	Height (m)
Wheat	-0.75	-0.48	-0.50	-0.84
Barley	-0.70	-0.65	-0.65	-0.85

4.3.2 Parameter estimation

Non-linear regression analysis was used to study the accuracy of crop parameter estimation. Crop height and soil cover of beet and potato, and crop height and canopy biomass of wheat and barley were estimated from the radar backscattering at 50° incidence angle. The crop parameters were estimated from

second order polynomial or logarithmic equations. As an example, the logarithmic equations that best described the relationship between the crop parameters and the radar backscattering are given for beet and wheat:

Beet:

$$h = -0.473*10\log[-(\gamma-0.334)/10.90] \quad (1)$$
$$f = -0.648*10\log[-(\gamma+0.084)/10.26] \quad (2)$$

Wheat:

$$h = 2.21 - 10\log[-(339.38/\gamma+6.37)+1]/1.40 \quad (3)$$
$$W_d = 5.08 - 10\log[-(8.19/\gamma+5.64)+1]/0.20 \quad (4)$$

where: h = crop height (m); f = soil cover of the crop (fraction); W_d = dry weight of the crop canopy (kg/m^2); γ = radar cross section (dB)

These equations are drawn as solid lines in the scatter diagrams of Figures 4.2 and 4.3. For beet, slightly better relationships were obtained by using higher order polynomial equations. The coefficients of correlation r and the residual standard deviations S(residual) between the measured and estimated crop parameters are given for all crops in Table 4.3. The S(residual) can be seen as a measure of accuracy of parameter estimation:

$$S(\text{residual}) = \sqrt{[\sqrt{(y-y')^2}/N-1]} \quad (5)$$

where: y = measured value of parameter; y' = estimated value of parameter; N = number of data pairs

For all parameters, the estimation accuracy [S(residual)] was about 20% of the total range in the parameter values from zero to its maximum value. The coefficients of correlation were not very high, with the highest values for beet.

These poor results were caused by 1) a large variability in the radar backscattering curves of the same crop type in different years, and 2) relatively large fluctuations in the individual backscattering curves. The large variability was explained by differences in crop variety and management practices (e.g. row spacing), and by differences in growth conditions and environment (e.g. soil background). The relatively large fluctuations in the curves were caused by variation in the soil moisture content and by changes in the canopy architecture induced by weather (Bouman and van Kasteren; 1990a, 1990b).

Table 4.3. Results of the estimation of crop parameters from the VV radar backscattering at 50° incidence angle. The coefficients of correlation r and the residual standard deviations S(residual) were calculated between the measured and estimated crop parameters from empirical regressions.

Crop	parameter	r	S(residual)
Beet	height	0.86	0.14 m
	cover	0.87	0.21 fraction
Potato	height	0.78	0.12 m
	cover	0.70	0.19 fraction
Wheat	height	0.83	0.19 m
	biomass	0.79	0.22 kg/m^2
Barley	height	0.85	0.18 m
	biomass	0.73	0.23 kg/m^2

The estimation accuracies in Table 4.3 are empirical averages over different fields and years, and over the whole growing season. A theoretic example illustrates the effect of deviations in radar backscattering from the regression line on the accuracy of crop parameter estimation, along the range in crop parameter values from its minimum to a maximum. The inverse of equation 2 was used to calculate the radar backscattering of a hypothetical beet crop for a range in soil cover from 0.0 to 1.0. Equation 2 was then used again to estimate the soil cover from the calculated radar backscattering with deviations of +/- 0.5, +/- 1 and +/- 2 dB. Estimated soil covers below 0.0 and above 1.0 were set on these boundaries to avoid unrealistic values. In Figure 4.4, the estimated soil cover is plotted against true soil cover of the hypothetical crop. The effect of deviations in the radar backscattering on parameter estimation depended on the magnitude of the estimated parameter itself. At values close to 0 the estimation error was about 0.05 and 0.08 with deviations of 0.5 and 1 dB respectively. With increasing fraction soil cover the errors increased to values of more than 0.30 and 0.45 at full cover.

Fluctuations in the order of 1 dB, and sometimes even larger, were common in the temporal backscattering curves of beet and other crops. This means that the estimation of soil cover from each single radar measurement has an accuracy that ranges from 0.05 to 0.45. For application in, for instance, crop growth modelling, this accuracy should be in the order of 0.05.

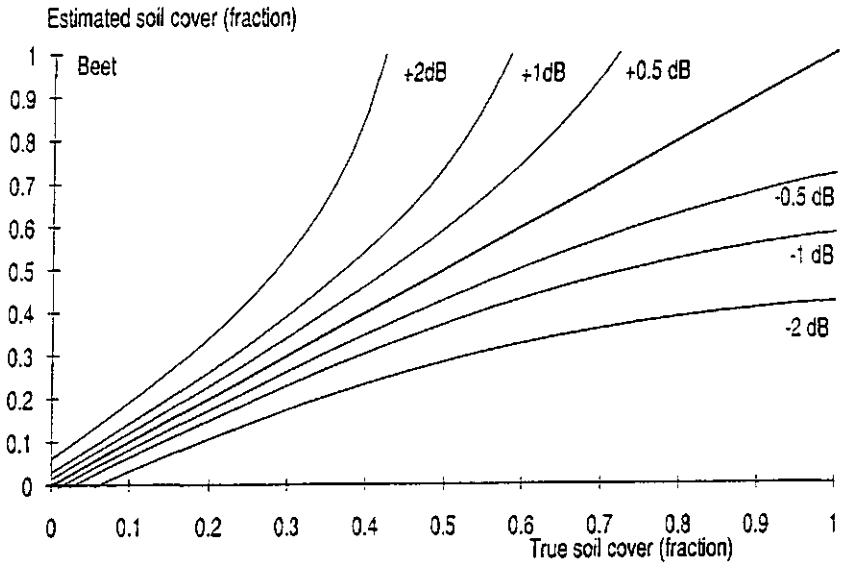

Figure 4.4. Theoretical sensitivity of the estimation of soil cover of beet on deviations in the radar backscattering from an empirically fitted curve, at 50° incidence angle. The estimated soil cover is plotted on the vertical axis and the true soil cover on the horizontal axis.

4.4 The simple physical 'Cloud' equations

Attema and Ulaby (1978) have modelled the radar backscattering from vegetation by representing the vegetation canopy as a cloud of isotropic water droplets. The driving parameters in their 'Cloud' model are the amount of water in the vegetation layer and the volumetric moisture content in the top soil (for X-band radar, typically the layer of first 5 cm):

$$\gamma = C(\theta)(1-\exp(-DW/\cos(\theta)))+ G(\theta)\exp(Km-DW/\cos(\theta)) \qquad (6)$$

where: γ = radar cross section (m^2/m^2), W = crop water per unit soil surface (kg/m^2), m = volumetric moisture content of top soil (%), θ = incidence angle (°), D = coefficient of attenuation per unit of crop water (m^2/kg), K = moisture coefficient of top soil per volumetric moisture content (-), $C(\theta)$ = backscattering coefficient of an optically thick vegetation cover (m^2/m^2), $G(\theta)$ = backscattering of dry soil (m^2/m^2).

In this formulation (equations 6 and 7), γ is expressed in m^2/m^2 instead of in dB. The 'Cloud' model was calibrated for a number of crops in different growing conditions with ground-based data collected by the University of Kansas and by the

Dutch ROVE team. The residual standard deviation between the measured radar backscattering and the calculated backscattering with the 'Cloud' equations averaged about 1 dB for beet and potato. Hoekman et al (1982) extended the 'Cloud' model in a two-layer model to describe the radar backscattering of cereals. Because this model can not be analytically inverted it is less suitable for the estimation of crop parameters. Bouman and van Kasteren (1989) modified the original 'Cloud' model for wheat and barley by replacing the term $W/\cos(\theta)$ by the crop height h:

$$\gamma = C(\theta)(1-\exp(-Dh)) + G(\theta)\exp(Km-Dh) \qquad (7)$$

This model described the radar backscattering as accurate as the two-layer 'Cloud' model. The residual standard deviation between measured and calculated backscattering varied between 0.8 and 2.4 dB for various data sets of wheat and barley.

The model parameters of the 'Cloud' equations for beet, potato, wheat and barley in 1979 are given in Table 4.4.

Table 4.4. Model parameters and the residual standard deviation S(residual) of the 'Cloud' equations at 40° incidence angle for beet, potato (Hoekman et al, 1982), wheat and barley in 1979 (modified 'Cloud' equations, Bouman and van Kasteren, 1989).

Crop	$G(\theta)$	K	$C(\theta)$	D	S(residual) (dB)
Beet	0.061	0.051	0.929	0.76	0.83
Potato	0.078	0.051	0.994	0.25	0.94
Wheat	0.188	0.051	0.056	2.95	0.83
Barley	0.198	0.051	0.037	2.54	0.88

4.4.1 Single incidence-angle data

With the model parameters in Table 4.4, the radar backscattering at 40° incidence angle was calculated for a given range in crop water for beet, and for a given range in crop height for wheat. The soil moisture content was taken 5%. The inverse equations of 6 and 7 were then used to estimate crop water of beet and crop height of wheat respectively, from the calculated backscattering with deviations of +/- 0.5 to +/- 2 dB.

For *beet*, the error of estimation increased sharply with increasing amount of crop water (Fig. 4.5a). With a negative deviation of 0.83 dB in the radar backscattering, S(residual) in Table 4.4, the error increased from some 0.05 kg/m^2 at 0 kg/m^2 crop water to more than 1 kg/m^2 at 2 kg/m^2 crop water. With a positive deviation of 0.83, the error was already more than 2 kg/m^2 at values of 1.5 kg/m^2 crop water.

The main cause for these large errors was the early saturation of the radar backscattering in the growing season (Fig. 4.1). After saturation, the radar backscattering no longer reacted on any increase in crop water. Because of this insensitivity, small deviations in the radar backscattering near saturation resulted in large errors in the estimation of crop water.

For *wheat*, the errors in estimation of crop height were also quite large (Fig. 4.5b). Compared to beet, the estimation error varied less with crop height itself (within the realistic range of 0-1.2 m). With deviations of +0.83 dB, the error was about 0.1 m at 0 m crop height, and 0.3 m at 1 m crop height. With a negative deviation of 0.83 dB, the error increased already to 0.3 m at 0.8 m crop height.

In this case, the errors were mainly caused by a relatively low contrast in radar backscattering, only some 5 dB, from bare soil to that of the full crop (Fig. 4.1). Deviations of 0.83 dB were relatively large and resulted in correspondingly large errors of estimation. In general, the same ratio of average deviations in radar backscattering to total 'radar-growth' range (here some 100*0.83/5 = 17%) is returned in the ratio of average estimation error to total growth range of the estimated parameter.

4.4.2 Multi incidence-angle data

Radar data of the same crop can be collected at different angles of incidence. Model equations like 6 and 7 may be derived for each angle of incidence. This has two implications. First, with two independent equations, the estimation of a second driving parameter becomes possible. In the case of the 'Cloud' equations, this parameter is the moisture content in the top soil. Secondly, if the number of independent equations is larger than the number of driving parameters in the model, these parameters are over-determined and can be statistically estimated.

Beet

The possibilities of parameter estimation with two incidence angles will first be investigated for *beet* in 1979. The best combination of two incidence angles is a low and a medium angle. At a low angle, the microwaves penetrate the canopy best and the soil contribution to the radar backscattering is relatively large. This angle is therefore suitable for estimations of the soil

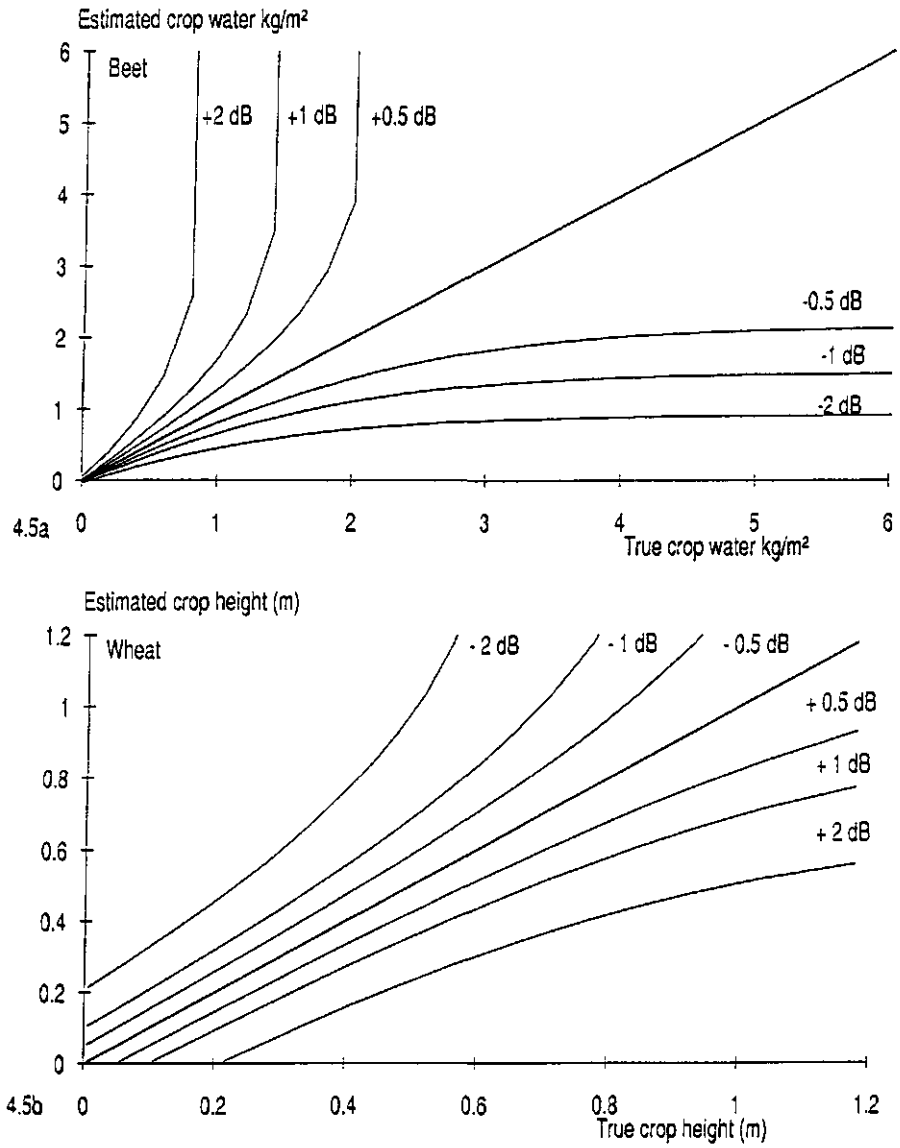

Figure 4.5. Theoretical sensitivity of the estimation of crop water of beet (4.5a) and crop height of wheat (4.5b) on deviations in the radar backscattering from the 'Cloud' equation, at 40° incidence angle. The estimated parameter is plotted on the vertical axis and the true parameter on the horizontal axis.

moisture content. At a medium angle of incidence, the contribution of the soil background is less, and the radar backscattering reacts strongly on crop water. When the angle of incidence is high, the backscattering also reacts strongly on crop water but the saturation of the backscattering takes place sooner than at medium angles of incidence (de Loor, 1985).

The estimation of crop water and soil moisture content from the radar backscattering at 10° and 50° incidence angle is graphically illustrated in Figure 4.6a. The 'Cloud' equations were used to calculate the radar backscattering at 10° and 50° incidence angle for a range in soil moisture contents and crop water values. 'Iso-crop water' and 'iso-soil moisture' lines were drawn in a nomogram with the radar backscattering at the two angles of incidence on the axes.

The measured radar backscattering pairs at 10° and 50° incidence angles were plotted in the nomogram. Interpolation between the iso-soil moisture and iso-crop water lines yielded estimated values of soil moisture and crop water (Fig. 4.7). The amount of crop water was estimated within 0.1 kg/m^2 accuracy until 1 kg/m^2. Between values of 1 and 2.5 kg/m^2 crop water, the estimation accuracy was about 0.4 kg/m^2, and after 2.5 kg/m^2 crop water the estimations became unrealistic. The decreasing estimation accuracy with increasing crop water was caused by the narrower spacing of the iso-crop water lines. The soil moisture content was estimated with an average absolute accuracy of some 3% until day 185. After day 185, the microwaves no longer penetrated the canopy sufficiently to give (reliable) information on the soil moisture status.

Both the amount of crop water and soil moisture content can be statistically estimated when more than two incidence angles are available. In this example, the radar backscattering of beet was measured at six angles of incidence from 10° to 80°. Crop water and soil moisture were estimated with non-linear optimization procedures from the software package GENSTAT5 (Reference manual, 1988). The results are again depicted in Figure 4.7. Between 1 and 2.5 kg/m^2, the estimations of crop water were slightly better than with two incidence angles only. With one exception, the estimations became again unrealistic at crop water values above 2.5 kg/m^2.

The soil moisture content was also estimated with an average absolute accuracy of about 3% until day 180.

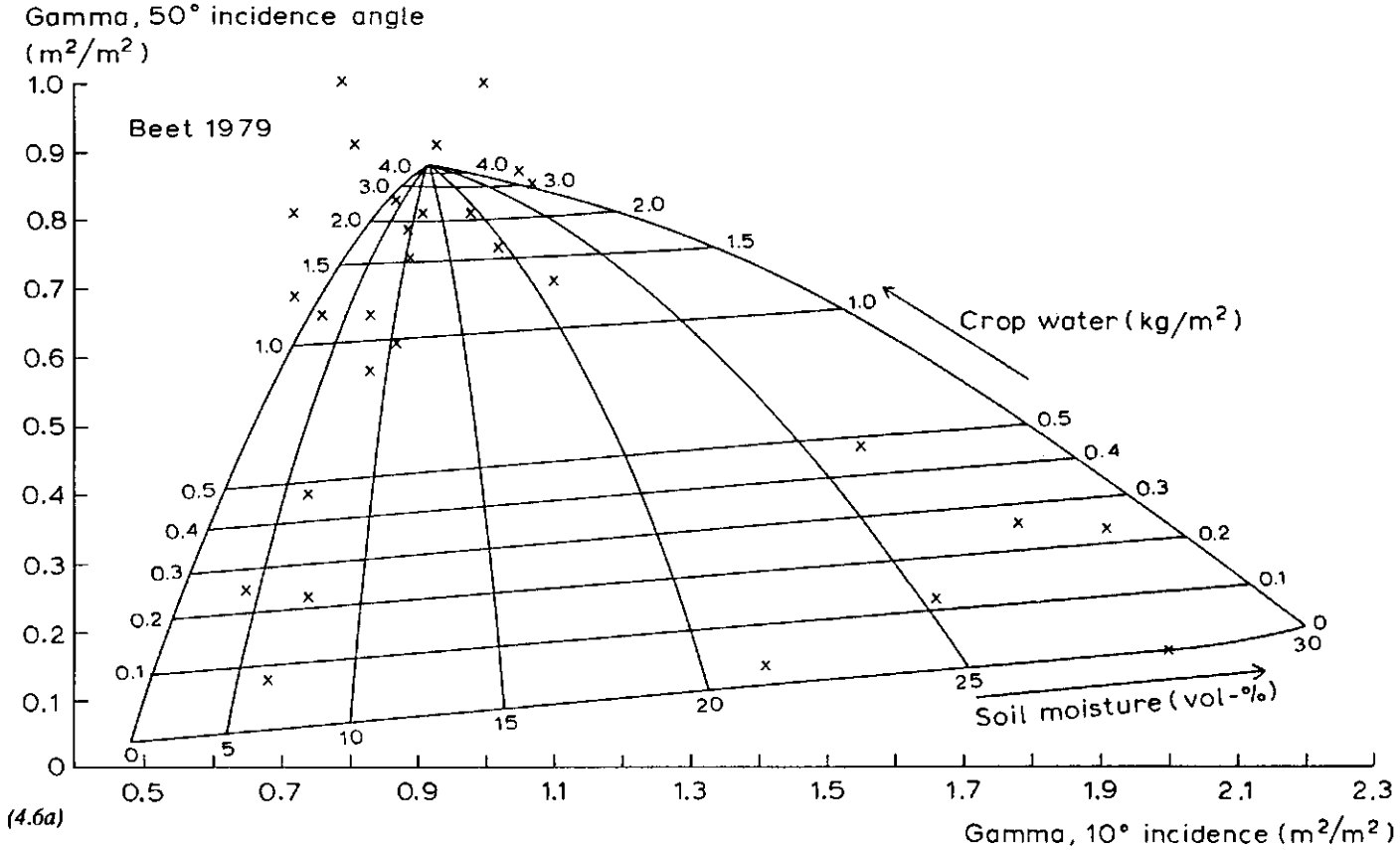
Gamma, 50° incidence angle
(m²/m²)
Beet 1979
Crop water (kg/m²)
Soil moisture (vol-%)
Gamma, 10° incidence (m²/m²)
1.0
0.9
0.8
0.7
0.6
0.5
0.4
0.3
0.2
0.1
0
0.5
0.7
0.9
1.1
1.3
1.5
1.7
1.9
2.1
2.3
4.0
3.0
2.0
1.5
1.0
0.5
0.4
0.3
0.2
0.1
0
5
10
15
20
25
30

(4.6a)

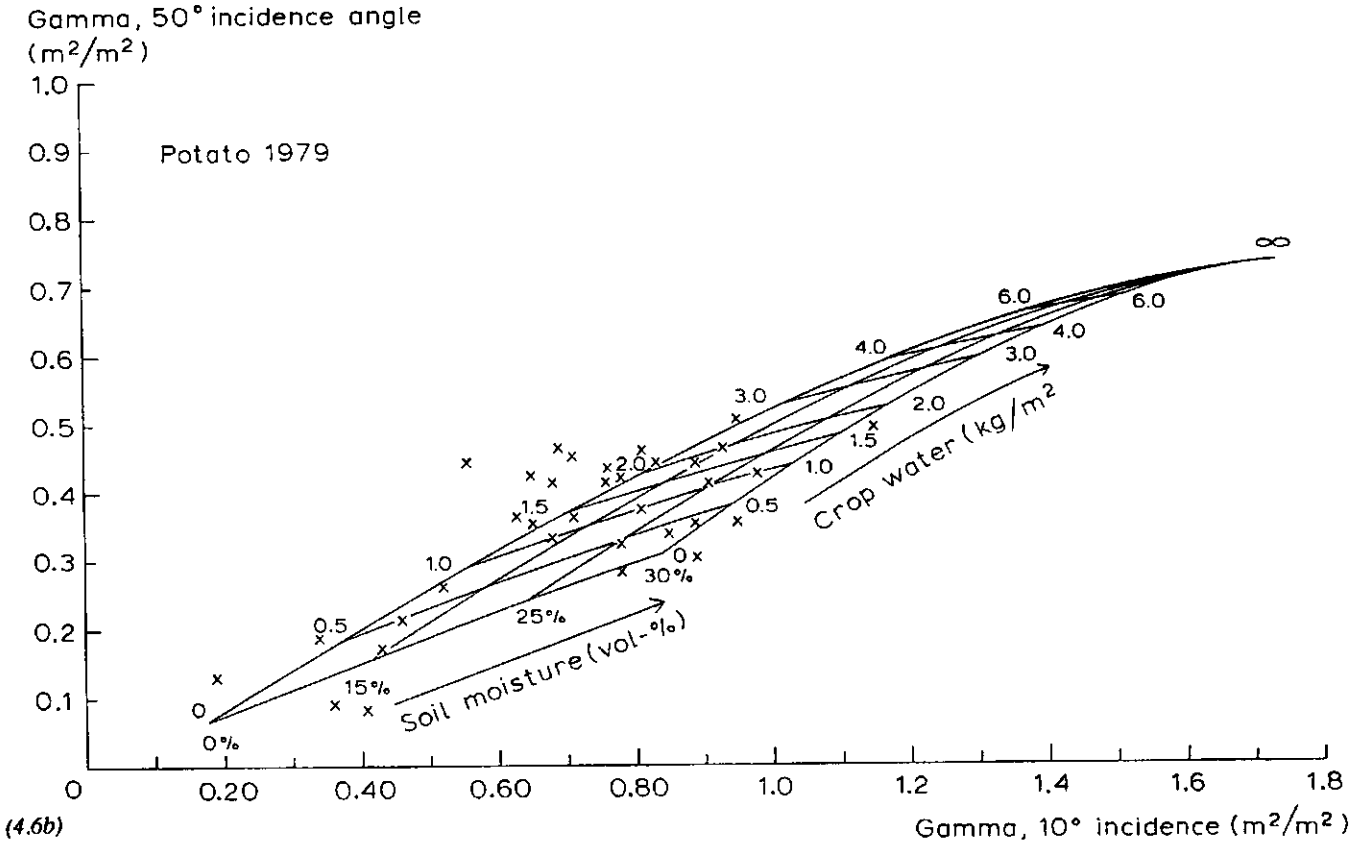

Figure 4.6. Nomogram for the estimation of the amount of crop water and the moisture content of the top soil for beet (4.6a) and potato (4.6b). The nomogram was constructed with the 'Cloud' equations for 10° and 50° incidence angle, calibrated for both crops at test farm De Bouwing in 1979. The crosses indicate the measured backscattering pairs. The radar backscattering is given in m^2/m^2 instead of in dB.

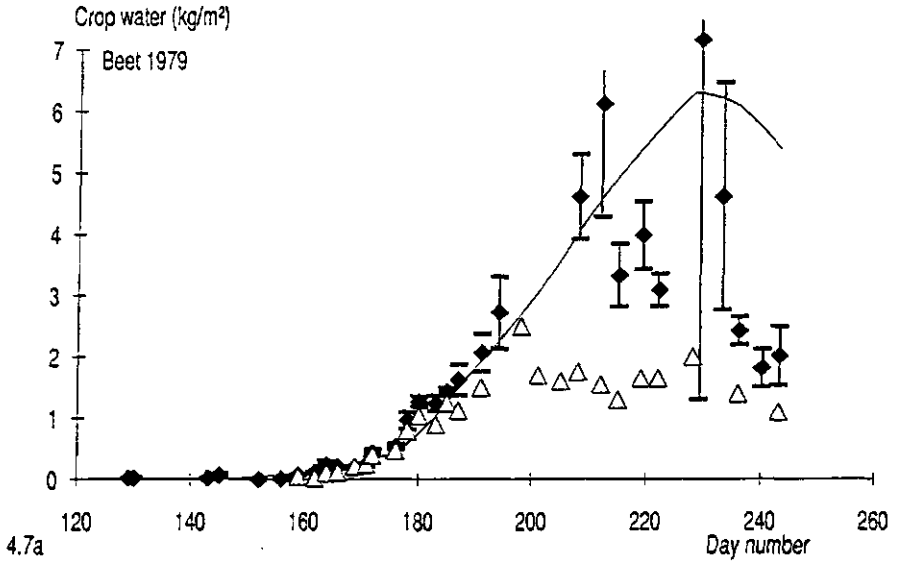

4.7a

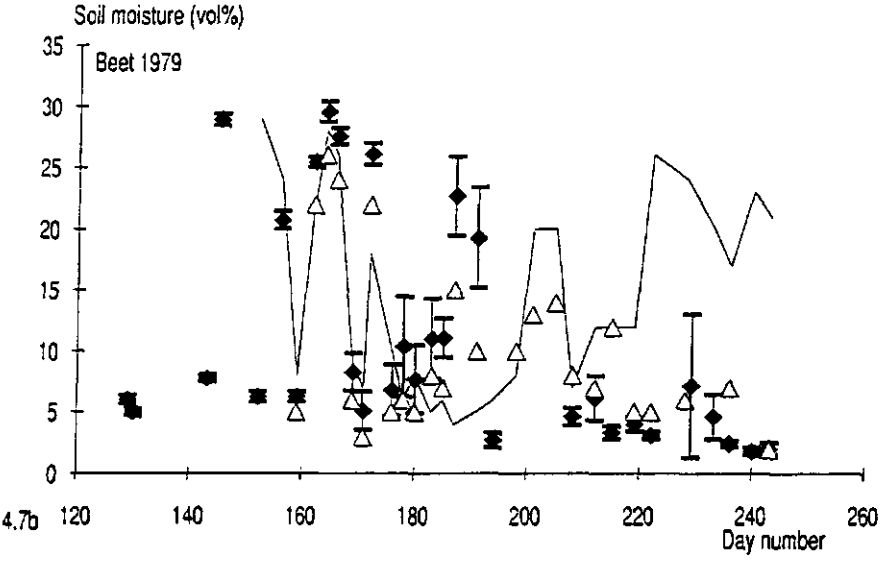

4.7b

Figure 4.7. Measured and estimated amount of crop water (4.7a) and moisture content of the top soil (4.7b) for beet in 1979. The drawn lines are smoothed curves from measured data. Δ indicates the estimated values using two angles of incidence, 10° and 50°. ♦ with the error bars indicate the estimated values using six angles of incidence, 10°, 20°...70°.

Wheat, barley and potato

For *wheat, barley and potato*, the temporal radar backscattering was similar at different angles of incidence (Bouman and van Kasteren; 1990a, 1990b). The temporal backscattering curves at the various angles of incidence were parallel and the correlations were high. The nomograms of the radar backscattering at two angles of incidence were therefore narrow, as illustrated for potato in Figure 4.6b. Because of this narrow spacing, the same magnitude of deviations in the measured radar backscattering from the fitted 'Cloud' equations as for sugar beet, resulted in relatively large errors of estimation.

Even when six angles of incidence between 10° and 80° were used, the estimation accuracies did not increase over the single-incidence angle approach. The reason for this was that the 'Cloud' equations were not independent at the different angles of incidence.

4.4.3 VV and HH polarization

Radar backscattering measurements can not only be made at different angles of incidence, but also at different states of polarization. For beet, potato, wheat and barley, however, both the trends and the absolute values in the radar backscattering were similar at VV and at HH polarization (Bouman and van Kasteren; 1990a, 1990b). Therefore, the accuracy of parameter estimation did not increase by considering radar data at both states of polarization.

4.5 Discussion

4.5.1 Conclusion

Empirical and simple physical relations were inapt for accurate estimations of crop parameters from X-band radar observations. The estimation accuracies were generally too low for agricultural applications like production estimations or crop growth modelling.

The low estimation accuracies may be attributed to specific features of X-band radar backscattering, and to the simplistic inversion schemes used here. An X-band specific problem appeared to be the early saturation of the radar backscattering with crop growth (beet). This suggests the use of other radar frequency bands. Lower frequency microwaves that (theoretically) penetrate the crop canopy deeper than X-band microwaves might give a longer sensitivity to crop growth. Another X-band specific problem was the low contrast between the backscattering of bare soil and that of a fully grown crop canopy (wheat). Small deviations in the radar

backscattering from the fitted regression or physical model, resulted then in relatively high errors in the estimation of a crop parameter. Deviations in the radar backscattering are caused by inaccuracies in the measurement (here only ≈ 0.5 dB) and by effects of other canopy-factors on the measured signal (e.g. 'canopy structure'). These effects render simple relationships between the backscattering and individual crop parameters relatively noisy.

4.5.2 Recommendations

Higher accuracies of crop parameter estimation may be obtained through the use of more physically based models that account for the variance and covariance of many variables simultaneously. However, 'multi' data are required to obtain unique solutions of the inversion of the model and to solve ambiguities. Within a single frequency band, like the X-band, 'multi' data may be multi-angle, multipolarization or multitemporal. In this study, it was shown that *multi-angle* data in the X-band were too highly correlated to help solve the inversion problem (except for beet in the early growing season). Moreover, multi-angle observations will not be very feasible from space platforms.

The aspect of *multipolarization* was only studied in the combination of vertical and horizontal co-polarization. Again, this 'multi' aspect did not improve the inversion accuracies because of the high correlation between the two states of co-polarization. However, cross-polarized backscattering (HV, VH) is generally not correlated with co-polarized backscattering (due to the multiple scattering within the canopy), and may be more useful. Also the introduction of radar polarimetry (Evans et al., 1988) may contribute to the solution of the inversion problem.

The aspect of *multitemporal* data may be used to improve the inversion algorithms through the linking with crop growth models. Crop growth is a dynamic process in which the state of the crop at one moment is not independent from that on a previous moment. The estimation of crop parameters from each single radar measurement in time does not take into account this temporal dependency. Improvement may be obtained when crop growth models are used to smooth the fluctuations in the radar backscattering curves (Bouman, 1991).

Finally, the (multi-variate) inversion scheme may be approached with *multifrequency* measurements. Because the interaction of microwaves with vegetation is wavelength dependent, the radar backscattering in different frequency bands may have a different information content.

Research into the multifrequency radar backscattering of crops was conducted in Europe during the Agriscatt 1987-1988 campaign (6 wavelengths between 1.7 and 25 cm; Attema, 1989). Preliminary results reported by Bouman et al. (1991) suggest that the L-band (25 cm wave) may be sufficiently decorrelated from the X-band (and smaller wavelengths) for combined use in agricultural applications.

5 ESTIMATION OF CROP GROWTH FROM OPTICAL AND MICROWAVE SOIL COVER

Abstract Direct derivation of biomass from radar backscattering gives erratic results so this paper discusses another method in which biomass was not estimated directly, but was found as the accumulated value of the estimated crop growth rate. The estimation was based on soil crop cover and global radiation. The relationship between soil cover in the optical and microwave regions was investigated. Analysis of the methodology showed that improvement is obtained in comparison with the direct estimation method. Despite variation in parameters for different years, a remarkable consistency in estimated biomass was observed. Nevertheless, measurements of radar backscattering still suffer from too much variation to be reliable for biomass estimation.

5.1 Introduction

In contrast to remote sensing in the optical region, radar remote sensing is hindered very little by clouds, fog or absence of global radiation during the night. Therefore, radar remote sensing provides a more reliable frequency for data collection and can be useful for a variety of land applications. In agriculture, a general demand exists for up-to-date inventories, and classifications of forests and field crops. Such inventories, however, only fulfil primary needs. Further interests are vested upon themes such as the monitoring of crop growth and development, and ultimately yield forecasting (ESA Land Applications Working Group, 1987). Up to now, much research work has been done in the field of classification with promising results (Hoogeboom, 1983, 1986; Binnenkade, 1986), but research in the field of growth monitoring and yield-prediction has made little progress. The great practical advantages of radar remote sensing are offset by the difficulties that have existed so far in the interpretation of the backscattering data, and in their conversion into biomass or into other meaningful crop characteristics.

In 1987, the MONISAR project (MONItoring with Synthetic Aperture Radar) was initiated in The Netherlands to investigate the possibilities of estimating crop growth and development from radar backscattering. For this purpose radar remote sensing data were integrated into crop growth models. These models are based on relationships between the physiological processes of plants and environmental factors such as solar radiation, temperature, day length, water and nutrient availability, etc. The development of these models for sub-optimal growing conditions is difficult and estimates of crop growth often turn out to be inaccurate. If remote sensing techniques can be used to yield information about the actual

status of a crop, growth models can be adjusted and more accurate predictions of crop growth can be made.

In this paper an attempt is made to develop a method for integrating radar remote sensing data and a basic crop growth model. The data used for this study have been derived from ground based radar experiments conducted by the ROVE (Radar Observation of VEgetation) team in the Netherlands in 1979 and 1980 (de Loor et al. 1976). The radar system utilized was an X-band scatterometer, operating at 9.5 GHzy frequency. Measurements made at vertical like-polarization VV on the crops beet, peas, and potatoes have been selected. These crops are important in European agriculture and have hardly been studied in radar remote sensing literature.

5.2 Outline of the methodology

5.2.1 The 'Cloud' equations

Radar remote sensing data can be converted into fresh weight by inversion of the so-called 'Cloud' equations. In these equations (Attema and Ulaby, 1978; Hoekman, 1980) the microwave backscattering is the weighted addition of a backscattering component of the bare soil, and that of the vegetation cover. The weighting coefficient is a function of the amount of plant water (water contained in plants), W, in the vegetation canopy, and can be called the microwave soil cover

$$f = 1\text{-}\exp(-DW/\sin\theta) \qquad (1)$$

The amount of plant water W is the fresh weight minus the dry weight of all the above-ground material of the crop canopy per unit soil surface. With the weighting coefficient, the microwave backscattering can be written as

$$\gamma = Cf + (1\text{-}f)G\exp(Km) \qquad (2)$$

where γ = normalized radar cross-section (m^2/m^2), θ = grazing angle, C = backscattering coefficient of an optically thick vegetation cover and is angle dependent (m^2/m^2), G = backscattering of dry soil, also angle dependent (m^2/m^2), W = plant water (kg/m^2), m = volumetric moisture content of the top soil (per cent), K = moisture coefficient of soil per volumetric moisture content, and D = coefficient of attenuation per unit plant water.

This relation is based on the exponential extinction of microwave radiation by the amount of plant water in the vegetation canopy. The parameter D is the coefficient of attenuation and gives the extinction of microwaves of a unit of plant water in the canopy. The parameter G is soil-specific and must be determined by regression on microwave backscattering data for bare soil. The parameter K is less

soil-specific and its value is about 0.051 (Hoekman et al., 1982). The parameters D and C are crop-specific and must be determined by regression on microwave backscattering data for crop-soil systems, using previously determined G and K values for the soil underneath the crop. If a series of measurements from bare soil exists throughout a growing season until the harvest, all four parameters can be determined in the same regression. Since the parameters C and G are dependent on the grazing angle of the radar, the regressions must be made for each grazing angle separately. The 'Cloud' equations comprise a set of the same equations with parameters for different grazing angles. An example of parameters collected in this way is given in Table 5.1.

If these parameters are known, inversion of the measured backscattering values is in principle possible in order to find W and m, by using data for different grazing angles θ. If the relative water content of the crop canopy is known from previous measurements, the amount of plant water can be used to calculate a direct estimate of dry canopy biomass.

In practice, this inversion turns out to be loaded with difficulties, especially when there is a lack of contrast between crop and soil, as occurs with potatoes (Bouman, 1988). Secondly in many crops, especially cereals, the parameters D and C have a strong azimuthal component governed by the orientation of the scatter elements, i.e. stems, leaves, and ears (van Kasteren, 1981; Ulaby and Allen, 1984). This orientation is influenced by meteorological conditions and thereby introduces a dependency of the radar backscattering on weather during measurements. Thirdly, the 'Cloud' parameters for the same crop may vary in different years (Table 5.1).

Beet causes fewer problems and attention was focussed on this crop for further analysis. Potatoes and peas have been used for comparison. The results of a direct inversion of backscattering data to dry canopy biomass, through the estimated amount of plant water and a measured value for the relative plant water content, are given for beet in two growing seasons (Fig. 5.1). The results have been obtained by using the 'Cloud' parameters collected for the same crop and the same year. To simulate future practical conditions only two angles were used for the inversion, 40° and 80° grazing angle. Because there are two parameters to be estimated, plant water and soil moisture, a minimum of two independent backscattering measurements are needed. The high grazing angles were chosen because the radar backscattering responds for a greater length of time to crop growth at high grazing angles than at low grazing angles. At a grazing angle of 20° the radar backscattering of beet reaches a saturation level relatively early in the growing season (Bouman, 1987).

Table 5.1. 'Cloud' parameters for some crops and soils, X-band radar (9.5 GHzy), vertical like-polarization. From Hoekman (1979) and van Kasteren (personal communication). The soils are alluvial clay at test farm "De Bouwing", 1979, and marine clay at test farm "De Schreef", 1980.

	C			*G*			*D*	*K*
Angle	20°	40°	80°	20°	40°	80°		
Beet 1979	0.72	0.87	0.92	0.02	0.04	0.48	0.76	0.05
Beet 1980	0.98	1.17	1.06	0.06	0.08	0.53	0.46	0.05
Peas 1979	0.39	0.41	0.22	0.03	0.06	0.43	0.41	0.05
Peas 1980	0.41	0.49	0.53	0.03	0.06	0.38	0.94	0.05
Potato 1979	0.37	0.73	1.73	0.03	0.07	0.18	0.25	0.05
Potato 1980	0.32	0.49	0.87	0.09	0.14	0.21	1.02	0.05

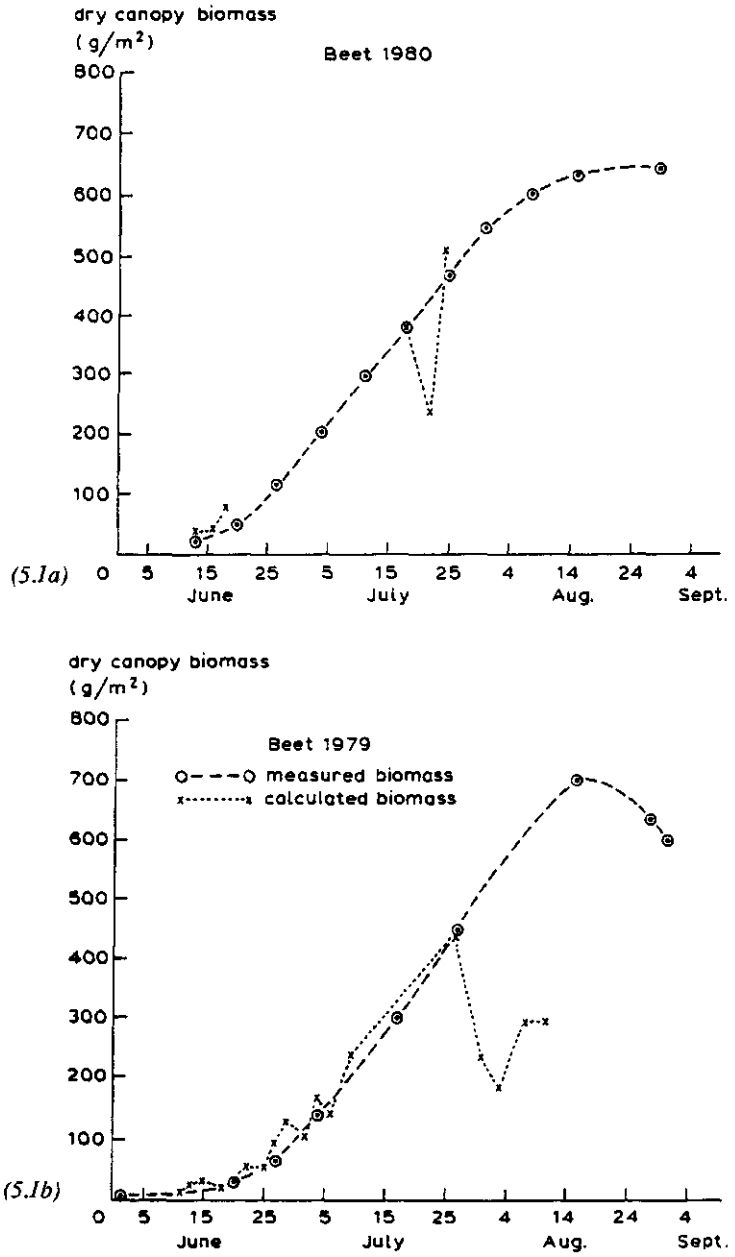

Figure 5.1. Measured and calculated dry canopy biomass as a function of time for beet (5.1a) in 1979 and (5.1b) in 1980. The calculated biomass is derived from the relative plant water content of a beet canopy, an average of 90 per cent, and from the amount of plant water estimated from inversion of the 'Cloud' equations.

In 1979, the calculated biomass followed the observed biomass with fluctuations until the end of July (Fig. 5.1a). In 1980, only 6 measurements out of thirty could be inverted to derive biomass values (Fig. 5.1b). Due to the fluctuating pattern of the backscattering measurements, twenty-four measurements fell outside the model range of grazing angles of 40° and 80° set by the factors $G\exp(Km)$ and C. When backscattering measurements at more than two grazing angles are used for the inversion, the parameters plant water and soil moisture are over-determined. Optimization techniques can then be used to arrive at a larger number of estimations of plant water with a better accuracy. However, a large number of grazing angles imposes practical problems for radar remote sensing from airborne or spaceborne platforms.

5.2.2 Crop growth rate and intercepted radiation

The poor quality of the results of this direct method necessitates another way of using the data, based on the presumption that the real crop does not fluctuate in biomass as Figure 5.1 suggests. Assuming continuity in biomass, the problem can be considered one of estimating the crop's growth rate. As shown by several authors such as Gallagher and Biscoe (1978), Milthorpe and Moorby (1979) and Monteith (1981), a crop's growth rate is closely correlated with intercepted global radiation, which can be estimated as the product of global radiation and soil cover. This means that the dry weight, W_d, of the crop is written as

$$W_d = \int R dt \qquad (3)$$

with

$$R = \alpha S f \qquad 4)$$

where R = growth rate of the crop (g/day), α = conversion efficiency to dry weight (g/J), S = incoming daily global radiation (J/m^2/day), f = fraction of green soil cover, and W_d = dry weight of the crop (g).

Our approach here was to estimate the soil crop cover from radar data and then multiply it by the global radiation collected in the conventional way. The following outlines the development of the method.

The first step was to derive the conversion efficiency α between crop growth rate, R, and intercepted global radiation, Sf, based on collected ground truth data (Fig. 5.2).

$$\left.\begin{array}{l} W_d \text{ (measured)} \\ \int Sf \text{ (measured)} \end{array}\right\} \; W_d = \alpha \int (\Sigma f)dt \rightarrow \alpha$$

Next, the regression coefficient β between the optical soil cover f, estimated in the field, and the microwave soil cover f', computed from the measured amount of plant water W, was calculated (Fig. 5.3).

$$\left.\begin{array}{l} f \text{ (estimated)} \\ f' \text{ (calculated from measured } W) \end{array}\right\} \; f = \beta f' \rightarrow \beta$$

Then, as in equations (3) and (4), the optical soil cover was replaced by the regression coefficient β, multiplied by the calculated microwave soil cover.

$$W_d = \alpha\beta \int (Sf')dt \qquad (5)$$

where f' is calculated from measured W.

Finally, the microwave soil cover calculated from the measured value for W was replaced by the microwave soil cover derived from radar backscattering measurements (Fig. 5.4).

$$W_d = \alpha\beta \int (Sf')dt$$

where f' is calculated from backscattering measurements

5.3 Calculation of the parameters α and β

5.3.1 Conversion efficiency α

Based on the ground truth collected in 1979 at test farm "De Bouwing", and in 1980 at test farm "De Schreef", the values for the efficiency factor α were derived (Table 5.2). The test farms are located in ecologically different areas some 50 kilometres apart.

Table 5.2. Conversion efficiency α of intercepted global radiation to dry weight of the crop canopy (μg/J)

	1979	1980	1979 + 1980
Beet	1.12	1.74	1.35
Peas	1.29	1.89	1.65
Potatoes	1.03	1.02	1.03

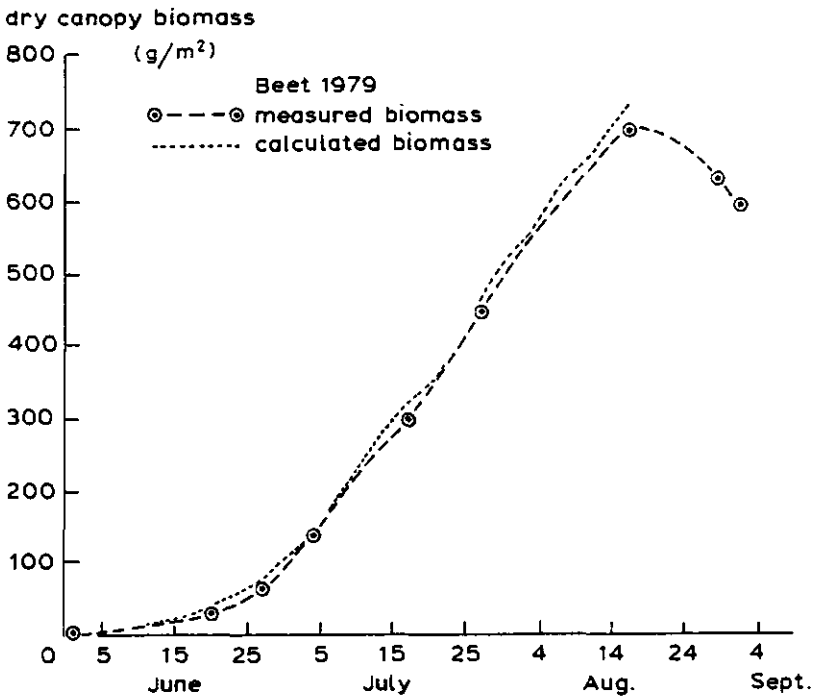

Figure 5.2. Measured and calculated dry canopy biomass of beet, 1979. The calculated biomass was found by accumulation of intercepted global radiation multiplied by the conversion efficiency derived from regression on the same data.

These data were derived from visually estimated crop cover and measured values of the canopy biomass. Due to the nature of the study, no ground truth was collected with regard to tuber biomass. Therefore, only data for the first two months of the growing season were taken into consideration in order to minimize disturbances caused by preferential growth of subsurface tubers. As a check for the method above, the integrated value of the crop growth rate of beet calculated in this way, and the measured canopy dry weight were plotted together (Fig. 5.2). The regression parameter, α, was not obtained independently of the data. Therefore, only the variability around the measured line can be used as an indication of the efficiency of this step in the method.

5.3.2 Optical and microwave soil cover

Given the good quality of the results in Figure 5.2, which were based exclusively on ground truth data, the next step was to extend the method to using radar data for estimating soil cover. To eliminate the disturbance from soil backscattering and meteorological influences on the crop canopy, microwave soil cover values were generated that were expected theoretically on the basis of equation (1). The input values for this equation were the ground truth data for the amount of plant water, W, and the values for D which gave the best correlations between the backscattering calculated by means of the 'Cloud' model and the measured backscattering (Bouman, 1987). The results are plotted against the visually estimated soil cover data for beet, peas and potatoes (Fig. 5.3). In Figure 5.3, the data for 1979 and 1980 are combined for beet and potatoes. In Figure 5.3a, the relationship between optical and microwave soil cover for beet is an S-shaped curve, although large linear stretches exist at all grazing angles. In Figure 5.3b, near-linear relationships are observed for potatoes. For peas (Fig. 5.3c), linear relationships only exist for the period of vegetative growth which agrees with the limited applicability of the 'Cloud' equations (Bouman, 1987). Because f' and f were almost linearly related over fairly large ranges, linear regression was used. The regression coefficients were calculated between the visually estimated soil cover and the theoretically expected microwave soil cover at an 80° grazing angle (Table 5.3).

Table 5.3. Regression coefficient, β, between optical soil cover, f, and calculated microwave soil cover, f', at 80° grazing angle, $f = \beta f'$

Beet	Peas	Potatoes
1.07	1.69	2.54

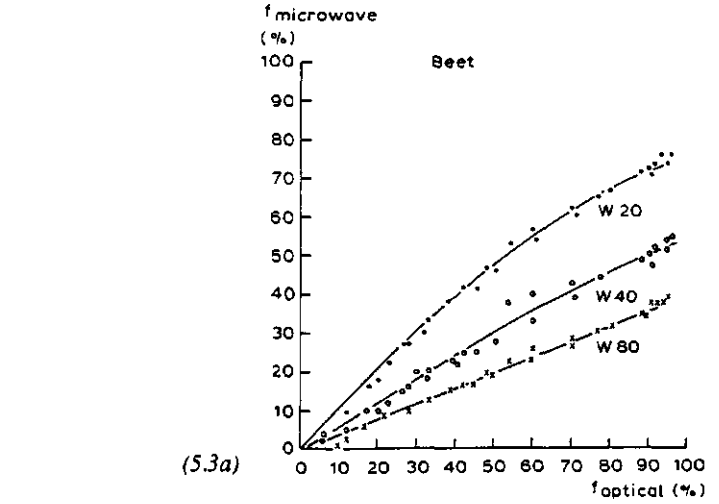

(5.3a)

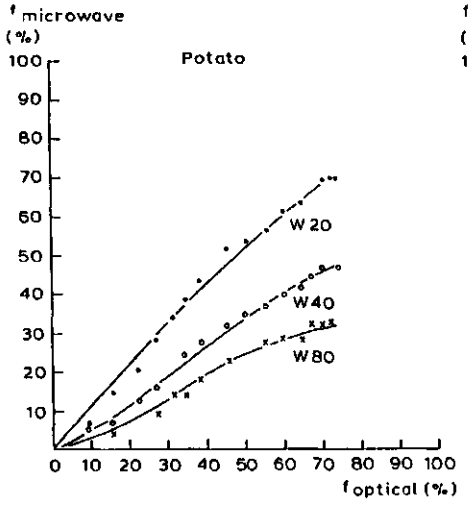

(5.3b)

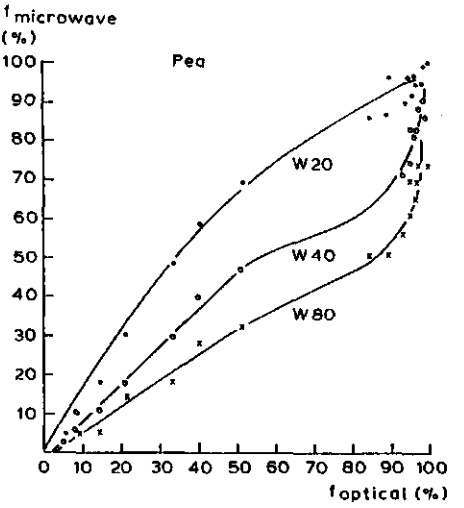

(5.3c)

Figure 5.3. Visually estimated soil cover, f, versus theoretically expected microwave soil cover, f', calculated from equation (1) from ground truth data and D values found by regression: beet (1979) D = 0.76, beet (1980) D = 0.46, potatoes (1979, 1980) D = 0.25, peas (1979, 1980) D = 0.41. Graphs are given (5.3a) for beet, (5.3b) for potatoes and (5.3c) for peas for different grazing angles: VV20, VV40 and VV80: vertical like-polarized radar waves at respectively 20°, 40° and 80° grazing angles.

The differences of the results for the crop species were due to the differences in transparency of the crop canopies to microwaves relative to the transparency in the optical region. A large value of the coefficient of attenuation D for beet coincided with a low coefficient of regression while a low value of D for potatoes coincided with a high value of the coefficient. The different values of D for beet in 1979 and 1980 coincided with similar differences in the optical transparency. Therefore, the relationship between optical and microwave soil cover of the crop was the same in both years (Fig. 5.3).

5.4 From microwave soil cover to canopy biomass

The two steps discussed above had to be combined and checked in their combined functioning. The dry weight of the crop canopy, W_d (in g) was written as

$$W_d = \alpha\beta\int(Sf')dt$$

Using the conversion efficiency and the coefficient of regression calculated above, and the microwave soil cover calculated from the measured amount of plant water, the integrated value of the crop growth rate was computed. Compared with Figure 5.2, this step in the method did not lead to an increase in the deviation of the calculated biomass from the measured biomass.

The last step was to derive the microwave soil cover from the radar observations instead of from the ground truth measurements as is described above. From inversion of the 'Cloud' equations, the amount of plant water was estimated from backscattering measurements. This estimation was used to calculate the microwave soil cover with the aid of equation (1). Using the microwave soil cover thus obtained, the integrated value of the crop growth rate could again be calculated with equations (3) and (4). In Figure 5.4, this value was plotted in time together with the measured dry biomass of the crop canopy. It should be remembered that the coefficient of regression, β, the conversion efficiency, α, and the 'Cloud' parameters were derived from the same set of data. The results were only used for comparison of the method with results from the direct estimation of canopy biomass (Fig. 5.1).

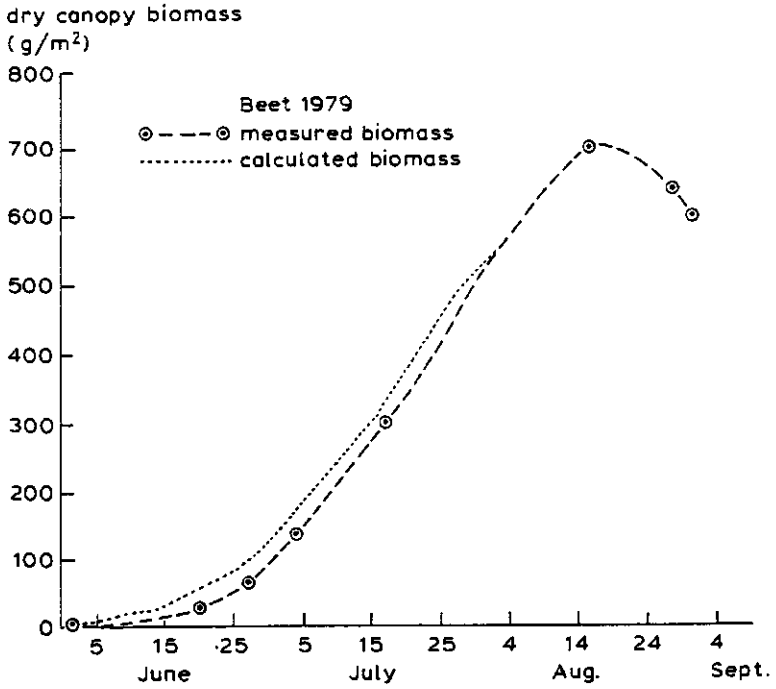

Figure 5.4. Measured and calculated dry canopy biomass of beet, 1979. See text for method of calculating dry biomass.

Compared with Figure 5.1, the method we developed led to an improvement in the calculation of the canopy biomass. The fluctuations in the curve of the calculated biomass in time had disappeared and a more realistic estimation of the biomass was obtained at the level of saturation of the backscattering. The calculated biomass, however, generally overestimated the measured biomass by some 25 g/m^2.

The method was used to predict the canopy biomass of beet from radar measurements during field experiments in 1981. That year, 15 radar measurements were made during the first two months of the growing season at the same location as in 1980. In Figure 5.5, the estimated canopy biomass is plotted together with the measured biomass. It shows the directly estimated biomass, calculated from the estimated amount of plant water by inversion of the 'Cloud' equations of 1980 and the relative water content of a beet canopy (90 per cent), and the continuously estimated biomass, based on the estimated microwave soil cover and the amount of

global radiation measured in the field. In Figure 5.5a the calculation of the estimated canopy biomass is based on the 'Cloud' parameters and conversion efficiency derived from the experiment in 1980. In Figure 5.5b the calculation is based on the 'Cloud' parameters and the conversion efficiency from the experiment in 1979.

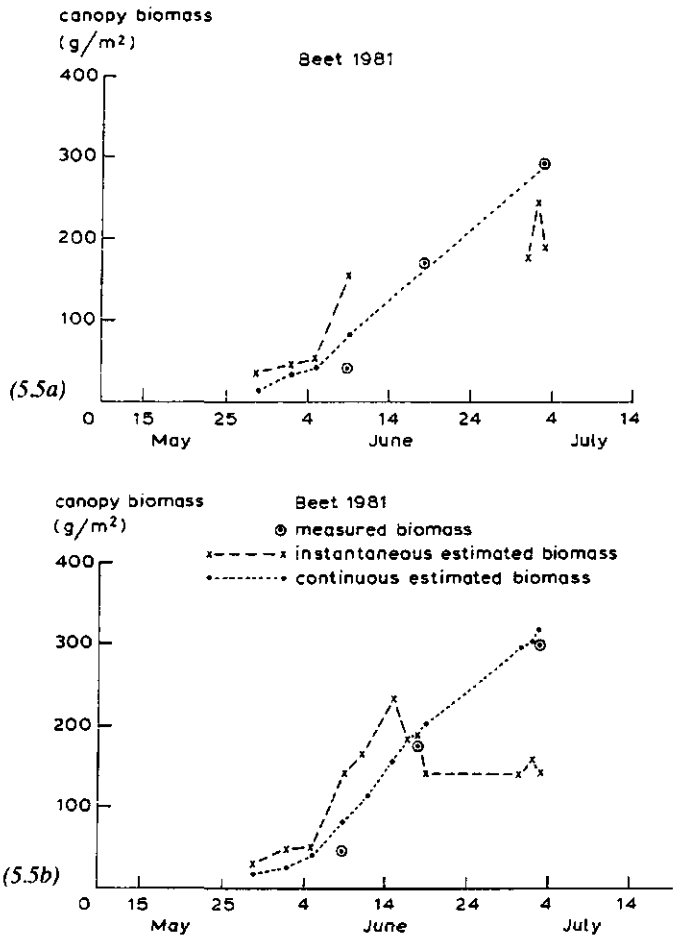

Figure 5.5. Measured and estimated dry canopy biomass of beet, 1981. Estimated biomass based on the 'Cloud' equations of (5.5a) 1980 and (5.5b) 1979.

When the 'Cloud' parameters in 1980 were used, 12 out of the 15 radar measurements could be inverted to yield estimates of the amount of plant water. By using the 'Cloud' parameters in 1979 only 7 radar measurements could be inverted.

The values of the backscattering from 10 June to 1 July exceeded the theoretical maximum of the 1979 C values (Table 5.1). This suggested that the 'Cloud' parameters from 1980 were better. The continuously estimated biomass based on the 'Cloud' parameters and the conversion efficiency from 1979 as on the parameters and the conversion efficiency from 1979, however, was just as efficient as those from 1980.

5.5 Discussion

The method of calculating dry biomass through the accumulation of the estimated rate of crop growth resulted in an improvement over the method of calculating the direct estimation of biomass. For potential use in the prediction of biomass from radar remote sensing, information should be available on the amount of daily incoming radiation for the site under consideration. This information is routinely gathered at most meteorological stations and can be input, along with other relevant information such as topographic data and crop type inventories, into any geographical information system. The radar system should deploy at least two, but preferably more, grazing angles from medium to high elevation. Based on the measurements used for this study, the backscattering measurements have to be calibrated with an absolute accuracy of 1 dB or less.

The prospects for the application of the method we have developed depends on the accuracy with which the 'Cloud' parameters and the conversion efficiencies can be determined. They also depend on the amount by which these parameters and efficiencies vary between different crop varieties and regional and climatological conditions.

Table 5.1 shows the variation that can exist in the *'Cloud' parameters* for the same crop. The parameters for the crops in 1980 were derived from experiments at a location different from the one in 1979. In a previous study, Bouman (1987) showed that the differences in 'Cloud' parameters for beet do not relate to differences in crop biomass or soil cover. The effects of the canopy structure and the plant water density on the 'Cloud' parameters is still, mostly, an unknown factor. Even if the 'Cloud' parameters are chosen correctly, the inversion of backscattering data to an estimation of the microwave soil cover still remains troublesome due to the variability in the radar measurements (Fig. 5.1b). Since much of this variation is caused by seasonal influences on the structure of the crop canopy, some improvement might be obtained by averaging the backscattering measurements over a number of sequential days.

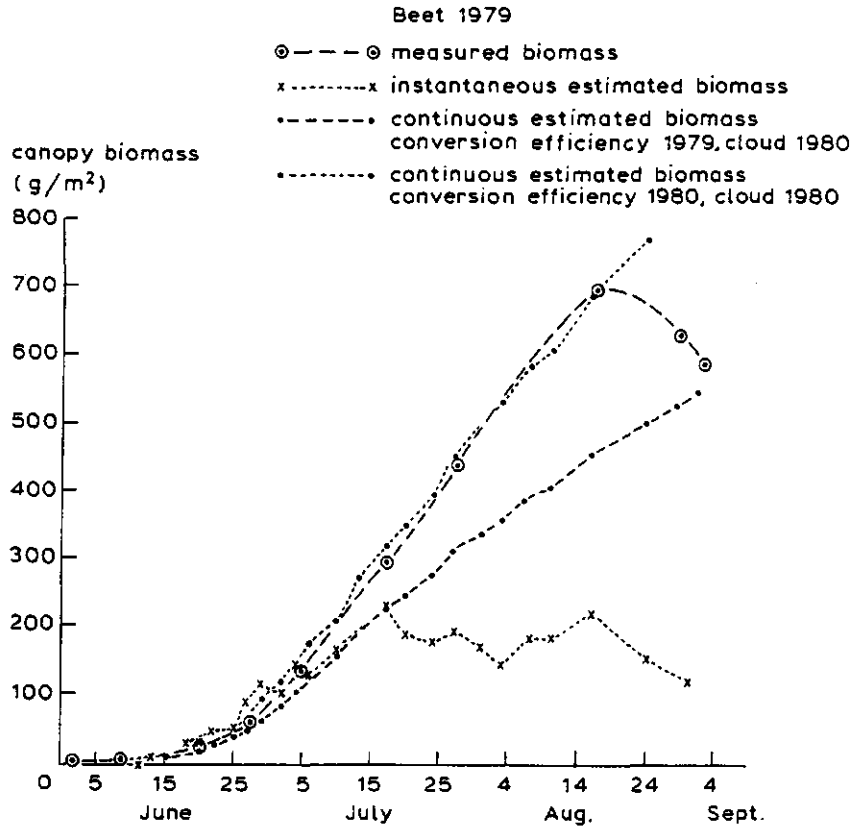

Figure 5.6. Measured and calculated dry canopy biomass of beet, 1979. The estimated biomass was found from the microwave soil cover through inversion of the backscattering data using the 'Cloud' parameters of 1980, and from the coefficient of regression β *and the conversion efficiency* α *derived from the experiments in both 1979 and 1980.*

The variation that occurs in the *conversion efficiencies* is demonstrated in Table 5.2. It is only for potatoes that this factor is the same for the two years. In theory, the linear relationship between the crop's growth rate and the intercepted global radiation is stable over a fairly wide range of external conditions. However, at various sites, deviations in the relationship for the same crop have been reported. These deviations could be due to errors in measurement, temperature differences, drought stress and diseases. Haverkort and Harris (1986) reported a range of conversion efficiencies for potato crops at the same location and related the variation to differences in air temperature. For potential use in the prediction of biomass, the method we developed should be extended to include the influences of external conditions and the limits of its applicability should be studied.

Despite the variations that occur in the 'Cloud' parameters and the conversion efficiencies for 1979 and 1980, a remarkable consistency was observed for beet when they were combined in the method we developed (Fig. 5.5). The lower value for the coefficient of attenuation, D, found in 1980, needed for the calculation of the microwave soil cover, was matched by a higher value for the conversion efficiency, α. When the biomass of beet in 1979 was calculated with the 'Cloud' parameters from 1980 and the conversion efficiency from 1979, the canopy biomass was seriously underestimated. When the canopy biomass in 1979 was predicted with all parameters from 1980, the biomass was estimated with the same accuracy as with the fitted parameters in 1979 themselves (Fig. 5.6). No explanation for this consistency in results has been found so far.

Acknowledgements

The authors would like to thank the Netherlands Remote Sensing Board (BCRS) for their financial support of this work.

6 ACCURACY OF ESTIMATING THE LEAF AREA INDEX FROM VEGETATION INDICES DERIVED FROM CROP REFLECTANCE CHARACTERISTICS, A SIMULATION STUDY.

Abstract The canopy radiation model EXTRAD was used to quantify the accuracy of Leaf Area Index (*LAI*) estimations from Vegetation Indices (VIs), derived from green and infra-red crop reflectance. The VIs were the infra-red/green (*IR/GR*) ratio, the Normalised Difference Vegetation Index *NDVI*, the Perpendicular Vegetation Index *PVI*, and the Weighted Difference Vegetation Index *WDVI*. The accuracy of *LAI* estimation was calculated in relation to variation in leaf green and infra-red colour, leaf angle distribution, soil background and illumination conditions. The theoretical calculations were supported with a field experiment on sugar beet.

Variation in illumination conditions and soil background gave relatively small estimation errors with all four VIs. The largest estimation errors resulted from variation in leaf colour and leaf angle distribution. With variation in green leaf colour, the estimation errors were lowest with the *WDVI*. With variation in leaf angle distribution, the errors were lowest with the *IR/GR* ratio and the *NDVI*. In practice, the magnitude of the error in *LAI* estimation will depend mostly on the magnitude and combination of occurring variation in leaf colour and leaf angle distribution.

In an average of 100 random combinations of disturbing conditions, and in a field experiment with sugar beet, the absolute estimation errors ranged between about 0.1 for $0<LAI<1$ and 0.35 for $3<LAI<5$.

6.1 Introduction

In the past 20 years, a number of vegetation indices (*VI*) has been constructed to aid the interpretation of remotely sensed data in the optical wavelength region. VIs are linear, orthogonal or ratio combinations of reflectances in the green (*GR*) and/or red (*R*), and infra-red (*IR*) part of the spectrum. Examples are the *IR/GR* ratio (first used by Jordan, 1969), the Normalized Difference Vegetation Index, *NDVI* (developed as '*VI*' by Rouse, 1973), the Perpendicular Vegetation Index, *PVI* (Richardson and Wiegand, 1977), and the Weighted Difference Vegetation Index, *WDVI* (Clevers, 1989). The calculation formulae are

$NDVI = (IR-GR)/(IR+GR)$
$PVI = \sqrt{[(IR-IR_s)^2+(GR-GR_s)^2]}$
$WDVI = IR-(IR_s/GR_s)GR$

where: *GR* and *IR* is the *GR* and *IR* crop reflectance respectively, and GR_s and $IR_s$is the *GR* and *IR* reflectance of (the underlying) bare soil respectively.

The main function of VIs is to minimize the effect of 'disturbing' factors on the relationship between reflectance and crop characteristics of interest such as crop type, Leaf Area Index (*LAI*) or canopy biomass. Disturbing factors may be illumination conditions, soil background and crop parameters of other interest such as leaf colour and canopy structure.

The choice and suitability of a *VI* for agricultural application is generally determined by its sensitivity to the crop parameter of interest, and/or to its sensitivity to disturbing factors (Bunnik, 1978; Clevers, 1988, 1989; Huete et al, 1984a, 1984b; Richardson and Wiegand, 1977; Tucker, 1979; Vygodskaya, 1989). However, the key property of a *VI* for application in agriculture lies in its inverse use, i.e. the *accuracy of crop parameter estimation*. Den Dulk (1989) is one of the few who systematically presented some errors in the estimation of *LAI* from a *VI*. He used the *LAI-NDVI* relationship, as calculated with the model TURTLE for a reference crop under reference conditions, to estimate the *LAI* with deviations in input parameters from the reference crop (Table 6.1).

In this paper, a theoretical sensitivity analysis will be given to quantify the accuracy of *LAI* estimation from VIs in relation to specific disturbing factors. The *LAI* was chosen as crop parameter because of its general importance in agriculture (e.g. crop growth and transpiration modelling). The analysis was based on model simulations with the canopy radiation model EXTRAD (Goudriaan, 1977) that describes the visible and infra-red reflection of leaf canopies. The simulation results were compared with a field experiment with sugar beet.

6.2 Method and materials.

The VIs were calculated from the nadir (90° angle with the horizontal plane) reflectances in the green (*GR*) and the infra-red (*IR*) spectral wavelength bands. The use of nadir reflectance corresponds with the general practice of remote sensing from satellites and with hand held radiometers. The choice of the green band rather than the more generally used red band was guided by the availability of field data for this study. For the (theoretical) sensitivity analysis, this choice did not make any difference since the studied range in leaf colour could apply to both the *R* and the *GR* band.

Table 6.1. Error in LAI estimation from the NDVI, with deviations in crop, soil and observation conditions from a reference crop. The reference crop had a spherical leaf angle distribution, isotropically scattering leaves, a soil background with an average reflection coefficient, and a sun's inclination angle of 60°. The calculations for the cotton plant were based on measurements presented by Lang (1973). Source: J.A. den Dulk (1989), The interpretation of remote sensing, a feasibility study, Thesis, Agricultural University Wageningen, p. 115.

LAI:	0.57	1.37	2.74
Bright leaves	0	0.01	0.01
Dark leaves	0	0	0.01
Specularly refl. leaves	0.02	0.01	0.02
Rough leaves	0.03	0.05	0.09
Erectophile crop	0.07	0.07	0.05
Planophile crop	0.16	0.14	0.10
Cotton	0.31	0.26	0.19
Dark soil	0.19	0.11	0.05
Bright soil	0.03	0.03	0.02
Sun's inclination 45°	0.09	0.07	0.06
Minimum observed value	0	0	0
Maximum observed value	0.16	0.16	0.27
Erectophile, rough leaves	0.11	0.11	0.15
Planophile, rough leaves	0.13	0.09	0.02
Cotton, min. sun's incl.	0.24	0.20	0.17
Cotton, max. sun's incl.	0.53	0.44	0.26

6.2.1 The canopy radiation model EXTRAD

GR and *IR* nadir crop reflectance was calculated with the canopy radiation model EXTRAD developed by Goudriaan (1977). It is beyond the scope of this paper to discuss in detail the formulae and computation procedures. Goudriaan (1977, pp 143-145)) gave a complete listing of the model, and Bunnik (1978, pp 26-29) presented a condensed summary of the calculation procedures.

A brief description of EXTRAD is as follows. The canopy is subdivided into a number of horizontal infinitely extended layers. The optical behaviour of a layer is

calculated as a function of the scattering coefficient of the leaves (equal hemispherical reflection and transmission), and of the leaf angle distribution. The azimuthal orientation of the leaves is assumed to be uniform. Nine inclination intervals from 10° each are used to describe the leaf angle distribution, and to compute the fluxes of upward and downward radiation through the layers of the canopy.

The radiation profile in the canopy is calculated with a relaxation method. The boundary conditions are the soil with ideal diffuse reflectance, and the total incident radiation on the top layer of the canopy. The incident radiation is subdivided into a direct solar component and a diffuse sky component emanating from nine equal intervals in the upper hemisphere. The canopy reflectance in a given direction (10° interval) is then computed from the total radiance leaving the top layer of the canopy in that direction.

The model input of EXTRAD is given in Table 6.2.

Table 6.2. Input for the model EXTRAD for canopy reflectance and values chosen for sugar beet. The spherical leaf angle distribution is explained in Table 6.4.

Input parameter	Value	
Leaf GR scattering coefficient	0.294	(*)
Leaf IR scattering coefficient	0.974	(*)
Leaf angle distribution	spherical	
Hemispherical soil reflectance GR	0.146	(*)
Hemispherical soil reflectance IR	0.178	(*)
Fraction diffuse sky irradiance	0.7	
Sun's elevation angle	60°	

(*) = fitted values to data set

A comparative study between the EXTRAD model and the models SAIL (Verhoef, 1984) and TURTLE/HARE (Den Dulk, 1989) revealed a very close agreement in results between all three with equal input values (Clevers, pers. comm.).

6.2.2 Model calibration

For this study, the model EXTRAD was calibrated on (nadir) reflectance data on sugar beet. The data were collected using a portable radiometer at intervals of

two to three weeks during the growing seasons of 1987 and 1988, on six fields in the Dutch Flevopolder. These fields belonged to different farmers who cultivated different sugar beet varieties: Regina (2x), Accord (2x), Salohil and Univers.

The *GR* reflectance was measured at 548 nm with a bandwidth of 31 nm, and the *IR* reflectance at 823 nm with a bandwidth of 80 nm. At each field and day of observation, ten measurements were averaged at each wavelength band. The radiometer was calibrated at construction and the stability was monitored by measuring panels of known reflectance values at the end of the growing season. The *LAI* of the crops was measured on the same day as the reflectance measurements. The total number of reflectance and *LAI* data was 33 (all fields, two years).

The model EXTRAD was calibrated on the data in the individual spectral bands of all six fields together. The calibration procedure was based on a controlled random search algorithm as developed by Price (1979) and extended by Klepper (1989) and Rouse (in prep.). Fitted values were obtained for the *GR* and *IR* scattering coefficients of the leaves, and for the hemispherical reflection coefficients of the soil. All parameters were assumed to be constant during the growing season. The calibrated values of the model parameters are given in Table 6.2.

6.3 Model simulations

The set of model parameters given in Table 6.2 was used to calculate the *IR/GR* ratio, the *NDVI*, the *PVI* and the *WDVI* for *LAI* values from 0 to 5. This parameter set was the standard set and the obtained curves were the standard curves around which the effects of disturbing factors were studied. The disturbing factors were deviations from the standard parameter set, and are given in Table 6.3. They were grouped in three general classes: 1) illumination condition (fraction diffuse sky irradiance and sun elevation angle), 2) soil background, and 3) canopy condition (leaf *GR* and *IR* colour, leaf angle distribution).

Ad 1) illumination condition. The fraction diffuse sky irradiance ranged from a completely clear sky, a minimum of 0.2, to a fully clouded sky, 1.0. The minimum sun's elevation angle was determined by the angle at which accurate reflection measurements could still be made in the field, about 30°. The maximum was set for Mid-North European latitudes, about 70°.

Ad 2) Soil background. Since the soil type under consideration had a medium reflection coefficient, disturbing effects were calculated for a light and a dark soil. The input values were the same as those used by Vygodskaya et al. (1989, p. 1860). A difference in soil moisture was implicitly present in the choice of the light and the dark soil with GR_s:IR_s respectively 0.06:0.09 and 0.25:0.35.

Table 6.3. Variations in model parameters (Table 6.2) as used for the sensitivity analysis.

Parameter	Values
Leaf *GR* scattering coefficient	0.25, 0.35
Leaf *IR* scattering coefficient	0.95, 0.99
Leaf angle distribution	planophile, erectophile, plagiophile, extremophile, uniform
Hemispherical soil reflectance GR_s	0.06, 0.25 (*)
Hemispherical soil reflectance IR_s	0.09, 0.15, 0.35 (*)
Fraction diffuse sky irradiance	0.2, 0.4, 0.6, 0.8, 1.0
Sun's elevation angle	30°, 40°, 50°, 70°

(*) soil reflectance only in the combinations:
GR_s:IR_s = 0.06:0.09, 0.06:0.15, 0.25:0.35

The IR_s/GR_s ratio of these soils was about the same, thus representing a dry and a wet condition respectively of a same soil type (Clevers, 1988).

Ad 3) canopy condition. The range in leaf *GR* and *IR* scattering coefficient was derived from reflection and transmission measurements on individual green and yellowish leaves. The measured range in the *GR* scattering coefficient was twice as large as that in the *IR*. The leaf angle distributions were taken from Bunnik (1978, pp 35-36), and are given in Table 6.4.

Table 6.4. Leaf angle distribution functions according to Bunnik (1978). θ is the angle between the leaf axis and the horizontal plane.

Planophile	$2(1+\cos 2\theta)/\pi$
Erectophile	$2(1-\cos 2\theta)/\pi$
Plagiophile	$2(1-\cos 4\theta)/\pi$
Extremophile	$2(1+\cos 4\theta)/\pi$
Spherical	$\sin\theta$
Uniform	$2/\pi$

6.3.1 The sensitivity of VIs

As an example, the effect of deviations in leaf angle distribution and in *GR* leaf colour on the *NDVI-LAI* and the *WDVI-LAI* relationship is given in Figure 6.1.

First it is noted that the *WDVI* was sensitive to *LAI* over a larger *LAI* range than the *NDVI*. Where the *NDVI* 'saturated' at an *LAI* of about 3, the *WDVI* 'saturated' only after an *LAI* of 5. The *WDVI* was more sensitive to *leaf angle distribution* than the *NDVI*, thus offsetting its larger sensitivity to *LAI*. Compared to the effect of leaf angle distribution, that of *GR leaf colour* was much smaller for the *WDVI*, and a bit larger for the *NDVI*. The *WDVI* was slightly less sensitive to *GR* leaf colour than the *NDVI*.

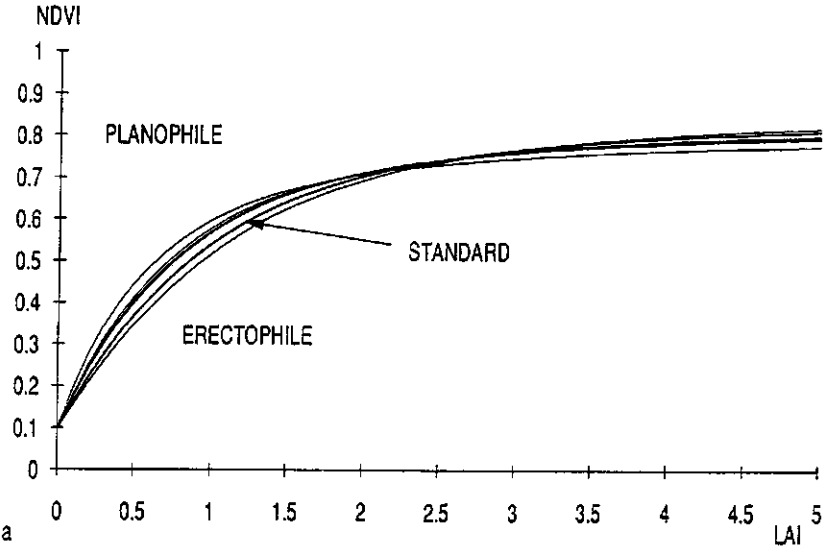
NDVI
1
0.9
0.8
0.7
0.6
0.5
0.4
0.3
0.2
0.1
0
PLANOPHILE
STANDARD
ERECTOPHILE
0
0.5
1
1.5
2
2.5
3
3.5
4
4.5
5
LAI

6.1a

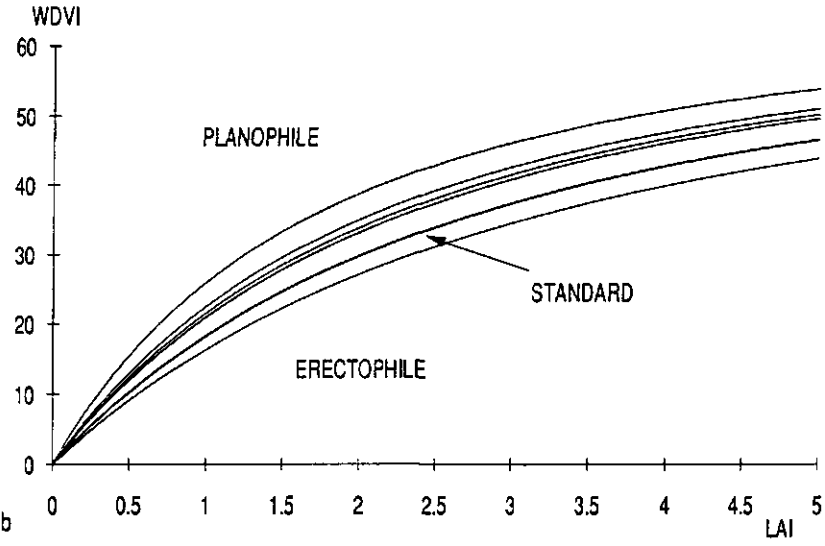
WDVI
60
50
40
30
20
10
0
PLANOPHILE
STANDARD
ERECTOPHILE
0
0.5
1
1.5
2
2.5
3
3.5
4
4.5
5
LAI

6.1b

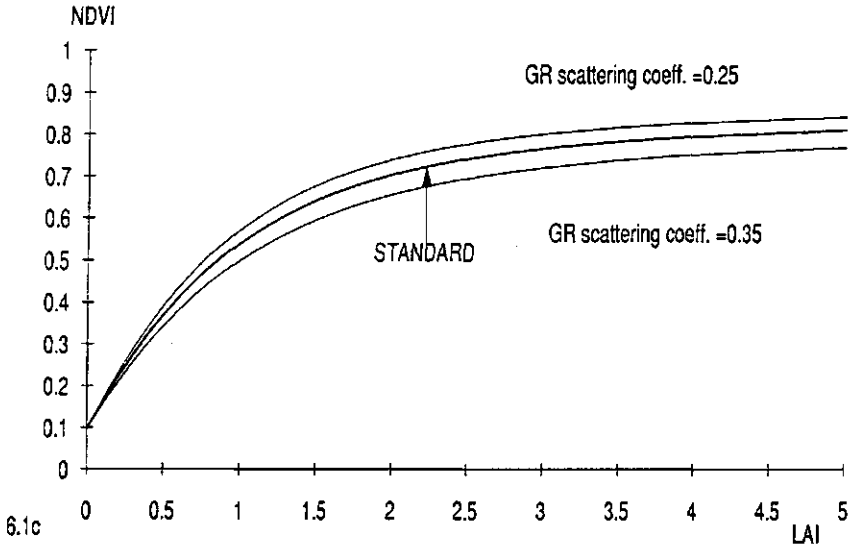

6.1c

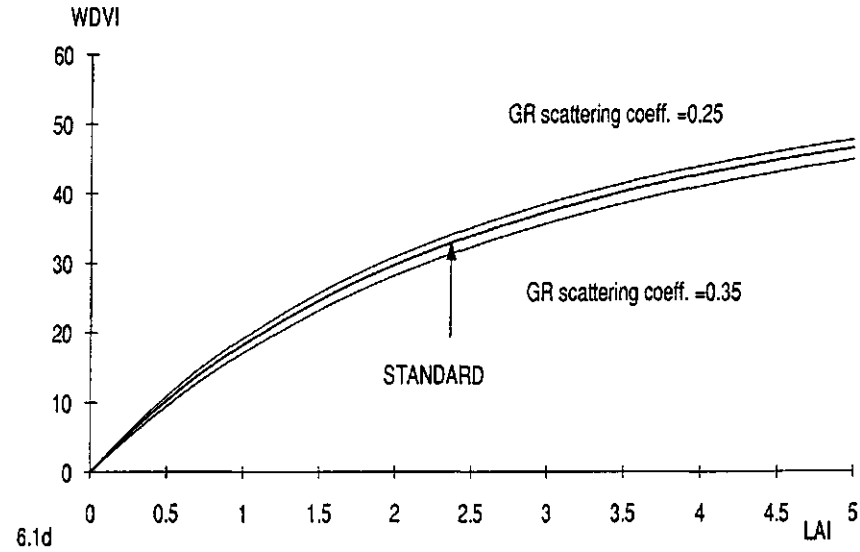

6.1d

Figure 6.1. The effect of canopy properties on the theoretical relationship between LAI and the computed vegetation indices NDVI and WDVI. Figs. 6.1a and 6.1b give the effect of leaf angle distribution, and Figs. 6.1c and 6.1d for the green scattering coefficient of the leaves.

To compare the effects of the variation in parameter values (disturbing factors) on the VIs, the sensitivity to these parameters was calculated as a normalized standard deviation S':

$$S' = S/\overline{VI}$$

where S is the standard deviation:

$$S = \sqrt{[\sum(VI'-VI)^2/N-1]}$$

where VI = VI at standard parameter and LAI value; VI' = VI at alternative parameter value and standard LAI value; $\overline{VI}$ = average value of VI in the 0-5 LAI range; N = number of VI calculations in the 0-5 LAI range.

S' indicated the sensitivity of the VI to changes in parameter values as an average over the whole LAI range. It was normalized to the average value of the VI to compare the values for the different VIs. Table 6.5 gives the average S' per parameter listed in Table 6.4.

Table 6.5. Average sensitivity S' of the VIs to variations in canopy properties, soil background and illumination conditions (Table 6.3).

Parameter	*IR/GR*	*WDVI*	*NDVI*	*PVI*
Leaf GR	26.8	5.3	9.1	1.9
Leaf IR	10.1	12.0	3.1	14.6
Leaf angle distribution	9.1	18.4	5.0	26.5
Soil background	10.8	19.3	14.2	24.6
Fraction diffuse sky irradiance	3.2	4.4	2.5	4.6
Sun's elevation angle	1.4	2.8	1.1	3.6

From this Table, two general conclusions were drawn. 1) All VIs were comparatively least sensitive to changes in illumination conditions. 2) The *PVI* was most sensitive to all disturbing factors, except for *GR* leaf colour, and the *NDVI* was generally the least sensitive to disturbing factors.

6.3.2 The accuracy of LAI estimation

The next step consisted of analysing the effect of the disturbing factors on the accuracy of *LAI* estimation. Therefore, the standard curves of the VIs, calculated with the standard parameter set from Table 6.2, were inversely used to estimate *LAI*. The VIs calculated with the deviating parameters from Table 6.3 resulted in *LAI* estimations *LAI'* which deviated with *dLAI* from the true *LAI*:

LAI(*true*) ----------> *VI*(*true*)
with disturbing factor

VI(*true*) ----------> *LAI'*
inverse standard relationship

$$dLAI = |LAI - LAI'|$$

The estimated *LAI'* was limited to a maximum of 5 to avoid unrealistic values. It is important to consider the values of *dLAI* along the 0-5 *LAI* range and not to analyse the results on an average basis over the whole *LAI* range (see example of Fig. 6.1). The values of *dLAI* were averaged per disturbing factor for each *VI*, and are presented as function of *LAI* in Figure 6.2. For all disturbing factors but soil background, the estimation accuracy was lowest at low values of *LAI* and generally increased with *LAI*.

Illumination conditions had the smallest effect on the accuracy of *LAI* estimation for all four VIs (note the difference in *dLAI* scale between Figs. 6.2a/b and 6.2c-f). Errors in *LAI* estimation were generally not higher than 0.25 at high levels of *LAI*. The *IR/GR* and the *NDVI* had generally the lowest estimation errors. The low errors implicate that no further correction on remotely sensed optical data for illumination condition is needed.

Soil background had the second smallest effect on the estimation accuracy. The *IR/GR* ratio and the *NDVI* limited the error to 0.25, the *WDVI* and the *PVI* to about 0.4. The errors were constant over the whole *LAI* range.

Canopy properties had relatively the largest effect on the estimation accuracy. *GR* leaf colour largely affected the estimation errors with the *IR/GR* ratio and the *NDVI*: the errors sharply increased from about 0.5 at an *LAI* of 2, to 3.5 at an *LAI* of 4.5. The *PVI* and the *WDVI* limited the errors to 0.1 and 0.4 respectively at a high *LAI* of 5.

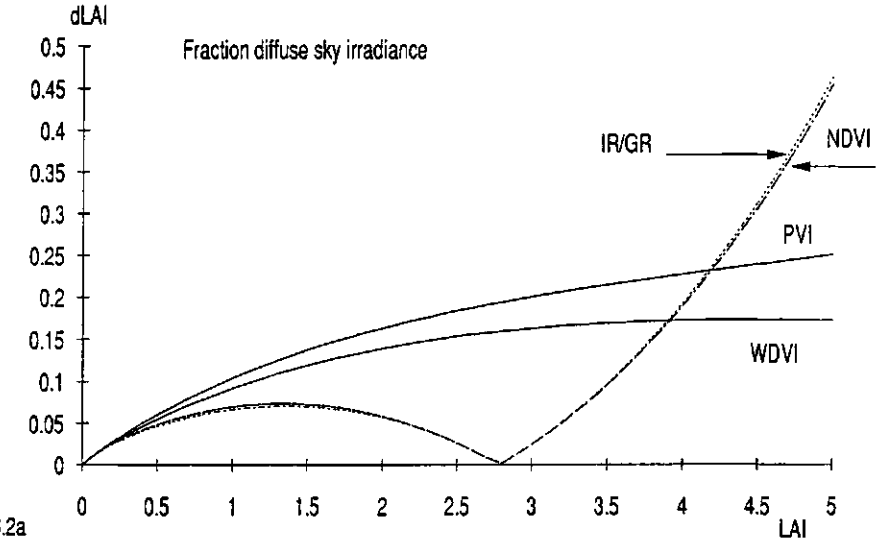
dLAI
Fraction diffuse sky irradiance
IR/GR
NDVI
PVI
WDVI
0.5
0.45
0.4
0.35
0.3
0.25
0.2
0.15
0.1
0.05
0
0
0.5
1
1.5
2
2.5
3
3.5
4
4.5
5
LAI

6.2a

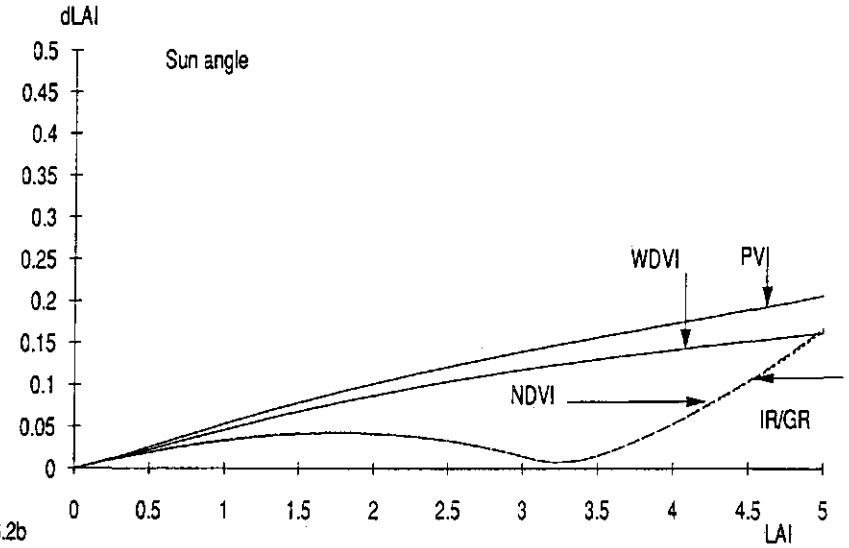
dLAI
Sun angle
WDVI
PVI
NDVI
IR/GR
0.5
0.45
0.4
0.35
0.3
0.25
0.2
0.15
0.1
0.05
0
0
0.5
1
1.5
2
2.5
3
3.5
4
4.5
5
LAI

6.2b

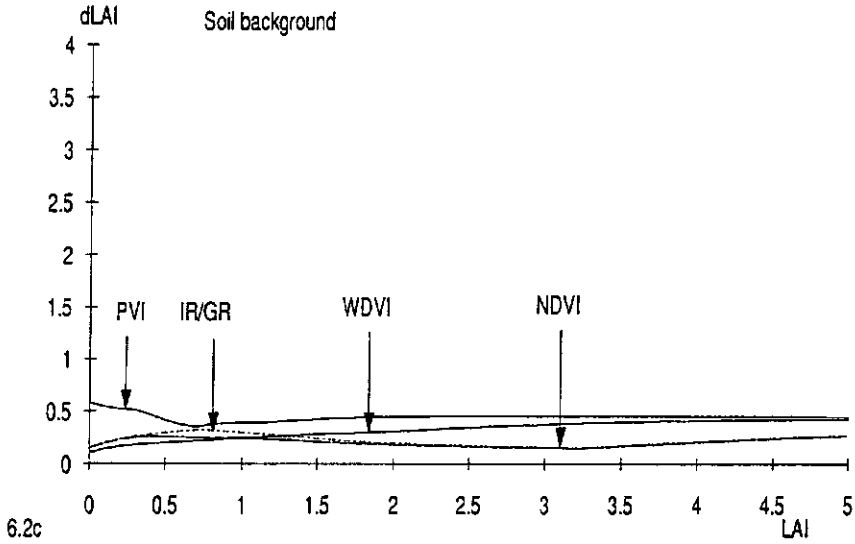
dLAI
Soil background
4
3.5
3
2.5
2
1.5
1
0.5
0
PVI
IR/GR
WDVI
NDVI
0
0.5
1
1.5
2
2.5
3
3.5
4
4.5
5
LAI

6.2c

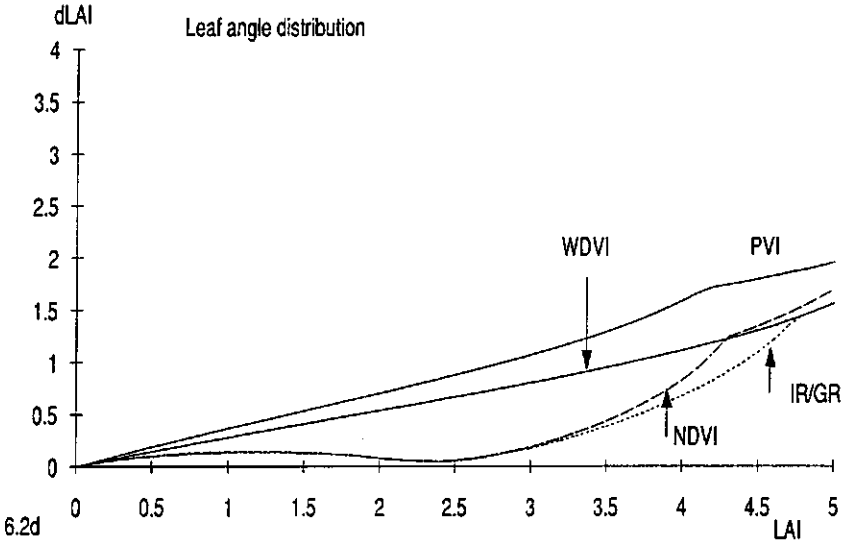
dLAI
Leaf angle distribution
4
3.5
3
2.5
2
1.5
1
0.5
0
WDVI
PVI
IR/GR
NDVI
0
0.5
1
1.5
2
2.5
3
3.5
4
4.5
5
LAI

6.2d

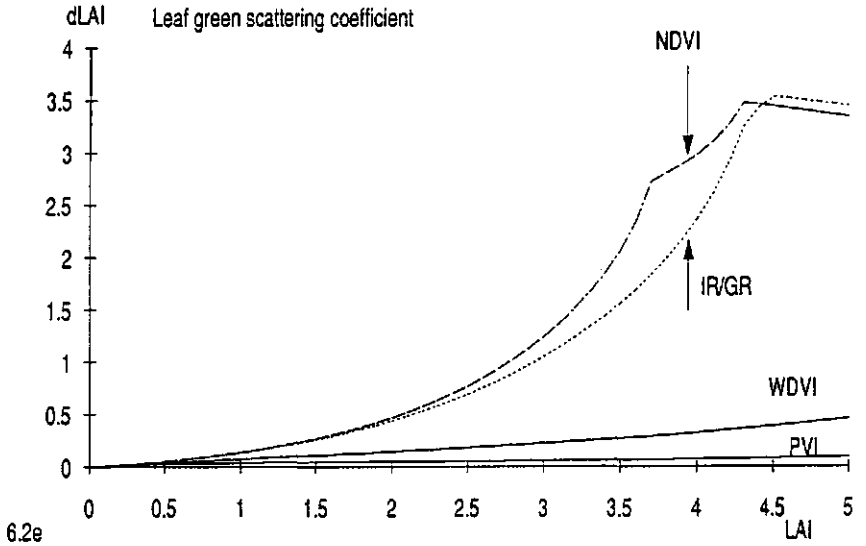

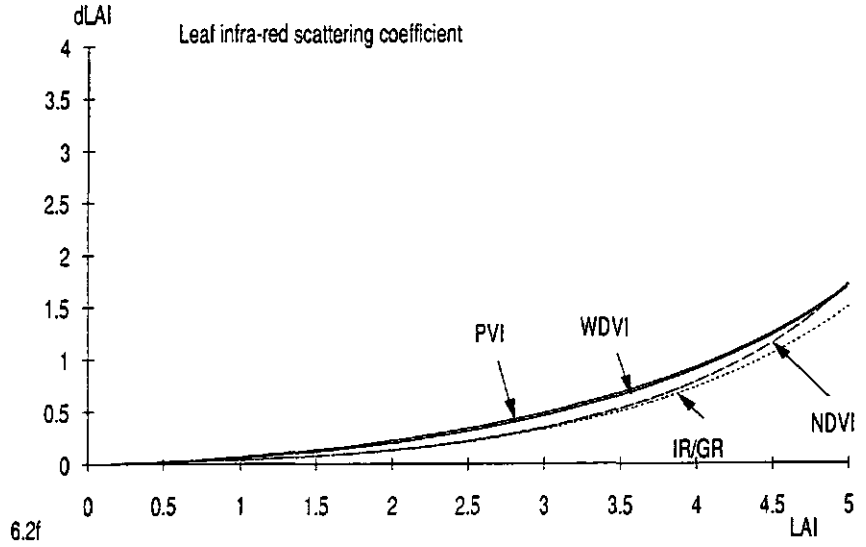

Figure 6.2. Theoretical error in LAI estimation from the IR/GR ratio, the NDVI, the WDVI and the PVI, as a function of LAI. The errors were due to variations in fraction diffuse sky irradiance (6.2a), sun angle (6.2b), soil background (6.2c), leaf angle distribution (6.2d), leaf green scattering coefficient (6.2e), and leaf infra-red scattering coefficient (6.2f).

The effect of *IR* leaf scattering coefficient was comparable with all four VIs. The errors ranged from about 0.5 at medium *LAI* levels to 1.5 at high *LAI* levels.

The estimation errors caused by leaf angle distribution were again lowest with the *IR/GR* ratio and the *NDVI*; they limited the errors to 0.25 at *LAI* values up to 3. The estimation errors with the *PVI* and the *WDVI* steadily increased from 0 at an *LAI* of 0, to 1.5 at an *LAI* of 5.

The example of the effect of *GR* leaf colour clearly demonstrated the necessity to evaluate the performance of the VIs in terms of estimation accuracy. From Table 6.5 it is read that the average sensitivity *S'* of the *IR/GR* ratio to *GR* leaf colour was three times larger than that of the *NDVI*. The lower *S'* of the *NDVI* however, was counter-affected by its lower sensitivity to *LAI*. The end result, the accuracy of *LAI* estimation, was similar for both.

Figure 6.2 suggests that, in practice the optimum *VI* for estimation of *LAI* will be largely determined by occurring variations in *GR* leaf colour. With a stable *GR* leaf colour, the estimation errors will be lowest with the *IR/GR* ratio and the *NDVI*. When *GR* leaf colour is variable, the estimation errors will probably be lowest with the *WDVI*. The estimation errors were largest with the *PVI* for all other disturbing factors.

The final error in *LAI* estimation in field situations will depend on the combination and magnitude of occurring disturbing factors, especially *GR* leaf colour and leaf angle distribution. The effect of variation in one factor might either counter-affect or reinforce that in another factor. To simulate possible field situations, the model EXTRAD was run 100 times with a random selection of parameter values chosen between the boundary values given in Table 6.3. The errors in *LAI* estimation were averaged over these 100 runs and given in Figure 6.3a. In this example, the estimation errors were lowest nearly throughout the whole 0-5 *LAI* range with the *IR/GR* ratio and the *NDVI* (exactly the same errors). The estimation error was limited to 0.15-0.25 between *LAI* values of 0 and 2.5, and increased to 1.25 at an *LAI* of 5. The estimation error was only smaller with the *WDVI* at *LAI* values lower than 0.5. The estimation errors were largest with the *PVI* because of the accumulation of large errors with all disturbing factors (except *GR* leaf colour).

6.4 Field verification

The data set of the radiometer measurements used to calibrate the EXTRAD model comprised variations in disturbing factors. Reflectance measurements were made with either a dry or a wet top soil, depending on the natural whims of rainfall. They were also made in the course of a whole day so that variation in illumination

conditions was present. Furthermore, the data set consisted of measurements on different fields in two years. This set was therefore suitable to study the accuracy of *LAI* estimation from VIs in a specified, regional agricultural situation.

The VIs were calculated from the measured *GR* and *IR* reflectances and plotted against measured *LAI*. The model EXTRAD was fitted to these data for each *VI* separately to obtain the best curve per *VI*. This resulted in only minor differences in the fitted parameters for the four VIs. An example is given in Figure 6.4 for the *IR/GR* ratio and the *WDVI*. For both VIs, the fitted curve ran nicely through the data set. For the *IR/GR* ratio, the scatter around the curve was larger at high values of *LAI* than at low values, suggesting variation in *GR* leaf colour (compare Fig. 6.2e). For the *WDVI*, the scatter around the curve at high values of *LAI* was smaller.

The fitted curves through the *VI-LAI* data sets were now used to estimate *LAI* from the measured VIs. The estimated *LAI* was compared with the measured *LAI* to give the error in estimation *dLAI*. For graphical presentation, the errors were smoothed by taking the average of a *dLAI* value with two neighbouring values (Fig. 6.3b). The best *VI* for accurate estimations of *LAI* in this data set was the *WDVI*: the estimation error was about 0.1 at low values of *LAI* and averaged 0.35 at high values of *LAI*. The estimation errors with the *IR/GR* ratio and the *NDVI* were mutually nearly identical and averaged 0.1 at low levels of *LAI*, and 0.8 at high levels.

The magnitude of the errors of estimation in Figure 6.3b compared favourably with those of the simulation study in Figure 6.3a up to *LAI* values of 3. After *LAI* values of 3, the errors were smaller in the field experiment than in the simulation study. In both cases, the estimation errors were highest with the *PVI* at all values of *LAI*. In the simulation study, however, the estimation errors were lowest with the *IR/GR* ratio and the *NDVI*. In the field experiment, the errors were lowest with the *WDVI*. The lower estimation errors with the *WDVI* in the field experiment again suggested a relatively large variation in *GR* leaf colour compared to that in other disturbing factors, especially leaf angle distribution. Field observations and literature (De Wit, 1965; Loomis and Williams, 1969) indicate that sugar beet has a high consistency in leaf angle distribution throughout the growing season.

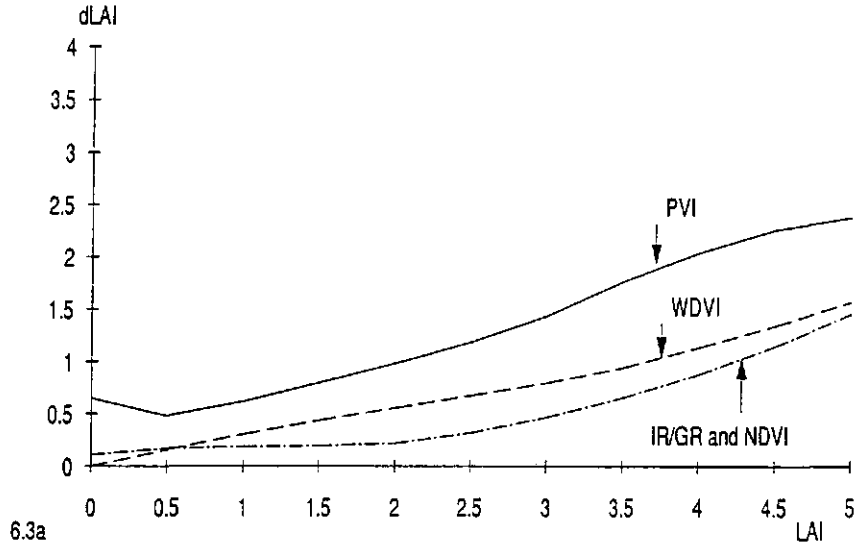

6.3a

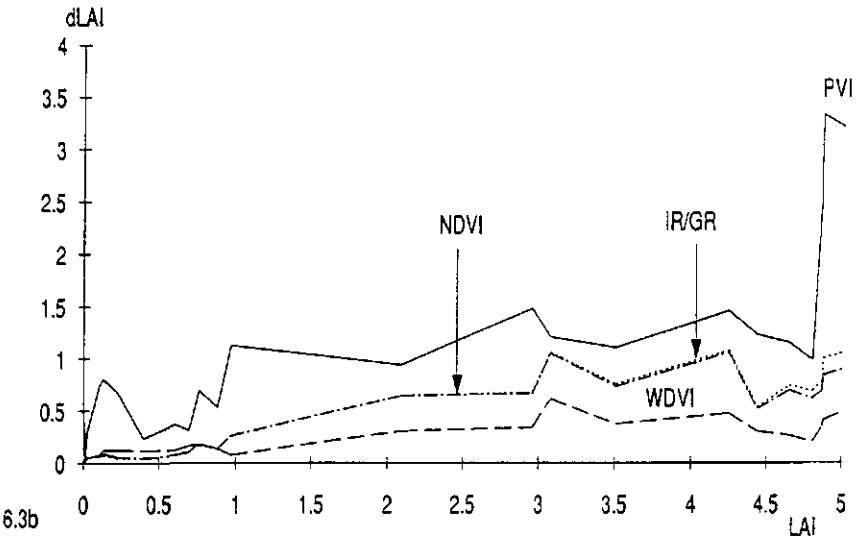

6.3b

Figure 6.3. Comparison between theoretical and experimental error in LAI estimation. In 6.3a, the theoretical error in LAI estimation was averaged over hundred selections of random combinations in disturbing factors (Table 6.3). In 6.3b, the errors were calculated from experimental data on sugar beet.

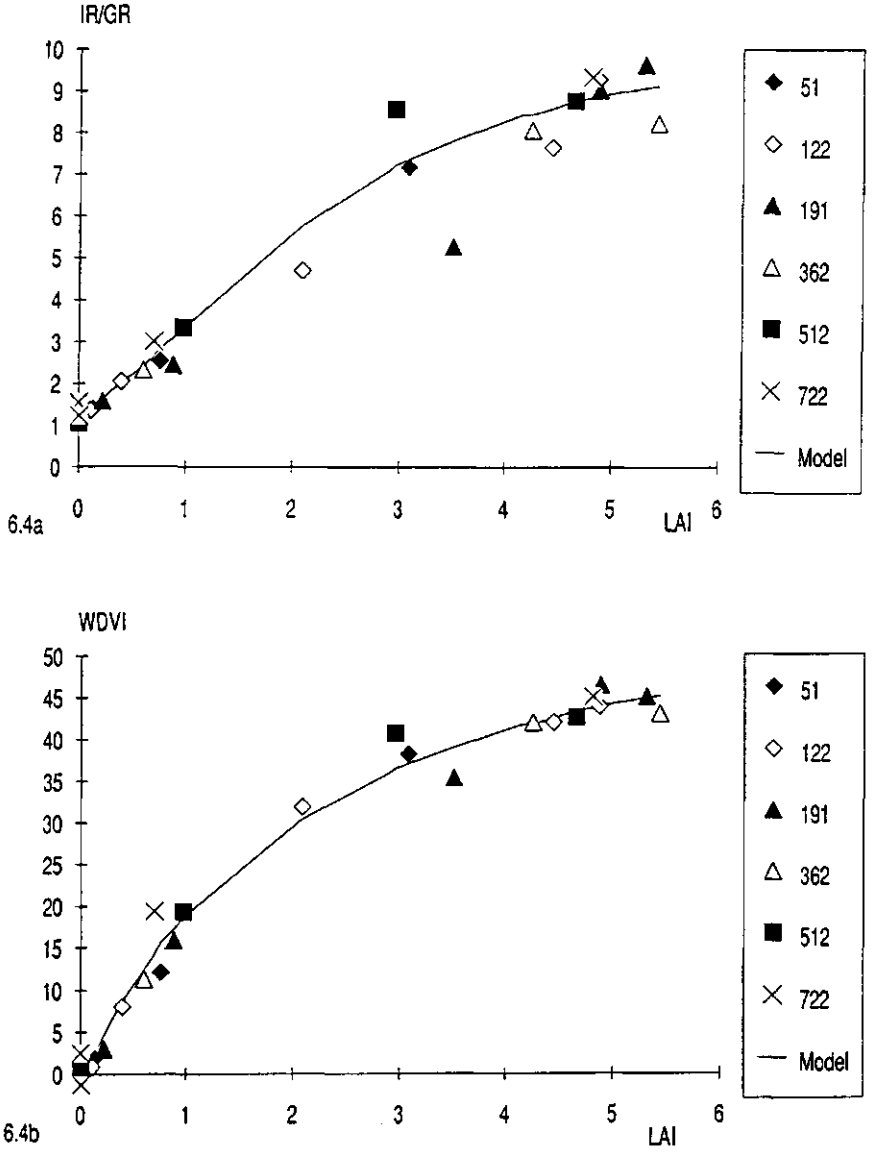

Figure 6.4. Measured IR/GR reflectance ratio (6.4a) and WDVI (6.4b) versus LAI for sugar beet. The fitted curve with the model EXTRAD is given by the solid line. The numbers in the legend refer to different sugar beet fields.

6.5 Discussion

The simulation study for average disturbing conditions, and the field experiment indicated that the *LAI* could be estimated from either the *IR/GR* ratio and the *NDVI*, or the *WDVI*, with accuracies that ranged between about 0.1 for $0<LAI<1$ and 0.35 for $3<LAI<5$. These values agree with the magnitude of the errors given in Table 6.1 (Den Dulk, 1989). In practice, the accuracy of estimating *LAI* will depend largely on the occurring variation in leaf colour. Even in sugar beet that has no phase of ripening and yellowing of the canopy, the *WDVI* was the best *VI* for estimating *LAI*.

In the analysis of the field experiment, the error in the standard *LAI* determination through leaf surface measurements (typically 0.25 to 0.4 at *LAI* values around three; van Keulen, pers. comm.) was tacitly neglected. All differences between the *LAI* determined by the standard method ('*LAI* true'), and that estimated from the VIs were attributed to estimation errors from the VIs. Since part of these differences should be attributed to errors in the standard *LAI* determination, the accuracy of the *VI-LAI* estimation is in reality probably higher than that given in Figure 6.3b.

The effect of (*GR*) leaf colour on the estimation accuracy of *LAI* from the *IR/GR* ratio and the *NDVI* was relatively large. In preliminary reflection and transmission measurements on individual leaves, the variation in scattering properties was, on an absolute scale smaller in the red band than in the green band. This suggests that the red band would be more suitable than the green band for the estimation of *LAI* from vegetation indices.

In this study, the crop parameter of interest was *LAI* while leaf colour and canopy structure were treated as disturbing factors. However, leaf colour and canopy structure may also be properties of interest (e.g. in the relationship between leaf colour and rate of photosynthesis). The presented analysis can be repeated for any selection of properties of interest and 'disturbing' factors.

Acknowledgements

The author thanks C.J.T. Spitters (Centre for Agrobiological Research; † 1990) and J.G.P.W. Clevers (Agricultural University Wageningen) for their comments on this manuscript.

7 LINKING PHYSICAL REMOTE SENSING MODELS WITH CROP GROWTH SIMULATION MODELS, APPLIED FOR SUGAR BEET

Abstract In recent years, remote sensing and crop growth simulation models have become increasingly recognized as potential tools for growth monitoring and yield estimation of agricultural crops. In this paper, a methodology is developed to link remote sensing data with a crop growth model for monitoring crop growth and development. The 'Cloud' equations for radar backscattering and the optical canopy radiation model EXTRAD were linked to the crop growth simulation model SUCROS: SUCROS-Cloud-EXTRAD. This combined model was initialized and re-parameterized to fit *simulated* X-band radar backscattering and/or optical reflectance values, to *measured* values. The developed methodology was applied for sugar beet. The simulated canopy biomass after initialization and re-parameterization was compared with simulated canopy biomass with SUCROS using standard input, and with measured biomass in the field, for 11 fields in different years and different locations.

The seasonal-average error in simulated canopy biomass was smaller with the initialized and re-parameterized model (225-475 kg/ha), than with SUCROS using standard input (390-700 kg/ha), with 'end-of-season' canopy biomass values between 5500 and 7000 kg/ha.

X-band radar backscattering and optical reflectance data were very effective in the initialization of SUCROS. The radar backscattering data further adjusted SUCROS only during early crop growth (exponential growth), whereas optical data still adjusted SUCROS until late in the growing season (at high levels of *LAI*, 3-5).

7.1 Introduction

In agriculture, monitoring of crop growth and development, and early estimates of the final yield to be expected are of general interest. Traditionally, yield forecasts are made on the basis of samples at individual farmers, i.e. field visits or written enquiries. Problems encountered concern subjectivity in responses, respondent differences and non-response (Heath, 1990). On regional and (inter-) national scales, the processing of these sample data is an expensive and time-consuming procedure. In general, there is a need for an objective, standardized and possibly cheaper and faster methodology for collecting yield estimations. The last few years, attention has been paid to the possibilities of crop growth models and remote sensing techniques (King, 1988; Toselli and Meyer-Roux, 1990). In this paper, a methodology is developed to link radar and optical remote sensing data

with a crop growth simulation model for the monitoring of crop growth. The description of the methodology is preceeded by a short literature review to sketch some approaches and problems encountered so far.

In the integration with growth models, remote sensing data are mostly used to estimate some measure of light interception, e.g. Leaf Area Index (*LAI*) or green soil cover (Wiegand et al., 1986; Birnie et al., 1987). The rate of crop growth is then calculated from the product of light interception with global solar radiation and an efficiency factor with which crops convert radiant energy to biomass (Steven et al., 1983; Garcia et al., 1988; Bouman and Goudriaan, 1989). Using more elaborate, cyclic growth models, Kanemasu et al. (1984) and Maas (1988) replaced the *LAI* simulated in time by the model itself, with the *LAI* estimated from remote sensing data. However, Maas pointed out that a high accuracy of simulation results is dependent on frequent remote sensing observations. He developed a technique to initialize and re-parameterize a crop growth model to the *LAI* estimated from remote sensing data.

For practical reasons, *LAI* or soil cover is often estimated from (semi-) empirical regressions on remote sensing data. Such regressions are generally only valid for the specific environment and growth conditions under which they were derived. Moreover, they are non-explanatory and ignore existing knowledge on the interaction of radiation (light, microwaves) with vegetation canopies. Deterministic remote sensing models that explain the remote sensing signals from crop canopies have a wider applicability. However, the inversion of these models for the estimation of crop variables is often a difficult and cumbersome procedure (Goel et al., 1983, 1984). Finally, with (X-band) radar data, the accuracy of crop parameter estimation, like soil cover, is often too low for use in crop growth models (Bouman, 1991).

The synergistic use of remote sensing data from different types of sensors in crop growth models is, up to now, hardly being addressed. Researchers have suggested to relate optical and microwave remote sensing signals to crop parameters through common physical concepts (Goel, 1985; Clevers, 1988a). The estimation of, for instance *LAI*, may be improved with the introduction of independent equations that relate *LAI* to different remote sensing signals. However, this approach does not benefit from sensor-specific information and will not be pursued here.

In this paper a methodology of integrating remote sensing data with crop growth models is presented, that allows for the use of data from different types of sensors. Theoretic remote sensing models were not analytically inverted, but used in their original, explanatory formulation. The remote sensing models were 'Cloud' for canopy radar backscattering (Attema and Ulaby, 1978), and EXTRAD (EXTinction of RADiation) for optical canopy reflectance (Goudriaan, 1977). The radar backscattering was taken in the X-band (3-cm waves), and the optical

reflectance in the visible and near infra-red wavelengths. The used crop growth model was SUCROS (Simple and Universal CROp growth Simulator; Spitters et al., 1989). The methodology was tested on data of 11 fields of sugar beet, in different years and different locations.

7.2 Methodology

The crop growth simulation model SUCROS was extended with the 'Cloud' equations and the reflectance model EXTRAD. The combined SUCROS-Cloud-EXTRAD model simulated crop variables, such as biomass and *LAI*, together with radar backscattering and canopy reflectance during the growing season. SUCROS-Cloud-EXTRAD was then initialized and parameterized to fit the simulated remote sensing signals to the measured signals (Fig. 7.1).

7.2.1 The crop growth model SUCROS

SUCROS is a mechanistic crop growth model that describes the potential growth of a crop from irradiation, air temperature and crop characteristics. Potential growth means the accumulation of dry matter under ample supply of water and nutrients, in an environment that is free from pests and diseases.

A schematic illustration of the model is given in Figure 7.2. The light profile within a crop canopy is computed on the basis of the Leaf Area Index (*LAI*) and the extinction coefficient (based on the formulations in EXTRAD, see §7.2.3). At selected times during the day and at selected depths within the canopy, photosynthesis is calculated from the photosynthesis-light response of individual leaves. This response curve is characterized with its initial slope (the initial light use efficiency) and the asymptote (the light saturated photosynthesis). Integration over the canopy layers and over time within the day gives the daily assimilation rate of the crop (partly from Spitters, 1990).

Assimilated matter is first used to maintain the present biomass (maintenance respiration) and for the remainder converted into new, structural plant matter (with loss due to growth respiration). The newly formed dry matter is partitioned to the various plant organs through partitioning factors introduced as a function of the phenological development stage of the crop. Multiplication of the simulated leaf dry matter with the specific leaf area of new leaves gives the increase in leaf area (*LAI*). The increase in leaf area contributes to next day's light interception and hence to next day's rate of assimilation.

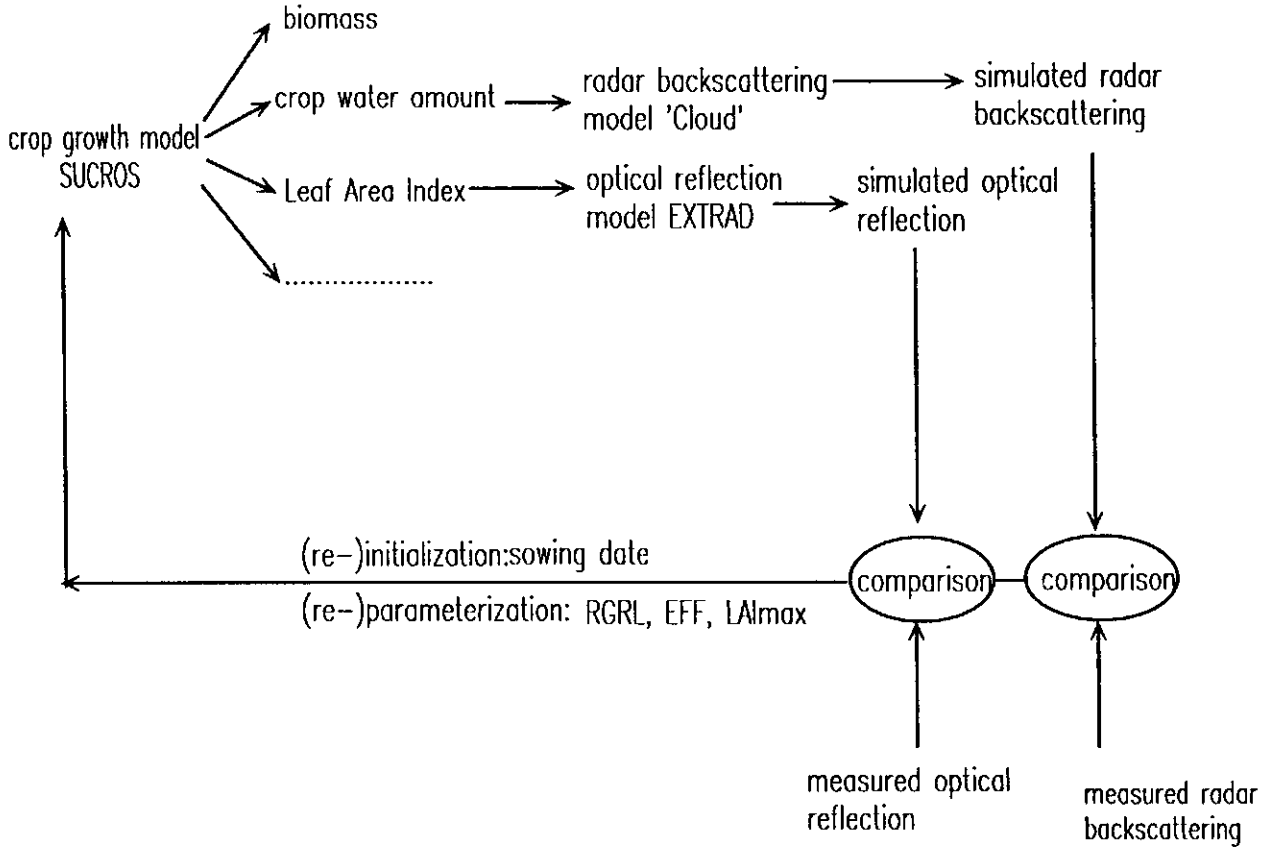

Figure 7.1. Methodology of (re-)initializing and (re-)parameterizing the crop growth model SUCROS with simulated and measured radar and optical remote sensing data.

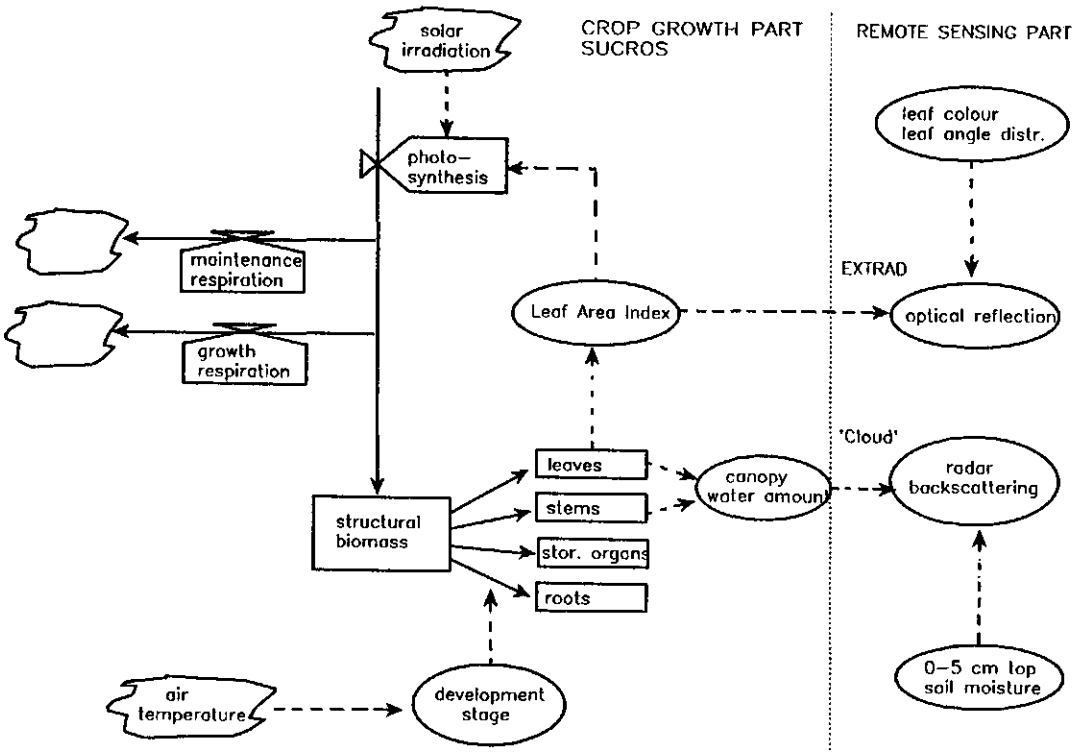

Figure 7.2. Functioning of the crop growth model SUCROS, and the linkage with the remote sensing models 'Cloud' (radar backscattering) and EXTRAD (optical reflectance). Rectangles represent quantities, valve symbols represent flows, circles represent auxiliary variables and clouds the atmosphere/environment; drawn lines represent flows of material and broken lines flows of information.

The parameters of the model can be divided into species parameters (e.g. partitioning factors, light use efficiency), location parameters (latitude), initialization parameters (e.g. sowing date, number of plants/m^2) and driving variables (daily irradiance, daily maximum and minimum temperature). Species parameters have to be estimated from field and laboratory measurements. Location and initialization parameters have to be known for each simulation condition, and driving variables have to be measured daily throughout the growing season.

7.2.2 The 'Cloud' equations for radar backscattering

Attema and Ulaby (1978) have modelled the radar backscattering from vegetation by representing the vegetation canopy as a cloud of isotropic water droplets. Their 'Cloud' equations belong to the class of semi-empirical models. The driving variables are the amount of water in the vegetation canopy and the volumetric moisture content in the top soil (for X-band radar, typically the layer of 0-5 cm). The radar backscattering is calculated at different angles of incidence:

$$\gamma = C(\theta).[1-\exp(-DW/\cos\theta)] + G(\theta).\exp(Km-DW/\cos\theta) \qquad (1)$$

where γ = radar cross section per unit projected area (m^2/m^2), W = amount of water in the canopy per unit soil surface (kg/m^2), m = volumetric soil moisture content (%), θ = incidence angle (°), D = coefficient of attenuation, K = soil moisture coefficient, $C(\theta)$ = backscattering of an optically thick crop cover, $G(\theta)$ = backscattering of dry soil. The parameters $C(\theta)$, D, $G(\theta)$ and K have to determined from regression analysis for specific crop types (from theoretical considerations $K \approx 0.05$-0.06). An example of γ as function of the amount of canopy water is given for sugar beet in Figure 7.3. The γ increases mainly with the early growth ($\approx$ 0-1000 kg/ha) in canopy water.

The 'Cloud' equations were linked to SUCROS by calculating the amount of water in the canopy from the simulated canopy dry biomass and the water content of the canopy (Fig. 7.2). Canopy water content (defined as fresh canopy weight minus dry canopy weight, divided by fresh weight) was derived from field experiments for different crop types. In sugar beet, the canopy water content was stable throughout the growing season at about 91%.

For the time being, the input for soil moisture content was taken from measurements in the field (see § 7.5.2).

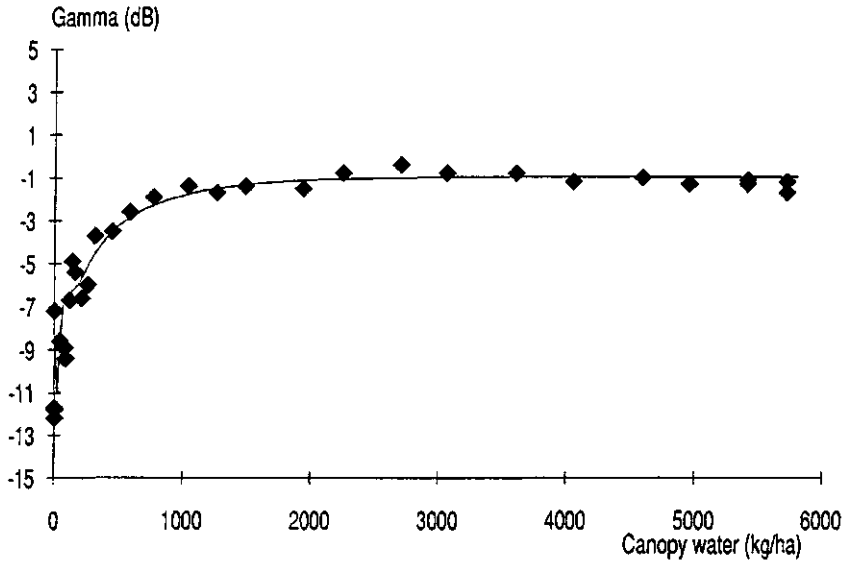

Figure 7.3. X-band radar backscattering (γ at 40° incidence angle) versus the amount of canopy water in sugar beet. ◆ are measurements on beet in 1979 and the drawn line is the fitted 'Cloud' curve.

7.2.3 The canopy radiation model EXTRAD

EXTRAD was developed by Goudriaan (1977) to calculate the (solar) radiation profile in crop canopies. A simplified version of EXTRAD is used in the photosynthesis subroutine of SUCROS to compute the extinction of photosynthetically active radiation (≈ 400-700 nm wavelength). However, the original, more detailed model was needed to calculate the directional reflectance from crop canopies at specific wavelengths up to the infrared region.

In EXTRAD, the canopy is subdivided into a number of horizontal infinitely extended layers. The leaves in these layers are assumed to have Lambertian scattering properties, and to have a uniform azimuthal distribution. The angle distribution of the leaves is described by nine inclination intervals from 10° each. The radiation profile in the canopy is then calculated with a relaxation method. The canopy reflectance in a given direction (in our study: nadir) is computed from the total radiance leaving the top layer of the canopy in that direction.

The input of the model are crop parameters (*LAI*, leaf scattering coefficient at specific wavelength, leaf angle distribution function), soil parameters (hemispherical reflection coefficient at specific wavelength) and illumination parameters (solar elevation angle, fraction diffuse sky irradiance). In principle, each parameter can be physically measured. Because a constant value is used as input for the reflection coefficient of bare soil, the influence of top soil (≈ 0-1 cm) moisture content on the reflectance of a crop-soil system is not modelled. However, the Weighted Difference Vegetation Index (*WDVI*), calculated from the infrared (*IR*) and the green (*GR*) (or red) reflectance, is relatively insensitive to variation in soil moisture content (Bouman, 1991; Clevers, 1989b):

$$\text{WDVI} = IR_c - (IR_s/GR_s)GR_c \qquad (2)$$

where IR_s and GR_s is the reflectance of the bare soil, and IR_c and GR_c is the reflectance of the crop. An example of the relation between *WDVI* and *LAI* is given for sugar beet in Figure 7.4.

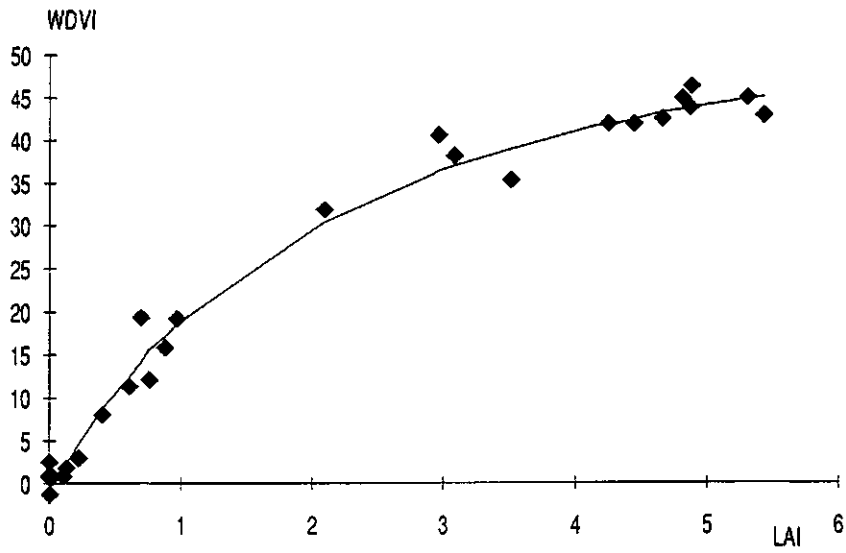

Figure 7.4. The Weighted Difference Vegetation Index (WDVI) versus Leaf Area Index (LAI) for sugar beet. ◆ are measurements on beet in 1987-1988 and the drawn line is the fitted EXTRAD curve.

EXTRAD was linked to SUCROS through the simulated *LAI* (Fig. 7.2). The other crop parameters were chosen according to crop type. In sugar beet, the leaf angle distribution was chosen spherical during the whole growing season. The scattering coefficients of the leaves were estimated from regression analysis on experimental data sets, and the hemispherical soil reflection coefficients were derived from measurements on bare soil. The input parameters for illumination conditions were chosen for each simulation condition. In principle, solar elevation angle and fraction diffuse sky irradiance can be set to actual conditions on days of remote sensing measurements.

7.2.4 Combined model functioning.

An example of simulated canopy biomass, *LAI*, X-band radar backscattering γ and *WDVI* with the combined SUCROS-Cloud-EXTRAD model is given for a hypothetical sugar beet crop in Figure 7.5.

In the early crop growth, γ reacted strongly on the first increase in canopy water (compare Fig. 7.3): γ increased already on day 140 with no significant dry biomass accumulation. The γ also saturated relatively soon, at day 180 with only some 2500 kg/ha dry biomass, and after day 180, no information on crop growth could be derived from γ.

The *WDVI* developed parallel to the *LAI*. It increased on about day 150 and reached a maximum value together with *LAI* on day 195. Because the maximum value of the *WDVI* was related to the maximum value of *LAI*, the *WDVI* still yielded information on *LAI* development at high levels of *LAI*.

Figure 7.5 illustrates the (potential) gain by considering both radar backscattering and optical reflectance data. (X-band) radar data extended the range over which information on crop growth can be derived in the 'early-growth' direction, and optical data in the 'mid-season' direction.

7.2.5 Initialization and (re-)parameterization

In reality, most crop species parameters in SUCROS do not have one specific value but are characterized by a 'biologically plausible range' (Rouse et al., 1991). This variation in parameter values allows for a range in simulation results from SUCROS-Cloud-EXTRAD. The model may thus be (re-)parameterized within the biologically plausible ranges to fit the simulated remote sensing signals to the measured remote sensing signals. Parameterization of the starting conditions (e.g. sowing date, number of plants/m^2) of SUCROS is called initialization.

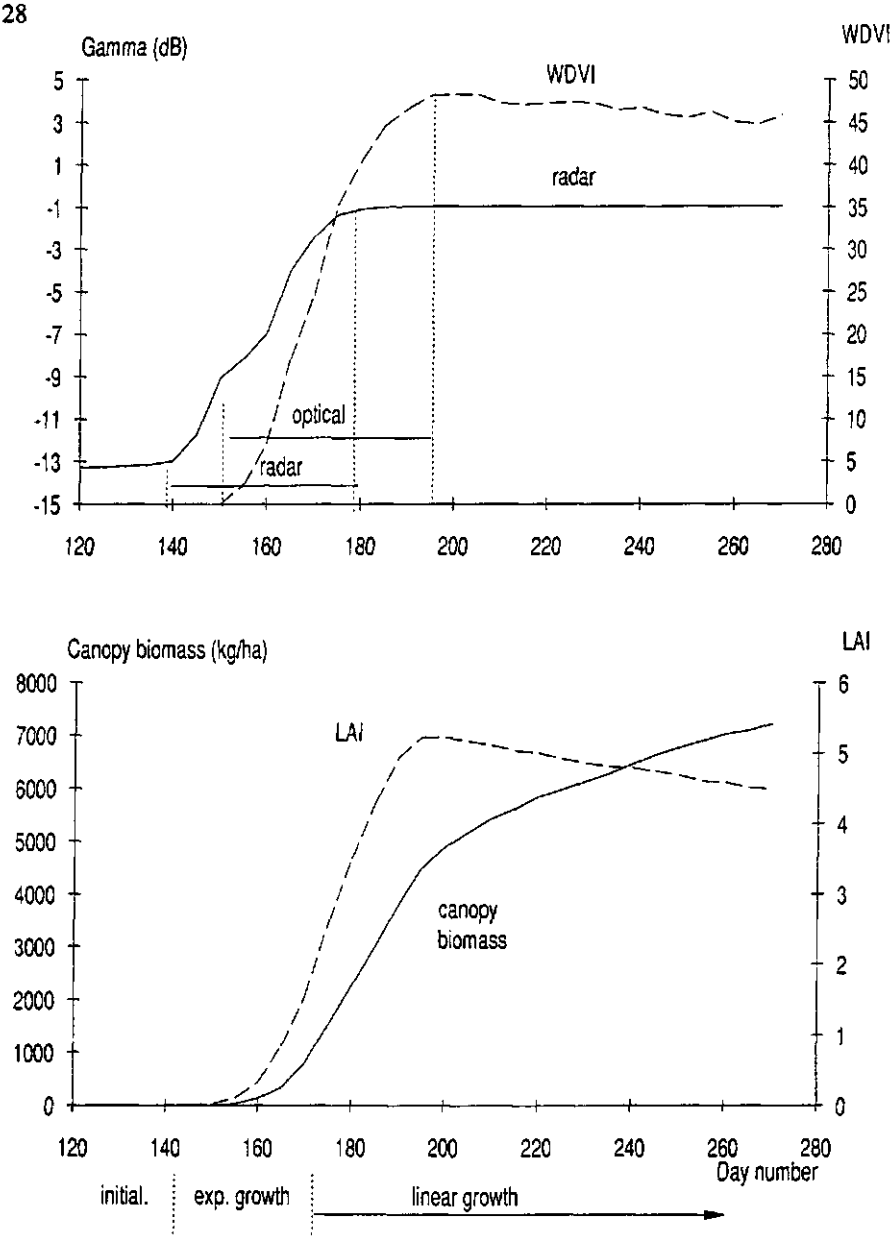

Figure 7.5. Simulated canopy biomass, Leaf Area Index, X-band radar backscattering (γ at 40° incidence angle) and optical reflection (WDVI) of a hypothetical sugar beet crop with the combined SUCROS-Cloud-EXTRAD model. The simulation environment was the Flevopolder with weather data from 1988.

Initialization and (re-)parameterization of SUCROS-Cloud-EXTRAD was based on a controlled random search procedure as developed by Price (1979) and extended by Klepper (1989) and Rouse et al. (1991). This procedure yielded per simulation condition 'optimum' initialization conditions and species parameter values. Optimum refers to parameter values that resulted in the smallest (absolute) difference between simulated and measured remote sensing signals (either optical or radar, or both), averaged over the whole growing season. With optimum parameter values, the simulated time course of remote sensing signals best fitted the measured signals. The procedure provided for the optimization of any number of parameters, to any number and combination of measured remote sensing signals. Thus, SUCROS-Cloud-EXTRAD could be optimized simultaneously to both optical and radar remote sensing measurements, at any combination of (radar) incidence angles.

A sensitivity analysis was used to select the initialization conditions and crop species parameters to be (re-)parameterized. The growing season was divided into three distinct growth periods: initialization, exponential growth, and linear growth (Fig. 7.5). Per growth period, parameters were selected that had a large effect on both the remote sensing signal and the canopy biomass and/or the *LAI* (Table 7.1). Because of the redundancy in the effect of parameter changes, the selection of parameters was kept to a minimum. With only radar data, 'sowing date' and 'relative growth rate' were selected. Changes in parameter values during linear growth had hardly any effect on γ (see also Fig. 7.5). With optical data, 'sowing date', 'relative growth rate', 'light use efficiency' and 'maximum leaf area' were selected. 'Maximum leaf area' (defined here as the leaf area above which dying occurs due to shading) had especially a large effect on the *WDVI* and the *LAI* in the second half of the period of linear growth.

Because the parameterization procedure optimized a number of parameters at the same time, the obtained optimum values may deviate from the true physical values. Optimum values only fitted the simulated remote sensing signals to the measured signals in order to improve the simulations of canopy biomass.

7.3 Description of experiments

The developed methodology was tested on a historical data set of 11 fields of sugar beet, both on experimental stations (1975-1983) and on farms in agricultural practice (1987-1988). The experiments were held in two different regions in The Netherlands: Wageningen and South-Flevoland (Table 7.2). The choice of this data set was solely guided by the availability of data (optical, radar, groundtruth).

Table 7.1. Sensitivity of canopy biomass, LAI, X-band radar backscattering (γ at 40° incidence angle) and WDVI to changes in SUCROS parameter values from the mean. The sensitivity was calculated as the maximum change in variable value during the whole growing season, divided by the seasonal mean of the variable. The change in SUCROS parameter values is given behind brackets in absolute values, or percentages from the mean.

	Canopy biomass	LAI	Radar	WDVI
Initialization:				
Sowing date (10 days)	.30	.40	.65	.60
Plant density (2 pl/m^2)	.04	.06	.07	.07
Exponential growth:				
Relative growth rate (10%)	.20	.40	.20	.35
Linear growth:				
Specific leaf area (10%)	.03	.16	.01	.08
Potential CO_2 assimilation rate (10%)	.06	.05	.02	.03
Light use efficiency (10%)	.17	.14	.04	.07
Extinction coeff. diffuse light (0.1)	.05	.07	.03	.05
Scattering coeff. leaves (0.1)	.05	.07	.03	.05
Maximum leaf area (2 LAI)	.07	.45	.01	.11

Table 7.2. Year, location (Wag = Wageningen, Fle = Flevoland), type and number of remote sensing observations of experiments on sugar beet.

Year	Location	Station name	Observation days Radar	Optical
1975	Wag	Droevendaal (1 field)	20	-
1979	Wag	De Bouwing („)	35	-
1980	Fle	De Schreef („)	36	34
1981	Fle	De Schreef („)	17	-
1983	Fle	De Schreef („)	-	32
1987	Fle	'Farmer' (3 fields)	-	6
1988	Fle	'Farmer' (3 fields)	-	9

The X-band radar backscattering was measured at 9.5 GHz, with a frequency sweep of about 0.4 GHz, using a ground-based FM-CW radar (van Kasteren and Smit, 1977; de Loor et al., 1982). Measurements were used here at different angles of incidence and at vertical co-polarization (VV: vertical transmitting and vertical receiving). The green (nadir) canopy reflectance was measured at 548 nm with a bandwidth of 31 nm, and the infra-red reflectance at 823 nm with a bandwidth of 80 nm, using a portable radiometer (van Kasteren, 1981). Both the radar system and the radiometer were frequently calibrated to ensure compatibility over the years.

Each year, canopy biomass and canopy water content were measured in the field at selected intervals during the growing season. The *LAI* was only measured in 1983-1988. On the experimental stations, canopy biomass was smoothed with growth functions, and values for the days of remote sensing observation were interpolated. In 1987 and 1988, the measurements coincided with the remote sensing observations.

In all years but 1975 and 1983, the volumetric moisture content of 0-5 cm top soil was measured on all days of remote sensing observation.

For this study, the empirical parameters of SUCROS, 'Cloud' and EXTRAD were determined/adapted for both the Wageningen and the Flevoland region.

SUCROS was originally developed and calibrated on field data in the Wageningen region (Spitters et al., 1989). For this study, the model was adapted for the Flevopolder region on the basis of the 1987 and 1988 data. Adaptations were made in the assimilate partitioning factors between leaf blades and leaf stems. Because of the prolonged growth of leaves (as compared to the Wageningen

region), the influence of temperature sum on the leaf photosynthesis rate and on the death rate of leaves, was removed.

The 'Cloud' equations were calibrated for the Wageningen region in 1979 (Hoekman et al., 1982) and for the Flevoland region in 1980 (Bouman and Goudriaan, 1989). EXTRAD was calibrated for the Flevoland region on the data of 1983, and on the data of 1987 and 1988.

7.4 Results

The simulations with the optimized SUCROS-Cloud-EXTRAD model were compared to those obtained with SUCROS-Cloud-EXTRAD with standard model input ('standard SUCROS'). Standard SUCROS runs were initialized with actual sowing dates. First, results will be discussed for a case study of beet in 1980 with optimization to radar data, to optical data, and to both radar and optical data (§ 7.4.1). Beet in 1980 are presented because only this year, both radar backscattering and optical reflectance were measured (Table 7.2). Next, the results of the methodology, expressed as seasonal-average difference between simulated and measured canopy biomass, are presented for all available data sets (§ 7.4.2). Finally, some limitations of the SUCROS-Cloud-EXTRAD model are indicated with a case study of beet in 1975 (§ 7.4.3).

7.4.1 Sugar beet in 1980

With *standard SUCROS* the simulated canopy biomass underestimated actual values during the whole growing season (Fig. 7.6). The corresponding simulated γ and *WDVI* were lower than the measured data in the early part of the growing season. The simulated *WDVI* was higher than the measured *WDVI* in the second half of the season.

After optimization to γ at 20°, 40° and 60° incidence angle, the simulated canopy biomass overestimated measured values for the largest part of the growing season (Fig. 7.6a). The description of the radar backscattering by the 'Cloud' equations was not adequate enough for better simulation results (of canopy biomass). In this case, a relatively large contribution of the soil background to the total radar backscattering from day 170 on (caused by high soil moisture contents) was 'misinterpreted' by the 'Cloud' equations as relatively high canopy water (and consequently high canopy biomass) values. However, the difference between simulated and measured canopy biomass, averaged over the whole growing season, was smaller than with standard SUCROS (Fig. 7.7).

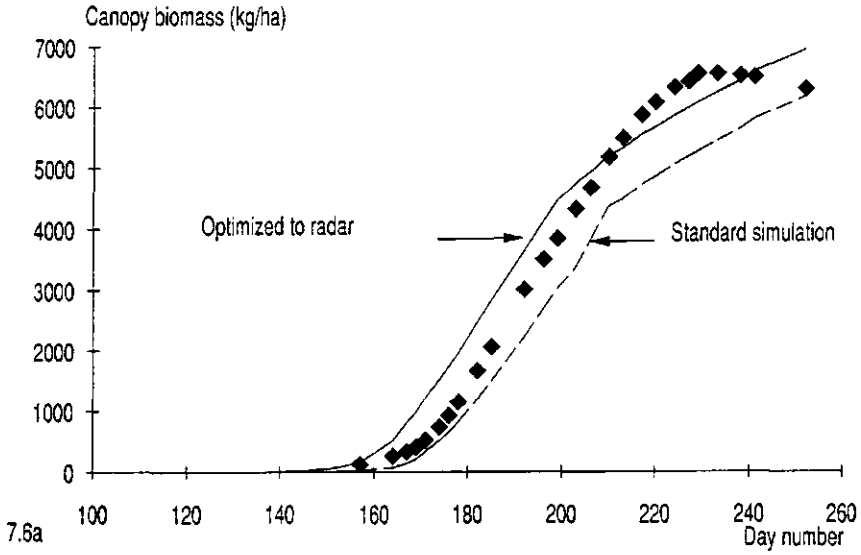
Canopy biomass (kg/ha)
7000
6000
5000
4000
3000
2000
1000
0
Optimized to radar
Standard simulation
100
120
140
160
180
200
220
240
260
Day number

7.6a

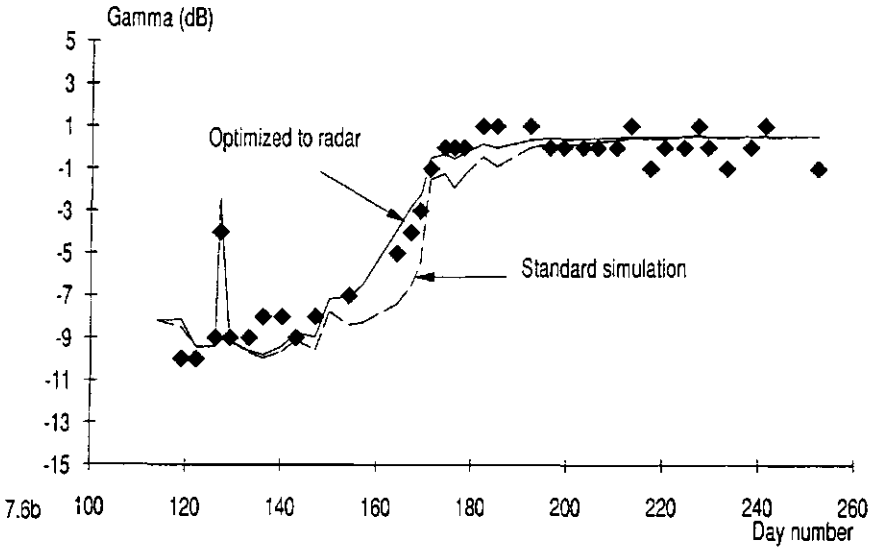
Gamma (dB)
5
3
1
-1
-3
-5
-7
-9
-11
-13
-15
Optimized to radar
Standard simulation
100
120
140
160
180
200
220
240
260
Day number

7.6b

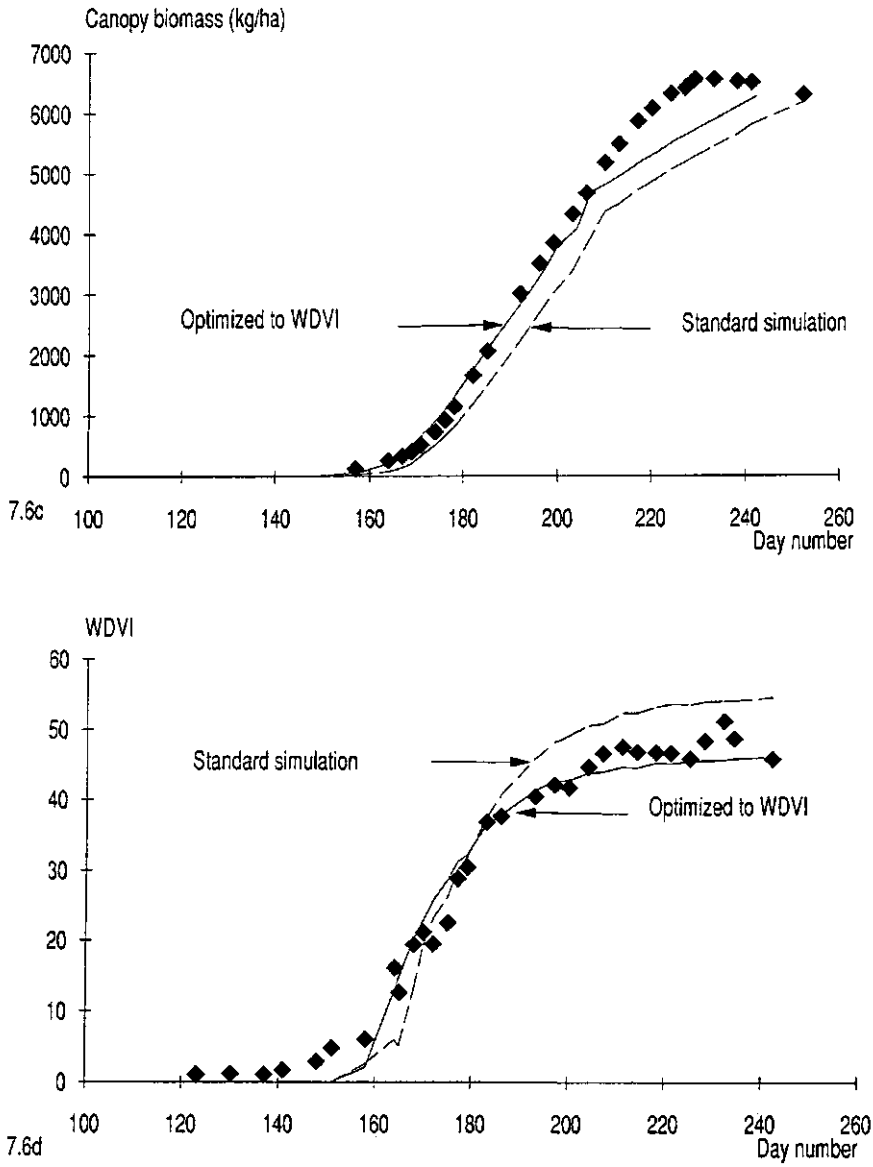

Figure 7.6. Simulated canopy biomass, X-band radar backscattering (γ at 40° incidence angle) and optical reflection (WDVI) for beet in 1980, with standard SUCROS and with SUCROS-Cloud-EXTRAD optimized to γ (7.6a/b) and optimized to WDVI (7.6c/d). ◆ are field measurements.

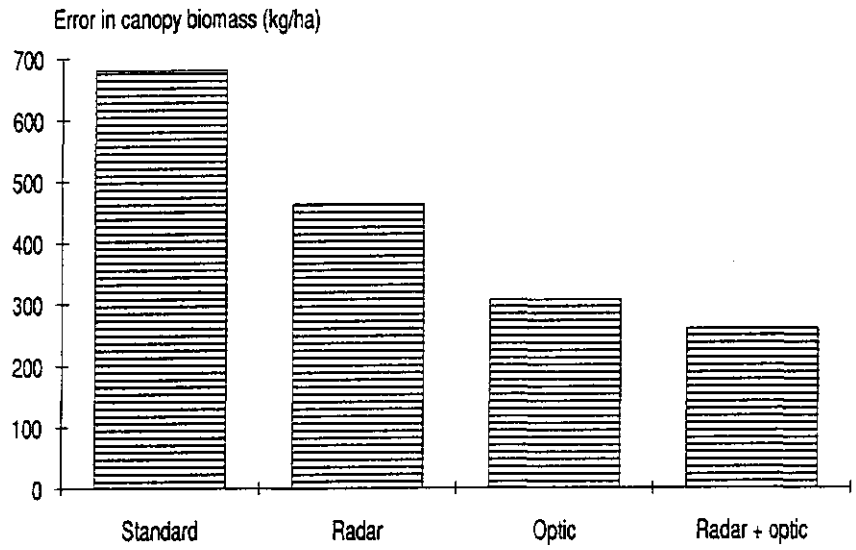

Figure 7.7. Seasonal-average error between measured and simulated canopy biomass for beet in 1980, with standard SUCROS, and with SUCROS-Cloud-EXTRAD optimized to γ (radar), to WDVI (optic) and to both γ and WDVI (radar + optic).

With optimization to *WDVI*, the simulated canopy biomass was in good agreement with measured data until day 205 (Fig. 7.6c). After day 205, SUCROS started to partition a larger portion of the assimilates to the underground crop parts, at the expense of the (above ground) canopy. The field measurements, however, showed that the growth of the canopy biomass after day 205 still took place at the same rate as before. After day 205, the (optimized) simulated *WDVI* remained a bit lower than measured *WDVI*. By optimizing SUCROS-Cloud-EXTRAD also to assimilate partitioning between canopy and root, simulated *WDVI* and canopy biomass could be brought in better agreement with measured values after day 205. However, because optical reflectance data only provide information on the above ground parts of the crop, the optimization to canopy-root assimilate partitioning seems a hazardous affair. Moreover, the optimized simulation of assimilate partitioning could not be verified due to the lack of measurements on root weight.

The seasonal-average difference between simulated and measured canopy biomass was smaller than with SUCROS-Cloud-EXTRAD optimized to γ (Fig. 7.7).

Figures 7.6a and 7.6c indicate that optimization of SUCROS-Cloud-EXTRAD to *both γ and WDVI* would not improve canopy biomass simulation over

optimization to *WDVI* only. However, the overestimation of canopy biomass with optimization to γ compensated somewhat for the underestimation with optimization to *WDVI* at the end of the growing season (Fig. 7.7).

7.4.2 All fields 1975-1988

The seasonal-average error in simulated canopy biomass with standard SUCROS and with optimized SUCROS-Cloud-EXTRAD was calculated for all available data sets (Fig. 7.8). The errors were averaged over data between crop emergence and harvesting. In 1975 and 1981, the errors were calculated over the first half of the growing season only, i.e. between crop emergence and some two weeks after closure of the canopy (≈ day 190). In 1975, a decrease in actual canopy biomass after day 190 hindered a meaningful comparison with simulations (see § 7.4.3). In 1981 biomass measurements were only made until day 190.

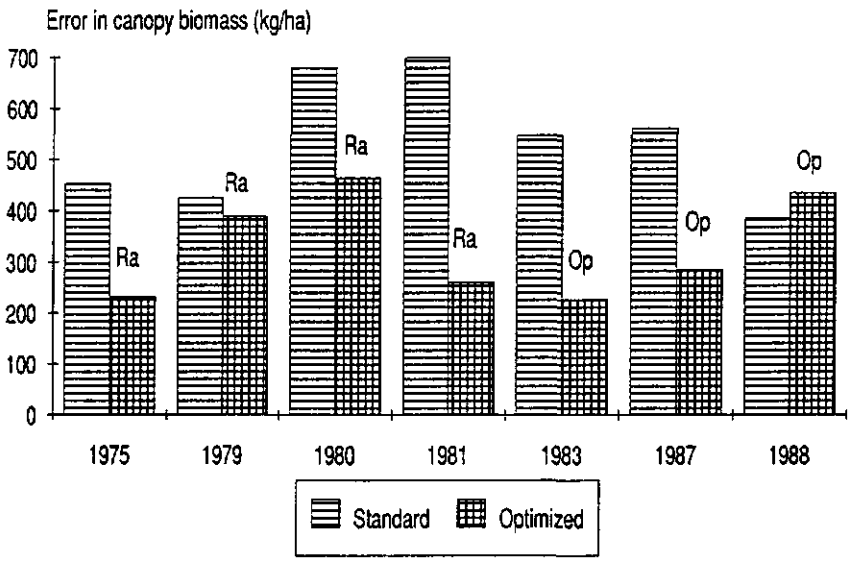

Figure 7.8. Seasonal-average error between measured and simulated canopy biomass for beet in 1975-1988, with standard SUCROS and with optimized SUCROS-Cloud-EXTRAD. 'Ra' means optimization to g, and 'Op' to WDVI.

In 1987 and 1988, the errors are averages over three fields, and in the other years, the errors relate to one field per year (Table 7.2).

Except for 1988, the errors with optimized SUCROS-Cloud-EXTRAD were lower than with standard SUCROS. The seasonal-average error in simulated canopy biomass with the optimized model ranged between 225 and 475 kg/ha, and with standard SUCROS between 390 and 700 kg/ha. For comparison: the 'end-of-season' canopy biomass values ranged between 5500 and 7000 kg/ha.

In 1988, the larger errors with optimized SUCROS-Cloud-EXTRAD were caused by a deviating (from other years) growth pattern of leaf-stems measured in the field (all three fields!). Only the biomass of leaf-blades was simulated accurately by the optimized model (to *WDVI*). The deviating measured growth pattern of leaf-stems could not be explained by the growth model SUCROS.

In 1975 and 1981 with radar data, and in 1980 with optical data, the model components of SUCROS-Cloud-EXTRAD were calibrated on independent data sets. In these years, the simulations of canopy biomass may be regarded as 'predictions'. In the other years, some or all SUCROS-Cloud-EXTRAD components were calibrated on the same data set used for comparison with simulations.

7.4.3 Model limitations

In 1975, crop growth of beet was seriously affected by drought in the second half of the growing season. Canopy biomass actually decreased after day ≈ 190 (Fig. 7.9). Simulations of canopy biomass with standard SUCROS already underestimated early crop growth. Moreover, because water stress is not modelled in SUCROS (§ 7.2.1: ample supply of water), the decrease in canopy biomass was not simulated.

SUCROS-Cloud-EXTRAD was optimized to γ at 20°, 50° and 70° incidence angle. Since no soil moisture contents were measured, this input in the 'Cloud' subroutine was fixed at 10% throughout the growing season. The optimized model simulated canopy biomass more accurately in the first half of the growing season (see also Fig. 7.8). Because γ was saturated above 2500 kg/ha canopy biomass (compare Fig. 7.5), the decrease in canopy biomass after day 190 was not noticed in the radar data and simulated canopy biomass kept on increasing.

Because no optical data were collected, the performance of SUCROS-Cloud-EXTRAD optimized to *WDVI* could not be evaluated. However, even if the *WDVI* did notice the decrease in canopy biomass (through decreasing *LAI*), the influence of water stress has to be included in SUCROS for correct simulations.

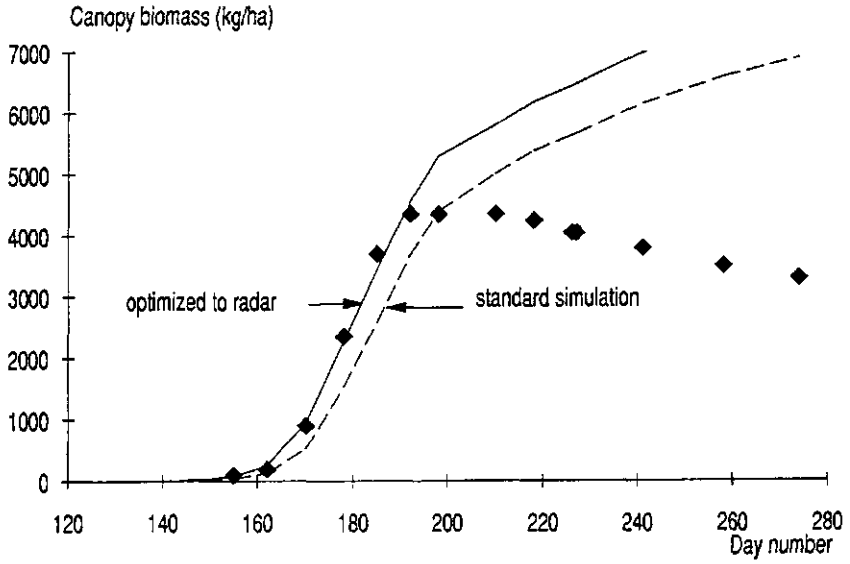

Figure 7.9. Simulated canopy biomass of sugar beet in 1975, with standard SUCROS and with SUCROS-Cloud-EXTRAD optimized to γ. ◆ are field measurements.

7.5 Discussion

7.5.1 Conclusion

Initialized and (re-)parameterized SUCROS-Cloud-EXTRAD to X-band radar (γ) and optical (*WDVI*) remote sensing data generally simulated canopy biomass more accurately than SUCROS with standard crop-species input and actual sowing date. Moreover, for growth monitoring on a regional scale, actual sowing dates of crops are generally not available as input for SUCROS.

The radar and optical remote sensing measurements adjusted the crop growth model mainly in the period of initialization and exponential growth. The γ saturated above canopy biomass values of about 2500 kg/ha and then no longer provided information on crop growth. The *WDVI* still yielded useful information on *LAI* development at high levels of *LAI* (3-5) in the second half of the growing season. Though the effect of *LAI* on net assimilation rate is relatively low at *LAI* values above three, a correct simulation of (high levels of) *LAI* is important for an accurate simulation of assimilate partitioning. This latter is important in crops where only specific parts have economic value, e.g. grains, roots, tubers. Furthermore, radar backscattering and optical reflectance data provide direct

information only on the (above-ground) crop canopy. The simulation of below-ground parts remains a 'derivative' of the optimized simulation of above-ground biomass.

7.5.2 Model improvements.

SUCROS-Cloud-EXTRAD may be improved by creating more links between SUCROS and the remote sensing model components. In the crop canopy, assimilate partitioning may be detected by remote sensing signals if the contribution of specific canopy parts to the total remote sensing signal of the crop is explicitly modelled. For example, in the two-layer 'Cloud' equations (Hoekman et al., 1982) a distinction is made between the contribution from the layer of ears in cereals, and that from the underlying vegetative matter. Up to now, more deterministic backscattering models that include canopy structure (Eom and Fung, 1984; Chuah and Tan, 1990) have been too complex for integration with crop growth models.

Again in cereals, the leaf angle distribution, canopy water content (in the ear-layer and in the vegetative layer) and leaf colour change with crop development. These three 'linking' parameters may be introduced in SUCROS as function of development stage. Possible links using the green leaf colour, that influences visible canopy reflectance and that may be related to leaf photosynthesis rate, have to be studied further.

In this study, measured top soil moisture contents were used as input in the 'Cloud' equations to calculate the radar backscattering. In practical applications, top soil moisture contents have to be estimated otherwise, for example from rainfall data, from C-band radar measurements (Bernard et al., 1982, 1984), or from radar measurements in combination with a water balance model (Prévot et al., 1984). The introduction of a soil water balance may also be used to extend SUCROS to account for effects of water stress, like for instance in WOFOST (van Diepen et al., 1989). Remote sensing models and observations in thermal bands may then be used to steer crop growth via the modelling of crop evapotranspiration (Thunnissen and Nieuwenhuis, 1989).

Finally, SUCROS-Cloud-EXTRAD may be extended with remote sensing models that operate in other radar bands or in the passive microwave region.

8 MAIN CONCLUSIONS AND DISCUSSION

This chapter synthesizes the main conclusions from the previous chapters, discusses implications and suggests possible directions for further research. First, the possibilities of specifically X-band radar remote sensing for use in monitoring crop growth and development are discussed. Next, two methods are described that were developed to link radar and optical remote sensing data with crop growth models for monitoring crop biomass.

8.1 The suitability of X-band radar for monitoring growth and development

The importance of canopy structure for X-band radar backscattering

An analysis was made of the main factors that influence radar backscattering of crop canopies. It was found that the X-band radar backscattering of crops was largely determined by canopy structure: the size, shape and orientation of canopy elements in three-dimensional space. Because the microwave dielectric constant of water is by an order of magnitude higher than that of dry biomass (Attema and Ulaby, 1978; Hoekman et al., 1982), water, for radar, is the most important constituent of canopy elements. It was found that even the spatial orientation of elongated canopy elements with a relatively low water content (≈ 10-20%), like straw and stubble, could still dominate the radar backscattering.

For a given crop type, variation in canopy structure may occur because of variety, ridge direction (potato), row spacing, wind and rain. In potato crops, the ridge direction was a major backscattering-infuencing factor from bare soil to ≈ 80% closure of the canopy. In wheat, barley and oats, the backscattering was greatly affected by lodging. In barley, the azimuthal orientation of the ears, as determined by wind direction and speed, was an important factor influencing radar backscattering. Canopy structure also changes due to morphological development in the course of the growing season.

Because of sensitivity to canopy structure, radar may be a tool to measure or monitor the morphology of crops. No instrument is as yet capable of doing so (non-destructively). Canopy structure is the basis of many morphological stages used to describe crop development (e.g. Zadoks et al., 1974). If the radar backscattering can be related to the morphological development of the crop, this information can be used in crop growth models. For instance in wheat, barley and oats, the temporal signature of the radar backscattering was shown to indicate general crop

development stages. Furthermore, canopy structure may give information about the general status of the crop, like lodging or wilting, which can affect crop growth. In wheat, for example, a sudden increase in radar backscattering suggested lodging. However, an interpretation such as this can be ambiguous sometimes because of unknown variables involved in determining radar backscattering. It can be expected that this problem will be solved by experienced interpreters by comparing other fields in the same region on radar imagery. (Other ways to solve ambiguities in the interpretation of canopy structure from radar data are given at the end of the end of this paragraph).

Another way of using the sensitivity of radar to canopy structure is in crop classification (Batliva and Ulaby, 1975; van Kasteren, 1981; Hoogeboom, 1983; Uenk et al., 1987; Wooding, 1988; Wegmüller, 1990). It is suggested here that crop types are differentiated mainly because of differences in canopy structure. For the monitoring of crop growth and yield estimations on a regional level, a classification of crops and an acreage inventory are the first steps that must be made.

Estimation of crop growth variables from X-band radar backscattering

Next, X-band radar data have been investigated in terms of the possibilities for estimating crop growth variables. Canopy biomass, canopy water, soil cover and height were estimated from radar data through empirical regressions and the semi-physical 'Cloud' equations. It was found that the estimation accuracies were generally too low for precise growth monitoring or for use in crop growth models. Out of the investigated crops (sugar beet, potato, wheat, barley, and oats), estimation of growth variables was only feasible for sugar beet in the early growing season. The amount of canopy water and the fraction soil cover were accurately estimated to values of about 2 kg/m^2 and 0.8 respectively, from radar data at a medium (40°-60°) and a high (60°-80°) angle of incidence.

The low estimation accuracies were caused by the simplicity of the estimation algorithms, and by specific features of the X-band: the relatively large influence of canopy structure, the early saturation of backscattering in the growing season (sugar beet, potato), and the relatively low crop-soil contrast (potato, wheat, barley). Even when regressions and the 'Cloud' equations are calibrated for specific crops, varieties and growth conditions, the effects of wind and rain on the canopy structure can not be accounted for (especially in cereals). It is suggested here that, for the estimation of crop growth variables from X-band radar data, the growth variable under consideration should be highly correlated with canopy structure. The following crop characteristics seem then to be important: uniform canopy geometry throughout the growing season, no azimuthal preference of canopy elements, absence of canopy elements with a pronounced narrow, longitudinal structure (e.g. ears and stems of wheat and barley), and relatively large and broad

leaves. From this reasoning, other crops that may be suitable for growth variable estimation, beside beet, are maize, sorghum and millet in the vegetative phase of the growing season.

Further research in radar remote sensing

More precise information on crop type, canopy structure and growth variables from radar remote sensing may be obtained from the analysis of so-called 'multi-parameter' data. Such data can be multi-angle, multi-temporal, multi-frequency or multi-polarization (polarimetry). To be useful, such data should be independent. In this study, it was found that multi-angle backscattering data in the X-band were generally too highly correlated to be useful for the estimation of growth variables (except for sugar beet; see above). In cereals, changes in canopy structure were often angle-dependent, and may be recognized by skilful interpreters. However, the use of a number of incidence angles is not suitable for observations from satellites. The use of multi-temporal radar data was elaborated in this study in combination with crop growth models, and will be summarized in the next paragraph. A first analysis of the usefulness of multi-frequency data was started in The Netherlands with the Agriscatt 1987-1988 (Bouman et al., 1991) and the Maestro 1989 campaigns. The Maestro campaign also initiated the study into radar polarimetry. Recent developments in this field of radar remote sensing seem especially promising (Kong, 1990; Ulaby and Elazhi, 1990).

The radar satellites planned for the near-future, ERS-1, JERS-1 and Radarsat, will only operate at one frequency, state of polarization and angle of incidence. The main feature of these satellites is that they will provide multi-temporal radar imagery of the surface of the Earth, unhindered by atmospheric conditions. This study has shown that, due to the many factors involved in determining radar backscattering, such data are generally not suitable for the precise estimation of crop canopy conditions in terms of quantitative growth variables or canopy structure. The use of future radar satellites in monitoring crop growth and development should focuss more on the spatial aspect of the radar data. The aim of satellite remote sensing is the observation of regional to global surface conditions, and not of detailed surface conditions on field level. Radar imagery can be used to spatially map and geo-code radar backscattering in relation to other types of geographic information such as topography, soil types, drainage conditions and rainfall patterns. Such combined data set can be used to extrapolate knowledge on the growth of crops on field level to regional and (inter-) national levels.

8.2 Methods of linking remote sensing data with crop growth models

Two methods were developed to link remote sensing data with crop growth models to monitor crop biomass. The first method was the estimation of soil cover from remote sensing data, and the use of this estimation as input into a light-interception growth model. The second method was the calibration of the crop growth model SUCROS on X-band radar backscattering and optical reflectance.

Estimation of soil cover from X-band radar data

In the first method, the growth rate of a crop was calculated from the fraction soil cover, the incident solar radiation, and a light use efficiency. The biomass of the crop was found by integration of the calculated growth rate of the crop in time. The fraction soil cover was estimated from X-band radar data. From the crops investigated (sugar beet, potato, wheat, barley, and oats), the use of X-band radar was only feasible for sugar beet (see above). In a case study of sugar beet for three different years, the canopy biomass was fairly accurately estimated throughout the growing season. The average error of estimation was about 250 kg/ha during the growing season. For operational use in biomass estimations, however, the consistency of the model parameters in the 'Cloud' equations needs to be further studied for differences in variety, and regional and climatological conditions.

Estimation of soil cover from optical reflectance data

The use of optical remote sensing data for the estimation of soil cover appears more promising. In this thesis, it was shown that the *LAI* (Leaf Area Index) of a crop can be fairly accurately estimated from the *WDVI* (Weighted Difference Vegetation Index). The *LAI* can then be converted into fraction soil cover f by the general expression $f = 1\text{-}\exp(-k\,LAI)$, where k is the light extinction coefficient.

The fraction soil cover can also be directly estimated from the *WDVI*, using empirical regressions. Figure 8.1 gives the *WDVI* versus fraction soil cover of nine fields of sugar beet (five different varieties, five different years, at four locations in the Flevopolder). A linear regression was fitted to this data set with an r^2 of 0.97. Using this regression, the average error of estimation of the fraction soil cover was the same as the estimation accuracy of the observer in the field, i.e. ≈ 0.05. The relationship between fraction soil cover and *WDVI* appears sufficiently stable to be used successfully in growth estimations. Stable relationships between soil cover and optical reflectance factors or Vegetation Indices have also been reported for other crops, e.g. potato (Birnie et al., 1987) and wheat (Kumar and Monteith, 1982; Lapitan, 1986; Garcia et al., 1988).

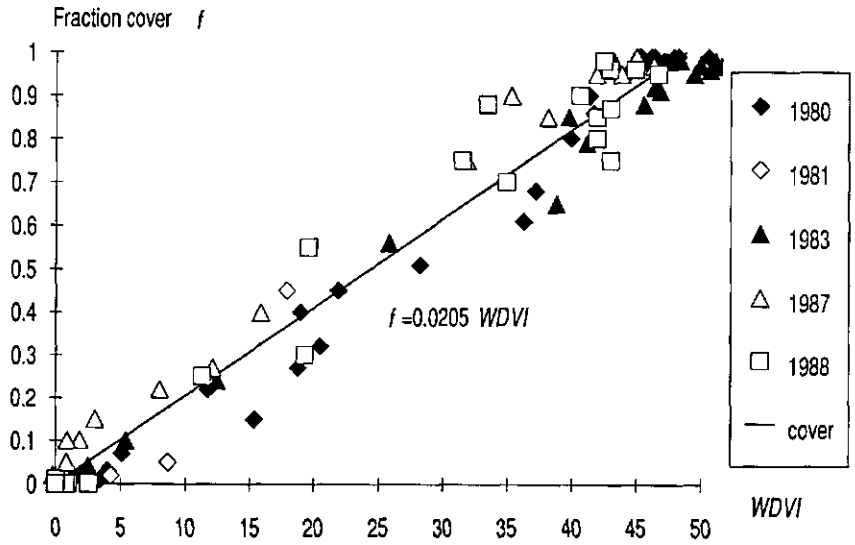

Figure 8.1. Fraction soil cover versus the Weighted Difference Vegetation Index (WDVI) for nine fields of sugar beet: one in 1980, 1981 and 183 each, and three in 1987 and 1988 each. The drawn line is the fitted regression, r^2=0.97, N=97.

Calibrating SUCROS on X-band radar backscattering and optical reflectance

In the second method used to link remote sensing data to crop growth models, the growth model SUCROS was extended with the remote sensing models 'Cloud' and 'EXTRAD' to calculate the radar backscattering and optical reflectance from the simulated crop. SUCROS was then calibrated by fitting the simulated remote sensing signals to a time series of actually measured remote sensing signals. In this method, the general shape of the growth curve is determined by SUCROS but the fine-tuning is done by the remote sensing data.

Important characteristics of this method are:

1) Remote sensing signals are calculated from the state of the crop canopy; physical remote sensing models are used in the original, explanatory way they were formulated. Inversion procedures, or the use of empirical regressions with limited applicability, are avoided.

2) Knowledge of the development of crop variables in time, incorporated into growth models, is optimally used. The fluctuations that occur in temporal

backscattering curves are nicely smoothed by the growth model, especially for radar.

3) Multi-sensor remote sensing data are applied in such a way that use is made of sensor-specific information. For beet, optical remote sensing data were related to the *LAI*, and X-band radar data to the amount of canopy water. When more sophisticated radar interaction models become available that are calibrated, these may be used to link radar data to the morphology of the canopy. SUCROS has then to be extended to include the simulation of canopy morphology. Furthermore, other remote sensing techniques, such as thermal infrared and passive microwave, may be incorporated by linking the interaction models to specific sub-processes of SUCROS.

The developed calibration method was tested on 11 fields of sugar beet. The accuracy of canopy biomass simulation was higher after calibration on remote sensing data than using standard model input in five out of six years. The seasonal-average error of estimation ranged between 225 and 475 kg/ha after calibration, and between 390 and 700 kg/ha before calibration, with 'end-of-season' canopy biomass values of 5500-7000 kg/ha.

Both X-band radar and optical remote sensing data were very effective in the initialization of SUCROS, i.e. the determination of the starting point of crop growth. This is one major contribution made by remote sensing to the operational application of growth models on regional levels. Information about the dates of sowing or emergence of crops to initialize growth models is generally not available.

After initialization, X-band radar data only adjusted SUCROS during early, exponential crop growth. Optical data still adjusted SUCROS in the middle part of the growing season. It is to be expected that in crops with a distinct ripening phase at the end of the growing season, such as cereals, optical data will again be very useful in calibrating that part of the growth model.

Further research in the application of radar and optical remote sensing with crop growth models for biomass monitoring

For the operational use of remote sensing and crop growth models in biomass monitoring, further research should be directed to calibration and validation of the model components for a number of crops under varying growth conditions. In root and tuber crops, like beet and potato, the simulation accuracy of the economically important under-ground parts should be investigated. This investigation was not carried out in this thesis because of lack of data. X-band radar and optical remote sensing data only provide direct information on the above-ground parts of a crop. In general, for biomass estimations of specific parts of a crop, the light-interception growth model presented here is too simplistic. On the other hand, the growth model

SUCROS requires many crop- and variety-specific input data that are often not available. Further research should be directed to the development of growth models of intermediate complexity that are specifically designed for, and calibrated on the scale of application. Such models may be linked with remote sensing data through either of the above developed methods.

The output of biomass estimations should be presented in terms of confidence intervals rather than in single, absolute values. This requires a sensitivity analysis of the model output in relation to the accuracy of model input, model parameters and remote sensing data.

SUMMARY

In agriculture, there is a general demand for monitoring crop growth and development for early yield estimations. New methodologies are being looked for that are more objective, standardized and possibly cheaper than traditional ways of monitoring and yield forecasting. Remote sensing and crop growth simulation models have become increasingly recognized as being new tools suitable for this purpose. Radar in particular seems suitable for monitoring purposes because its use is unhindered by weather conditions like clouds and fog.

This thesis describes an investigation into the suitability of X-band radar for monitoring crop growth and development, and into the possibilities of linking X-band radar backscattering and optical remote sensing data with crop growth models. The level of investigation is the field-level: radar backscattering and optical remote sensing data collected on experimental research stations and on fields of farmers are used.

In *Chapters 2 and 3*, six years of ground-based X-band radar observations were used to study the radar backscattering of sugar beet, potato, wheat, barley and oats in relation to crop growth and development. The radar data set included horizontal (HH) and vertical (VV) co-polarized radar data, at incidence angles from 10° to 80°. For beet and potato, the HH and VV radar backscattering increased at all angles of incidence until a level of saturation was reached at about 0.8 fraction soil cover. For wheat and barley, the HH and VV backscattering decreased with crop growth (after a small initial increase at low and medium incidence angles) until it fluctuated at a stable level from grain filling to the dying off of the canopy. The VV backscattering of oats at low to medium angles of incidence decreased during vegetative growth and sharply increased to a steady level with the appearance of the panicles.

The geometry of the crop-soil system was a major factor influencing radar backscattering. In potato, the orientation of the ridges with respect to the incident radar beam dominated the backscattering in the early growing season. The architecture of individual beet plants, and their distribution in space affected the radar backscattering of sugar beet.

Row spacing, crop variety and lodging influenced the radar backscattering of wheat, barley and oats. The effect of wind direction was sometimes very large for barley through changes in azimuthal ear-orientation. The architecture of the canopy also influenced the impact of the soil background on the radar backscattering. In cereal crops with a relatively wide row spacing, the influence of soil background was larger than in crops with a relatively close row spacing that had the same canopy biomass. Because of the many factors that influence canopy structure, the

radar backscattering of cereals was highly variable through the years. After harvesting, the radar backscattering was largely determined by the presence and spatial orientation of stubble and straw.

In *Chapter 4*, the possibilities of crop parameter estimation from X-band radar backscattering measurements were investigated using empirical and simple physical relationships. The crops investigated were sugar beet, potato, wheat and barley. The crop parameters investigated were dry canopy biomass, amount of canopy water, soil cover and crop height.

Empirical relations and the 'Cloud' equations were unsuitable for accurate estimations of crop parameters from X-band radar data at one angle of incidence at either HH or VV polarization. The use of both HH and VV polarized radar data did not improve the estimation accuracy. Using both a medium (40°-60°) and a high (60°-80°) angle of incidence, the amount of canopy water for sugar beet was estimated with an accuracy of 0.1-0.4 kg/m^2, to crop water values of about 2.5 kg/m^2. For potato, wheat and barley, the use of more than one angle of incidence did not result in higher accuracies of (any) parameter estimation.

The low estimation accuracies were attributed to the simplicity of the mono/bi-variate inversion schemes used, and to specific features of the X-band: 1) the disturbing influence of canopy structure on the radar backscattering, 2) the early saturation of the backscattering with crop growth, and 3) the low soil-crop contrast in backscattering. It was suggested that improvement of estimation accuracies might be obtained from radar remote sensing data using multi-frequency data, radar polarimetry and more sophisticated radar interaction models.

In *Chapter 5*, a method of growth monitoring was developed in which canopy biomass was not estimated directly, but was found as the accumulated value of the estimated crop growth rate. The crop growth rate was calculated from the fraction soil cover of the crop, the incident solar radiation, and a light use efficiency factor. The fraction soil cover was estimated from X-band radar data through the 'Cloud' equations and a regression with optical soil cover.

The method was applied on experimental data consisting of three sugar beet fields. In comparison with the direct estimation method, improved estimation accuracies of canopy biomass were obtained using 'Cloud' parameters and regression coefficients that were determined on the same data set. Using 'Cloud' parameter and regression coefficients that were determined in two different years, canopy biomass was fairly accurately estimated in a third year. Nevertheless, it was concluded that measurements of X-band radar backscattering still suffer from too much variation to be reliable for biomass estimation.

In *Chapter 6*, the optical canopy radiation model EXTRAD was used to quantify the accuracy of Leaf Area Index (*LAI*) estimations from Vegetation Indices (*VI*'s). The EXTRAD model was calibrated on sugar beet field data. The *VI*'s were the infrared/green ratio, [*IR/GR*], the Normalised Difference Vegetation Index, *NDVI* [*(IR-GR)/(IR+GR)*], the Perpendicular Vegetation Index, *PVI* [$\sqrt{((IR-IR_s)^2+(GR-GR_s)^2)}$], and the Weighted Difference Vegetation Index, *WDVI* [$IR-(IR_s/GR_s)GR$]. The accuracy of *LAI* estimation was calculated in relation to variation in so-called 'disturbing factors': green and infra-red leaf colour, leaf angle distribution, soil background and illumination conditions.

Variation in illumination conditions and soil background gave relatively small estimation errors with all four *VI*'s. The largest estimation errors resulted from variation in green leaf colour and leaf angle distribution. With variation in green leaf colour, the estimation errors were lowest with the *WDVI*. With variation in leaf angle distribution, the errors were lowest with the *IR/GR* ratio and the *NDVI*. In practice, the magnitude of the error in *LAI* estimation will depend on the magnitude and combination of occurring variation in leaf colour and leaf angle distribution.

In an average of 100 random combinations of disturbing conditions, and in a field experiment with six sugar beet fields, the absolute estimation errors ranged between about 0.1 for $0 < LAI < 1$ and 0.35 for $3 < LAI < 5$.

In *Chapter 7*, a method of calibrating crop growth simulation models on time series of remote sensing data was developed. The 'Cloud' equations for radar backscattering and the optical canopy radiation model EXTRAD were linked to the crop growth model SUCROS. SUCROS-Cloud-EXTRAD was then calibrated, i.e. re-initialized and re-parameterized, by fitting simulated X-band radar backscattering and/or optical reflectance (*WDVI*) to actually measured remote sensing data. The procedure developed allowed for the simultaneous calibration of any number of SUCROS parameters to any number and type of remote sensing data. Thus, SUCROS-Cloud-EXTRAD could be calibrated to both optical and radar measurements, individually or together, and at any combination of radar incidence angles.

The developed calibration method was applied to 11 fields of sugar beet in six different years. The simulated canopy biomass after calibration on remote sensing data was compared to simulations using SUCROS with standard model input. Except for one year, the seasonal-average error in simulated canopy biomass was smaller with the calibrated model (225-475 kg/ha) than using standard model input (390-700 kg/ha), with 'end-of-season' values of canopy biomass between 5500 and 7000 kg/ha.

X-band Radar backscattering and optical reflectance measurements were very effective in initializing SUCROS, i.e. the determination of the start of crop growth.

The radar backscattering further adjusted SUCROS only during early, exponential crop growth, while optical data still adjusted SUCROS until the late growing season at high levels of *LAI*, 3-5.

Chapter 8 brings together the main conclusions from the previous chapters, discusses implications and suggests possible directions for further research. The suitability of specifically X-band radar remote sensing for monitoring crop growth and development is discussed, together with its implications for radar remote sensing in general. The developed methods for linking optical and radar remote sensing data with crop growth models are also summarized.

SAMENVATTING

De koppeling van X-band radarreflectie en optische reflectie met gewasgroeimodellen.

In de landbouw bestaat een algemene behoefte aan het volgen van gewasgroei en -ontwikkeling ten behoeve van vroegtijdige oogstvoorspellingen. Hiervoor wordt naar nieuwe methoden gezocht die gestandaardizeerd, objectiever en mogelijk ook goedkoper zijn dan huidige methoden. Remote sensing en gewasgroeimodellen zijn veelbelovende technieken die hiervoor in aanmerking kunnen komen. Met name radar als remote sensing techniek lijkt bij uitstek geschikt voor monitoringsdoeleinden vanwege de ongevoeligheid voor weersomstandigheden als bewolking en mist.

In dit proefschrift wordt een onderzoek beschreven naar de mogelijkheden van X-band radar remote sensing voor het volgen van groei en ontwikkeling, en naar methoden om X-band radar en optische remote sensing data aan gewasgroeimodellen te koppelen. De schaal van onderzoek was het veldniveau: er zijn radar en optische reflectiemetingen gebruikt, verzameld met grondopstellingen op proefvelden en op praktijkpercelen.

In de *hoofdstukken 2 en 3* is de radarreflectie van suikerbieten, aardappelen, tarwe, gerst en haver beschreven in relatie tot groei en ontwikkeling. De radar data set bestond uit een meetserie van zes jaren, in horizontale (HH) en vertikale (VV) polarizatie, en in kijkhoeken tussen 10° en 80° van de vertikaal. Voor bieten en aardappelen nam de HH en VV radarreflectie bij alle kijkhoeken toe met de groei van het gewas tot een verzadigingsniveau vanaf ongeveer 80% bodembedekking. Voor tarwe en gerst daalde de HH en VV radarreflectie (na een kleine toename in het eerste begin van het groeiseizoen) tot het fluctueerde rond een stabiel niveau van korrelvulling tot afsterving. De VV radarreflectie van haver bij lage en middel kijkhoeken nam af gedurende de vegetatieve fase van gewasgroei, en nam scherp toe naar een stabiel niveau bij het verschijnen van de pluim.

De geometrie van het bodem-vegetatie systeem bleek een zeer groot effect te hebben op de radarreflectie. Bij aardappelen in het vroege groeiseizoen domineerde de richting van de ruggen ten opzichte van de kijkrichting van de radar de radarreflectie. De architectuur van individuele bietenplanten, en hun verspreiding in de ruimte beïnvloedde de radarreflectie van bieten.

Rij-afstand, gewasvariëteit en legeren beïnvloedde de radarreflectie van tarwe, gerst en haver. Het effect van windrichting op de radarreflectie van gerst was soms erg groot via de azimuthale richting van de aren. De geometrie van het gewas

beïnvloedde eveneens de mate waarin de onderliggende bodem aan de radarreflectie bijdroeg. Bij granen met een relatief grote rij-afstand was de bijdrage van de bodem groter dan bij granen met een relatief kleine rij-afstand en met een zelfde hoeveelheid biomassa. Vanwege de veelheid aan factoren die de gewasgeometrie bepaalt, was de radarreflectie van granen zeer variabel door de jaren heen. Na de oogst werd de radarreflectie met name bepaald door de aanwezigheid en ruimtelijke oriëntatie van stoppels en overgebleven stro (haksel).

In *hoofdstuk 4* zijn de mogelijkheden onderzocht om uit X-band radarreflectiemetingen gewasparameters te schatten met behulp van eenvoudige empirische of fysische modellen. De bestudeerde gewassen waren suikerbieten, aardappelen, tarwe en gerst. De bestudeerde gewasparameters waren bovengrondse droge biomassa, hoeveelheid bovengronds plantwater, bodembedekking en gewashoogte.

Schattingen van gewasparameters uit HH of VV radarreflectiemetingen bij één enkele kijkhoek, met behulp van empirische relaties of van het 'Cloud' model waren onnauwkeurig. Het gebruik van zowel HH als VV data verhoogde de nauwkeurigheid niet. Met gebruikmaking van een middel- (40°-60°) en een grote (60°-80°) kijkhoek, kon voor bieten de hoeveelheid bovengronds plantwater worden geschat met een nauwkeurigheid van 0.1-0.4 kg/m^2, tot een waarde van ongeveer 2.5 kg/m^2. Voor aardappelen, tarwe en gerst leidde het gebruik van meer dan één kijkhoek niet tot nauwkeurigere schattingen van gewasparameters.

De lage schattingsnauwkeurigheden werden toegeschreven aan de eenvoud van de gebruikte mono/bi-variabele inversie algoritmes, en aan enkele specifieke eigenschappen van de X-band: de invloed van gewasstructuur, de vroege verzadiging van de radarreflectie en het lage bodem-gewas contrast. Er werd voorgesteld dat hogere schattingsnauwkeurigheden verkregen zouden kunnen worden uit radar remote sensing met een aantal frekwenties, met radar polarimetrie en met meer geavanceerde interactiemodellen.

In *hoofdstuk 5* is een methode van het volgen van gewasgroei ontwikkeld waarbij de biomassa niet rechtstreeks geschat werd, maar bepaald werd door integratie van de geschatte gewasgroeisnelheid. De gewasgroeisnelheid werd berekend uit de fractie bodembedekking van het gewas, de hoeveelheid invallend zonlicht en een lichtbenuttingsefficiëntie factor. De fractie bodembedekking werd geschat uit X-band radar data met behulp van het 'Cloud' model en een regressie met optische bodembedekking.

De ontwikkelde methode werd toegepast op een experimentele dataset van drie jaar waarnemingen aan suikerbieten. In vergelijking met directe schattingen van biomassa uit radar metingen, leverde deze methode nauwkeurigere schattingen op

bij gebruikmaking van 'Cloud' parameters en regressiecoefficiënten die bepaald waren uit dezelfde dataset. Bij gebruikmaking van 'Cloud' parameters en regressiecoefficiënten die bepaald waren in twee verschillende jaren, werd in een derde, onafhankelijk jaar de biomassa geschat met een redelijk goede nauwkeurigheid. Desalniettemin werd geconcludeerd dat de variabiliteit in X-band radarreflectie data té groot was voor betrouwbare oogstschattingen.

In *hoofdstuk 6* is het optische stralingsmodel EXTRAD gebruikt om de schattingsnauwkeurigheid van het relatieve bladoppervlak (*LAI*) uit Vegetatie Indices (*VI*'s) te simuleren. Het EXTRAD model werd gecalibreerd op veldgegevens van suikerbieten. De *VI*'s waren de infrarood/groen ratio [*IR/GR*], de 'Normalized Difference Vegetation Index', *NDVI* [$(IR-GR)/(IR+GR)$], de 'Perpendicular Vegetation Index', *PVI* [$\sqrt{((IR-IR_s)^2+(GR-GR_s)^2)}$], en de 'Weighted Difference Vegetation Index', *WDVI* [$IR-(IR_s/GR_s)GR$]. De nauwkeurigheid van *LAI* schattingen werd gesimuleerd bij variaties in de volgende zogenaamde 'storende invloeden': groene en infrarode bladkleur, bladhoekverdeling, bodemachtergrond en belichtingsomstandigheden.

Variaties in belichtingsomstandigheden en in bodemachtergrond gaven relatief de kleinste schattingsfout bij alle vier *VI*'s. De grootste schattingsfouten werden veroorzaakt door variaties in groene bladkleur en in bladhoekverdeling. Bij variaties in groene bladkleur was de schattingsfout het kleinst met de *WDVI*, en bij variaties in bladhoekverdeling met de *IR/GR* ratio en de *NDVI*. In praktijk zal de schattingsfout afhangen van de grootte en de combinatie van voorkomende variaties in bladkleur en bladhoekverdeling.

In een gemiddelde van 100 willekeurige combinaties van variaties in storende invloeden, en in een veldexperiment met zes velden suikerbieten, varieerde de absolute schattingsfout van *LAI* van ongeveer 0.1 bij $0 < LAI < 1$ tot 0.35 bij $3 < LAI < 5$.

In *hoofdstuk 7* is een methode ontwikkeld waarbij een gewasgroeimodel gecalibreerd werd op remote sensing gegevens. De 'Cloud' vergelijkingen voor radarreflectie en het EXTRAD model voor optische reflectie werden gekoppeld aan het gewasgroeimodel SUCROS. SUCROS-Cloud-EXTRAD werd vervolgens gecalibreerd, d.w.z. ge-initialiseerd en ge-reparameteriseerd, door de gesimuleerde X-band radarreflectie en/of de optische reflectie (*WDVI*) te 'fitten' door de gemeten remote sensing data. In de fit procedure kon SUCROS gecalibreerd worden naar ieder aantal modelparameters, en op ieder aantal en type remote sensing metingen. SUCROS-Cloud-EXTRAD kon b.v. gecalibreerd worden op radar en optische data, zowel gelijktijdig als ieder afzonderlijk, en naar iedere combinatie van radar kijkhoeken.

De ontwikkelde calibratie methode werd toegepast op elf velden suikerbieten in zes verschillende jaren. De gesimuleerde bovengrondse biomassa ná calibratie werd vergeleken met díe verkregen met standaard model input. Op één jaar na, was de seizoensgemiddelde fout in biomassa schatting kleiner na calibratie (225-475 kg/ha) dan met standaard model input (390-700 kg/ha), bij biomassa waarden aan het eind van het groeiseizoen van 5500-7000 kg/ha.

X-band radarreflectie en optische reflectie data waren met name effectief in de initialisatie van SUCROS, d.w.z. in het bepalen van de start van gewasgroei. De X-band radarreflectie stelde SUCROS verder nog bij in het vroege groeistadium van exponentiële groei, en optische reflectie data tot laat in het groeiseizoen (bij hoge *LAI* waarden van 3-5).

Hoofdstuk 8 vat de belangrijkste conclusies van de vorige hoofdstukken samen, en bespreekt implicaties en mogelijke richtingen voor vervolgonderzoek. De bruikbaarheid van specifiek de X-band radarreflectie voor het volgen van gewasgroei en -ontwikkeling is besproken, met gevolgtrekkingen voor radar in grotere algemeenheid. De ontwikkelde methoden voor de koppeling van radarreflectie en optische reflectie gegevens aan gewasgroeimodellen zijn samen gevat.

REFERENCES

Allen, W.A. and A.J. Richardson, (1968), Interaction of light with a plant canopy, *Journal of Optical Society of America*, 58: 1023-1028.

Allen, W.A., T.V. Gayle and A.J. Richardson, (1969), Interaction of light with a compact leaf, *Journal of Optical Society of America*, 59: 1376-1379.

Allen, C.T. and F.T. Ulaby, (1984), Modelling the polarization dependence of the attenuation in vegetation canopies, in *Proceedings of IGARSS'84 Symposium, Strassbourg*, ESA SP-215: 119-124.

Asrar, G.M., M. Fuchs, E.T. Kanemasu and J.L. Hatfield, (1984), Estimating absorbed photosynthetic radiation and leaf area index from spectral reflectance in wheat, *Agronomic Journal*, 76: 300-306.

Attema, E.P.W., (1974), Short range vegetation scatterometry, in *Proceedings URSI Specialist Meeting: Microwave scattering and emission from the Earth*, Bern Switzerland, pp. 177-184.

Attema, E.P.W., and F.T. Ulaby, (1978), Vegetation modelled as a water cloud, *Radio Science* 13(2): 357-364

Attema, E.P.W., (1988), Radar signature measurements during the Agriscatt campaigns, in *Proceedings of IGARSS'88 Symposium*, Edinburgh, Scotland, 13-16 September 1988, ESA SP-284:1141-1144.

Batliva, P.P., and F.T. Ulaby, (1975), Crop identification from radar imagery of the Huntington County, Indiana test site, *The University of Kansas Space Technology Center, RSL Technical report* 177-58, Lawrence, Kansas.

Bernard, R., PH. Martin, J.L. Thony, M. Vauclin and D. Vidal-Madjar, (1982), C-band radar for determining surface soil moisture, *Remote Sensing of Environment* 12:189-200.

Bernard, R., O. Taconet, D. Vidal-Madjar, J.L. Thony, M. Vauclin, A. Chapton, F. Wattrelot and A. Lebrun, (1984), Comparison of three in situ surface soil moisture measurements and application to C-band scatterometer calibration, *IEEE Transactions on Geoscience and Remote Sensing*, GE-22(4): 388-394.

Binnenkade, P., (1986), The determination of optimum parameters for identification of agricultural crops with airborne SLAR data, in *Proceedings of the 7th International Symposium, ISPRS Commission VII: Interpretation of photographic and Remote Sensing Data*, Enschede 25-29, Augustus 1986, (Balkema Publishers, Rotterdam) pp. 111-115.

Binnenkade, P. and D. Uenk, (1987), Gewasidentificatie met behulp van microgolven (uitwerking SLAR-gegevens 1985), *BCRS report* bcrs-87-13, Delft, The Netherlands (Dutch).

Birnie, R.V., P. Millard, M.J. Adams and G.G. Wright, (1987), Estimation of percentage ground cover in potatoes by optical radiance measurements, *Research and Development in Agriculture*, 4, 1:33-35.

Bouman, B.A.M., (1987), Radar backscattering from three agricultural crops: beet, potatoes and peas, *CABO report* 71, Wageningen, The Netherlands.

Bouman, B.A.M. and D. Uenk, (1987), Quick-looks van IRIS op Flevoland, veldwerk bij radar opnames met de Canadese IRIS SAR, *CABO report* 73, Wageningen, The Netherlands (Dutch).

Bouman, B.A.M., (1988), The microwave backscatter from beets, peas and potatoes throughout the growing season, in *Proceedings of the 4th Internati onal Colloquium on Spectral Signatures of Objects in Remote Sensing*, Aussois (Modave), France 18-22 January, ESA SP-287: 25-30

Bouman, B.A.M., and H.W.J. van Kasteren, (1989), Ground-based X-band radar backscattering measurements of wheat, barley and oats 1975-1981, *CABO report 119*, Wageningen, The Netherlands.

Bouman, B.A.M. and J. Goudriaan, (1989), Estimation of crop growth from optical and microwave soil cover, *International Journal of Remote Sensing*, 10(12): 1843-1855.

Bouman, B.A.M. and H.W.J. van Kasteren, (1990a), Ground-based X-band (3 cm wave) radar backscattering of agricultural crops. I. Sugar beet and potato; backscattering and crop growth, *Remote Sensing of Environment*, 32: 93-105

Bouman, B.A.M. and H.W.J. van Kasteren, (1990b), Ground-based X-band (3 cm wave) radar backscattering of agricultural crops. II. Wheat, barley and oats; the impact of canopy structure, *Remote Sensing of Environment*, 32: 107-118

Bouman, B.A.M., M.A.M. Vissers and D. Uenk, (1991), Multifrequency radar measurements of potato, beet and wheat during the Agriscatt-88 campaign in The Netherlands, in *Proceedings Fifth International Colloquium on 'Physical Measurements and Signatures in Remote Sensing'*, Courchevel, France, 14-18 January 1991 (in press.).

Bouman, B.A.M., (1991a), The linking of crop growth models and multi-sensor remote sensing data, in *Proceedings Fifth International Colloquium on*

'Physical Measurements and Signatures in Remote Sensing', Courchevel, France, 14-18 January 1991 (in press.).

Bouman, B.A.M., (1991b), Crop parameter estimation from ground-based X-band (3-cm waves) radar data, *Remote Sensing of Environment* (in press).

Bouman, B.A.M., (1991c), Accuracy of estimating the leaf area index from vegetation indices derived from reflectance characteristics, a simulation study, *International Journal of Remote Sensing* (submitted)

Buiten, H.J. and J.G.P.W. Clevers (Eds), (1990), *Remote sensing, theorie en toepassingen van landobservatie*, PUDOC, Wageningen, The Netherlands (in Dutch),

Bunnik, N.J.J., (1978), The multispectral reflectance of shortwave radiation by agricultural crops in relation with their morphological and optical properties, *Thesis, Agricultural University Wageningen*, 78-1, The Netherlands.

Chuah, H.T. and H.S. Tan, (1990), A multiconstituent and multilayer microwave backscatter model for a vegetative medium, *Remote Sensing of Environment*, 31(2): 137-153.

Cihlar, J., R.J. Brown and B. Guindon, (1984), Microwave remote sensing of agricultural crops in Canada, In *Microwave remote sensing applied to vegetation*, ESA SP-227: 113-126.

Clevers, J.G.P.W., (1986), *Application of remote sensing to agricultural field trials*, Agricultural University of Wageningen paper 86-4, Wageningen, The Netherlands.

Clevers, J.G.P.W., (1988a), Crop monitoring for agricultural propositions, in *Proceedings 16th ISPRS Symposium*, Kyoto, Japan, July 1-10, pp: VII 206-215.

Clevers, J.G.P.W., (1988b), The derivation of a simplified reflectance model for the estimation of leaf area index, *Remote Sensing of Environment*, 25:53-69.

Clevers, J.G.P.W., (1989), The application of a weighted infrared-red vegetation index for estimating leaf area index by correcting for soil moisture, *Remote Sensing of Environment*, 29:25-37

Diepen, C.A. van, J. Wolf, H. van Keulen and C. Rappoldt, (1989), WOFOST: a simulation model of crop production, *Soil Use and Management*, 5(1): 16-24.

Dulk, J.A. den, (1989), The interpretation of remote sensing, a feasibility study, *Thesis, Agricultural University Wageningen*, The Netherlands.

Eom, H.J. and K.A. Fung, (1984), A scatter model for vegetation up to Ku-band, *Remote Sensing of Environment* 15: 185-200.

ESA Land Applications Working Group, (1987), *Remote Sensing for Advanced Land Applications*, ESA Report SP-1075 Revision 1, Paris: European Space Agency.

Evans, D.L, T.G. Far, J.J. van Zijl and H.E. Zebker, (1988), Radar polarimetry: analysis tools and applications, *IEEE Transactions on Geoscience and Remote Sensing*, GE-26(6): 774-789.

Fiumara, A., et al., (1988), Crops radar responses analysis based on Agrisar '86 data, in *Proceedings of IGARSS'88 Symposium*, Edinburgh, Scotland, 13-16 September 1988. ESA SP-284:1131-1132.

Gallagher, J.N., and Biscoe, P.V., (1978), Radiation absorption, growth and yield of cereals, *Journal of Agricultural Science* (Cambridge) 91, pp. 47-60.

Garcia, R., E.T. Kanemasu, B.L Blad, A. Bauer, J.L. Hatfield, D.J. Major, R.J. Reginato, K.G. Hubbard, (1988), Interception and use efficiency of light in winter wheat under differences in nitrogen regimes, *Agricultural and Forest Meteorology*, 44:175-186.

GENSTAT5 *Reference Manual*, (1988), Oxford Science Publication, England.

Goel, N.S., and D.E. Strebel, (1983), Inversion of vegetation canopy reflectance models for estimating agronomic variables I. Problem definition and initial results using Suits' model, *Remote Sensing of Environment* 13(6): 487-507.

Goel, N.S., D.E. Strebel and R.L. Thompson, (1984), Inversion of vegetation canopy reflectance models for estimating agronomic variables. II Use of angular transforms and error analysis as illustrated by Suits' model, *Remote Sensing of Environment* 14:77-111

Goel, N.S, (1985), Modelling of canopy reflectance and microwave backscattering coefficient, *Remote Sensing of Environment*, 18: 235-253.

Goodman, J.M., (1980), Environmental constraints in earth-space propagations, in *Agard Conference Proceedings*, CP-284: 35.1-35.27

Goudriaan, J., (1977), *Crop micrometeorology: a simulation study* (Wageningen, The Netherlands: Pudoc).

Haverkort, A.J., Harris, P.M., (1986), Conversion coefficients between intercepted solar radiation and tuber yields of potato crops under tropical highland conditions, *Potato Research* 29, pp. 529-533.

Heath, D.W., (1990), Introductory remarks, In *Proceedings of the Conference on The Application of Remote Sensing to Agricultural Statistics* (Edited by F. Toselli and J. Meyer-Roux), 10-11 october 1989, Varese, Italy (Publisher: Commission of the European Communities).

Hoekman, D.H., (1981), Modelvorming radar backscatter voor gewassen, *Delft University of Technology, Department of Electrical Engineering*, the Netherlands, Master's Thesis, Report 05-1-533-AV-90'81 ((Dutch).

Hoekman, D.H., L. Krul and E.P.W. Attema, (1982), A multilayer model for radar backscattering from vegetation canopies, *Digest of the 2nd IEEE International Geoscience and Remote Sensing Symposium*, Münich, West Germany, 1-4 June, pp. 4.1-4.7

Hoekman, D.H., (1990), Radar remote sensing data for applications in forestry, *Thesis Agricultural University of Wageningen*, The Netherlands.

Hoogeboom, P., (1983), Classification of agricultural crops in radar images, *IEEE Transactions on Geoscience and Remote Sensing*, GE-21(3): 329-336.

Hoogeboom, P., (1985), Optimization of agricultural crop identification in SLAR images: hierarchic classification and texture analysis, in *Proceedings EARSeL Workshop 'Microwave Remote Sensing Applied to Vegetation'*, Amsterdam, 10-12 December 1984, ESA Publication ESA SP-227, pp. 41-48.

Hoogeboom, P., (1986), Identifying agricultural crops in radar images, in *Proceedings of the 7th International Symposium, ISPRS Commission VII: Interpretation of photographic and Remote Sensing Data*, Enschede 25-29 Augustus 1986, (Balkema Publishers, Rotterdam) pp. 131-137.

Huete, A.R., D.F Post and R.D. Jackson, (1984a), Soil spectral effects on 4-space vegetation discrimination, *Remote sensing of environment*, 15:155-165.

Huete, A.R., R.D. Jackson and D.F Post, (1984b), Spectral response of a plant canopy with different soil backgrounds, *Remote sensing of environment*, 16.

Huete, A.R., (1988), A soil-adjusted vegetation index (SAVI), *Remote Sensing of Environment*, 25: 295-309.

Jones, C.A. and J.R. Kiniry (Eds.), (1986), *Ceres maize, a simulation model of maize growth and development*, Texas A & M University press, United States of America.

Jordan, C.F., (1969), Derivation of leaf area index from quality of light on the forest floor, *Ecology*, 50: 663-666.

Kanemasu, E.T., G. Asrar and M. Fuchs, (1984), Application of remotely sensed data in wheat growth modelling. In *Wheat growth modelling*: 357-369, Edited by Day, W. and R.K. Atkin (Plenum Press, New York and London, Published in cooperation with NATO Scientific Affairs Division).

Karam, M.A. and A.K. Fung, (1988), Electromagnetic scattering from a layer of finite length, randomly oriented, dielectric, circular cylinders over a rough surface with application to vegetation, *International Journal of Remote Sensing*, 9(6): 1109-1134.

Kasteren H.W.J. van, and M.K. Smit, (1977), Measurements on the backscattering of X-band radiation of seven crops, throughout the growing season, *NIWARS publication* 47, Delft, The Netherlands.

Kasteren, H.W.J. van, (1981a), Radar signatures of crops. The effect of weather conditions and the possibilities of crop discrimination with radar, in *Signatures spectrales d'objets en teledetection*, Avignon, 8-11 September 1981, pp. 407-415.

Kasteren, H.W.J. van, (1981b), A spectrometer to determine soil coverage and biomass in situ, in *Ist International Colloquium on Spectral Signatures in Remote Sensing* (ISP-INRA), Proceedings:125-132.

Keulen, H. van, and J. Wolf (Eds), (1986), *Modelling of agricultural production: weather, soils and crops*, Simulation monograph, PUDOC, Wageningen, The Netherlands.

Keulen, H. van, and Seligman, (1987), *Simulation of water use, nitrogen nutrition and growth of a spring wheat crop*, Simulation Monograph, PUDOC, Wageningen, The Netherlands.

King, D., (1988), Télédétection et modèles agrométéorologiques de prévisions de rendements, *Joint Research Centre* SP.1-88.40/FR, Ispra, Italy.

Klepper, O, (1989), A model of carbon flows in relation to macrobenthic food supply in the Oosterschelde estuary (S.W. Netherlands), *Thesis, Agricultural University Wageningen*, The Netherlands.

Kong, J.A. (Ed), (1990), *Polarimetric remote sensing*, PIER 3, Elsevier Publisher.

Krul, L., (1988), Microwave remote sensing and vegetation: problems, progress and solutions - a review, In *Microwave remote sensing applied to vegetation*, ESA SP-227: 3-9.

Kumar, M., and J.L. Monteith, (1981), Remote sensing of crop growth, In *Plants and the daylight spectrum*, H. Smith (Ed), pp. 133-144.

Kuusk, A. and T. Nilson, (1989), The reflectance of shortwave radiation from multilayer plant canopies, *Academy of sciences of the Estonian SSR section of physics and astronomy*, Tallinn, Estonia, USSR.

Laan, F.B. van der, (1989), The chance on cloud free imagery of The Netherlands, in *National Point of Contact, Products and Services*, detailed guide to imagery available, Emmeloord, The Netherlands.

Lang, A.R.G., (1973), Leaf orientation of a cotton plant, *Agricultural meteorology*, 11:37-51.

Lang, R.H., S. Saatchi and D.M. Levine, (1986), Microwave backscattering from an anistropic soybean canopy, in *Proceedings of IGARSS'86 Symposium*, ESA SP-254: 1107-1112.

Lapitan, R.L., (1986), Spectral estimates of absrobed light and leaf area index: effects of canopy geometry and water stress, *Ph.D. dissertation*, Kansas State University.

Lavin, E.P., (1971), *Specular reflection*, Monograph on applied optics, No. 2, Adam Hilger (Publisher), London, England.

Lillesand, T.M. and R.W. Kiefer, (1979), *Remote sensing and image interpretation*, J. Wiley and Sons, Inc., New York.

Loomis, R.S. and W.A. Williams, (1969), Productivity and the morphology of crop stands: patterns with leaves. In *Physiological aspects of crop yield*: 27-48, edited by Eastin, J.D. et al. (American Society of Agronomy and Crop Science Society of America, Madison, Wisconsin).

Loor, G.P. de, P. Hoogeboom and E.P.W. Attema, (1982), The Dutch ROVE program, *IEEE Transactions on Geoscience and Remote Sensing*, GE-20, 1:3-11.

Loor, G.P. de, (1985a), Variation of the radar backscattering of vegetation through the growing season, in *Proceedings EARSeL Workshop Microwave remote sensing applied to vegetation*, Amsterdam, 10-12 December 1984, pp. 63-67.

Loor, G.P. de, (1985b), Moisture determination in and under vegetation canopies, *Physics and Electronics Laboratory TNO*, Report 1985-52, The Hague, The Netherlands.

Loor, G.P. de, (1987), Moisture determination in and under vegetation canopies, part II: results after parameterization of the CLOUD model, *BCRS-87-03*, Delft, The Netherlands.

Maas, S.J., (1988), Use of remotely sensed information in agricultural crop growth models, *Ecological Modelling*, 41: 247-268.

Milthorpe, F.L. and Moorby, J., (1979), *An introduction to crop physiology* (Cambridge: Cambridge University Press).

Monteith, J.L., (1981), Does light limit production? In *Physiological processes limiting plant productivity*, edited by C.B. Johnson (London: Buttersworths).

Nilson, T., (1988), Spectral-temporal reflectance profiles for some cereals, *Academy of sciences of the Estonian SSR section of physics and astronomy*, Tartu, Estonia, USSR.

Prévot, L., R. Bernard, O. Taconet, D. Vidal-Madjar and J.L. Thony, (1984), Evaporation from a bare soil evaluated using a soil water transfer model and remotely sensed surface soil moisture data, *Water Resources Research*, 20(2): 311-316.

Prévot, L., I. Champion and G. Guyot, (1988), Extraction des caracteristiques du sol et de la végétation a partir de données de télédétection hyperfréquences, in *Fourth International Colloquium on Spectral Signatures in Remote Rensing*, Aussois France, ESA SP-287: 7-12.

Price, W.L., (1979), A controlled random search procedure for global optimisation, *The Computer Journal*, 20:367-370.

Richardson, A.J., and C.L. Wiegand, (1977), Distinguishing vegetation from soil background information, *Photogrammetric Engineering and Remote Sensing*, 43:1541-1552.

Rouse, J.W., R.H. Haas, J.A. Schell and D.W. Deering, (1973), Monitoring vegetation systems in the great plains with ERTS, in *Third ERTS Symposium*, NASA SP-351:309-317.

Rouse, D.I., W. Stol and O. Klepper, (1991), A fortran program for calibration and uncertainty analysis of crop growth models: description with users guide and program listing, *CABO report* (in press), Wageningen, The Netherlands.

Schanda, E., (1986), *Physical fundamentals of remote sensing*, Springer-Verlag Berlin Heidelberg, Germany.

Schellberg, J., (1990), Die spektrale Reflexion von Weizen - ein Beitrag zur Zustandsbeschreibung landwirtschaftliger Kulturpflanzenbestände durch Fernerkundung, *Inaugural-Dissertation, Institut fur Pflanzenbau der Rheinischen Friedrich-Wilhelm-Universität Bonn*, Germany.

Smit, M.K., (1978), Radar reflectrometry in The Netherlands: measurement system, data handling and some results, in *Proceedings OST Conference Earth Observation from Space and Management of Planetary Resources*, Toulouse, France, ESA SP-134.

Spitters, C.J.T., H. van Keulen and D.W.G. van Kraalingen, (1989), A simple and universal crop growth simulator: SUCROS87, In *Simulation and systems management in crop protection*: 147-181, edited by R. Rabbinge, S.A. Ward and H.H. van Laar (PUDOC Wageningen, The Netherlands).

Spitters, C.J.T., (1990), Crop growth models: their usefulness and limitations, *Acta Horticulturae* 267: 345-363

Steven, M.D., P.V. Biscoe and K.W. Jaggard, (1983), Estimation of sugar beet productivity from reflection in the red and infrared spectral bands, *International Journal of Remote Sensing*, 4(2): 325-334.

Suits, G.H., (1972a), The calculation of the directional reflectance of a vegetation canopy, *Remote Sensing of Environment*, 2: 117-125.

Suits, G.H., (1972b), Verification of a reflectance model for mature corn with application to corn blight detection, *Remote Sensing of Environment*, 2: 183-192.

Suits, G.H., (1975), The nature of electromagnetic radiation, in *The manual of remote sensing*, vol.1 , chapter 3, American Society of Photogrammetry, Falls Church, Virginia.

Thunnissen, H.A.M., and G.J.A. Nieuwenhuis, (1989), An application of remote sensing and soil water balance simulation models to determine the effect of groundwater extraction on crop evapotranspiration, *Agricultural Water Management*, 15: 315-332

Toselli, F. and J. Meyer-Roux, (1990), (Eds), *Proceedings of the Conference on The Application of Remote Sensing to Agricultural Statistics*, 10-11 october 1989, Varese, Italy (Publisher: Commission of the European Communities).

Tucker, C.J., (1979), Red and photographic infrared linear combinations for monitoring vegetation, *Remote Sensing of environment*, 8:127-150.

Tucker, C.J., B.N. Holben, J.H. Elgin and J.E. McMurtrey III, (1980), Relationship of spectral data to grain yield variation, *Photogrammetric Engineering and Remote Sensing*, 46: 657-666.

Uenk, D., H.W.J. van Kasteren and P. Binnenkade, (1987), Classificatie van landbouwgewassen met radar, radarvluchten 1983 en 1984 in Groningen, Oostelijk Flevoland en West Brabant, *BCRS-87-17*, Delft, The Netherlands.

Ulaby, F.T., R.K. Moore and A.K. Fung, (1981), *Microwave remote sensing*, Vol. I, Addison-Wesley, Reading Massachusettes, United States of America.

Ulaby, F.T., R.K. Moore and A.K. Fung, (1982), *Microwave remote sensing*, Vol. II, Addison-Wesley, Reading Massachusettes, United States of America.

Ulaby, F.T, and R.P. Jedlicka, (1984), Microwave dielectric properties of plant materials, *IEEE Transactions on Geoscience and Remote Sensing*, GE-22(4): 406-415.

Ulaby, F.T, C.T. Allen, G. Eger III and E. Kanemasu (1984), Relating the microwave backscattering coefficient to leaf area index, *Remote sensing of environment* 14: 113-133.

Ulaby, F.T. and E.W. Wilson, (1985), Microwave attenuation properties of vegetation canopies, *IEEE Transactions on Geoscience and Remote Sensing*, GE-23(5): 746-753.

Ulaby, F.T., R.K. Moore and A.K. Fung, (1986), *Microwave remote sensing*, Vol. III, Artech House, Washington, United States of America.

Ulaby, F.T. and C. Elazhi (Eds.), (1990), *Radar polarimetry for geoscience applications*, Artech House Publishers.

Verhoef, W., (1984), Light scattering by leaf layers with application to canopy reflectance modelling: The SAIL model, *Remote Sensing of Environment*, 16:125-141.

Vygodskaya, N.N., I.I. Gorshkova and Ye. V. Fadeyeva, (1989), Theoretical estimates of sensitivity in some vegetation indices to variation in the canopy condition, *International Journal of remote sensing*, 10(12): 1857-1872.

Waite, William P., Ali M. Sadeghi and H. Don Scott, (1984), Microwave Bistatic Reflectivity Dependence on the Moisture Content and Matric Potential of Bare Soil, *IEEE Transactions on Geoscience and Remote Sensing*, GE-22, 4:394:405.

Wegmüller, U., (1990), Remote sensing signature studies on agricultural fields with ground-based radiometry and scatterometry, *Phd. Thesis, University of Bern (Philosophisch-naturwissenschaftlichen Fakultät)*, Bern, Switzerland.

Wendlandt, W.W.H. and H.G. Hecht, (1966), *Reflectance spectroscopy*, Interscience Publishers.

Wiegand, C.L., A.J. Richardson and E.T. Kanemasu, (1979), Leaf area index estimates for wheat from Landsat and their implications for evapotranspiration and crop modelling, *Agronomic Journal*, no. 71: 336-342.

Wiegand, G.L., A.J. Richardson and P.R. Nixon, (1986), Spectral components analysis: a bridge between spectral observations and agrometeorological crop models, *IEEE Transactions on Geoscience and Remote Sensing*, GE-24(1): 83-88.

Wit, C.T. de, (1965), Photosynthesis of leaf canopies, *Agricultural Research Report* 663, Centre for Agricultural Publications and Documentation (PUDOC), Wageningen, The Netherlands.

Wooding, M. (Ed.), (1988), *Imaging radar applications in Europe*, ESA TM-01.

Zadoks, J.C., T.T. Chang and C.F. Konzak, (1974), A decimal code for growth stages of cereals, *Eucarpia Bulletin* 7.

BIOGRAPHY

Bas Antonius Maria Bouman was born in Groesbeek, The Netherlands, on 27 September 1960. In 1979 he obtained his Gymnasium diploma at the Rijksscholengemeenschap Wageningen. That same year he started his study 'Tropische Cultuurtechniek' at the Agricultural University Wageningen. He received the degree of Ingenieur 'cum laude' in 1987, with main courses in Remote Sensing, Soil Science, and Irrigation and Civil Engineering. In the last two years of his study, he worked as assistant to students in Remote Sensing.

After graduation, he was employed at the Centre for Agrobiological Research in Wageningen, doing his research work for this thesis. He was also involved in the international radar remote sensing campaigns Agriscatt (1987-1988), of which he was the Dutch Principal Investigator, and Maestro (1989). In 1987, he became secretary of the Commission 'Radar Observation on Vegetation', ROVE, and between 1988-1991, he was secretary of the 'Netherlands Remote Sensing Society'.